VIRGINIA POLYTECHNIC INSTITUTE
AND STATE UNIVERSITY

The Charles E. Via, Jr. Department
of Civil and Environmental Engineering
Blacksburg, VA 24061

Structural Engineering and Materials

YIELD LINE PATTERNS FOR END-PLATE MOMENT CONNECTIONS

by

Matthew R. Eatherton, S.E., Ph.D.
Associate Professor

Trai N. Nguyen

Graduate Research Assistant

Thomas M. Murray, P.E., Ph.D.
Emeritus Professor

Report No. CE/VPI-ST-21/05

December 2021

EXECUTIVE SUMMARY

The purpose of this report is to summarize the yield line patterns and associated yield line parameters for end-plate moment connections. Both the end-plate yield line patterns and the column side yield line patterns are provided. For each yield line parameter, either the derivation is given or details about how the yield line parameter was obtained from one of the other derived yield line parameters is described.

TABLE OF CONTENTS

1 INTRODUCTION

Yield line analysis is a method for determining the plastic collapse capacity of ductile steel plates or reinforced concrete slabs. In the yield line method, a plastic collapse mechanism is assumed consisting of rigid facets of the plate connected by lines where the plate undergoes plastic hinging, usually called yield lines. Figure 1-1a demonstrates the concept of facets and yield lines for an end-plate moment connection while Figure 1-1b shows the three-dimensional deformed shape associated with this yield line pattern. It is noted that yield lines at supports are generally shown with a slight offset (e.g., the yield lines adjacent to the flanges in Figure 1-1a are slightly offset from the face of the flange) to make them visible in sketches, but located at the support in all calculations. A yield line mechanism is considered admissible if every facet is planar and there are no displacement discontinuities (i.e. breaks in the plate) at the edges of the facets.

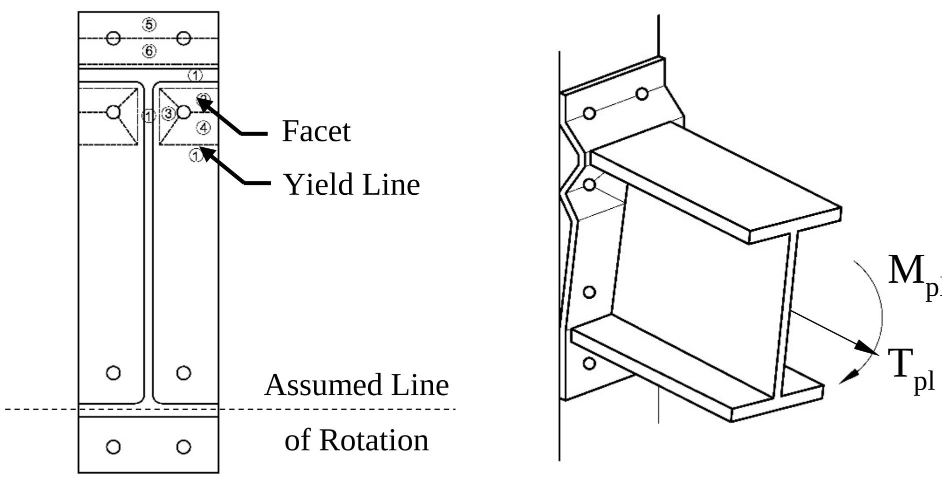

(a) Two-dimensional drawing of yield line pattern

(b) Three-dimensional representation of the yielded end-plate

Figure 1-1 Yield Line Pattern Representing End-Plate Yielding Failure Mode

Yield line analysis is typically conducted using virtual work and thus results in an upper bound solution for the collapse load. That means that the theoretically correct collapse load for a plate will be less than the collapse load calculated using virtual work. The most appropriate choice for the yield line pattern is therefore the one which produces the smallest yield line parameter and associated collapse load. In most configurations described in this document, the yield line pattern presented produces the smallest yield line parameter and associated moment strength. In some cases, however, a yield line pattern that does not produce the smallest yield line parameter was used in prior research and found to accurately predict the strength of an end-plate connection experiencing end-plate yielding. For those cases, the experimentally validated yield line parameter is presented first, and then the alternate yield line pattern is presented which predicts a smaller strength. In all cases, yield line parameters that have been experimentally validated are recommended for use in design.

The process of calculating an end-plate's moment strength for the limit state of end-plate yielding using yield line analysis consists of several steps: 1) assume an arbitrary amount of beam rotation, θ, 2) determine the rotation at each yield line associated with the beam rotation, 3) calculate the internal work associated with plastic hinging along the yield lines, 4) calculate external work associated with the moment and axial force acting through a rotation and translation, respectively, 5) set internal work equal to external work and simplify the resulting equation, and 6) extract the yield line parameter, Y.

The internal work is calculated as the plastic moment strength of the end plate per unit length multiplied by the rotation of each yield line:

$$W_I = m_p \sum_i \left(\theta_x + \theta_y \right)_i \tag{1-1}$$

Where:

W_I is the total internal work

m_p is plastic moment capacity per unit length which is calculated in Eq. (1-2);

θ_x and θ_y are the plastic rotation angles with respect to x and y axes, respectively.

$$m_p = \frac{1}{4} F_{yp} t_p^2 \tag{1-2}$$

Where:

F_{yp} = yield stress of the end-plate

t_p = thickness of the end-plate

The external work, W_E, is defined as the summation of external work associated with moment and axial force acting through a rotation and translation, respectively, as given by Eq (1-

3). However, the contribution of axial force to the external work is relatively small compared to the contribution of the moment so the external work is often approximated as shown in Eq (1-4).

$$W_E = M_{pl}\theta + T_{pl}\theta\frac{d}{2} \tag{1-3}$$

$$W_E \cong M_{pl}\theta \tag{1-4}$$

Where:

M_{pl} = moment strength of the end-plate associated with the yield-line mechanism

T_{pl} = axial strength of the end-plate associated with the yield-line mechanism

θ = rotation angle of the end-plate relative to the support

d = depth of the beam

Internal work and external work are set equal as given in Eq. (1-5) and the equation is simplified. The resulting equation is put in the form shown in Eq. (1-6) where the yield line parameter, Y is a function of the geometry of the end-plate connection and has units of length. Eq. (1-6) is a generic form of the equation for end-plate moment strength and is applicable to all configurations, whereas the resulting equation for the yield line parameter, Y, is unique to the specific configuration.

$$W_I = W_E \tag{1-5}$$

$$M_{pl} = F_{yp}\, t_p^2\, Y \tag{1-6}$$

Where:

Y = yield line parameter for the specific configuration of bolts

Moment strength associated with end-plate yielding M_{pl} is used to design the end-plate thickness of moment connection and the design procedure is presented in AISC Design Guide 4+16 (Eatherton and Murray 2021). Yield line parameters derived in this report are identical to those used in Design Guide 4+16 and this report is intended to be a companion to the Design Guide which gives the background for how the yield line parameters were obtained.

2 END-PLATE YIELD LINE SOLUTIONS

2.1 Summary of End-Plate Yield Line Parameters

There are a total of 14 end-plate configurations considered herein. All of these configurations have been studied previously, although the yield line derivation may not have been included in the original published literature. Table 2-1 provides a summary of the yield line parameter with variables defined in the respective sections. The following sections show the derivation of each yield line parameter.

The original work conducted on these end-plate moment connection configurations is summarized in Table 2-2. In most of these references, the yield line pattern and yield line parameter were presented and then validated against full-scale moment connection test results.

Table 2-1a Summary of Yield Line Parameters for Flush End-Plate Configurations

Configuration	Yield Line Parameter	Notes
Two-Bolt Flush Unstiffened	$Y=\frac{b_p}{2}\left[h_1\left(\frac{1}{p_{fi}}+\frac{1}{s}\right)\right]+\frac{2}{g}\left[h_1\left(p_{fi}+s\right)\right]$	
Four-Bolt Flush Unstiffened	$Y=\frac{b_p}{2}\left[h_1\left(\frac{1}{p_{fi}}\right)+h_2\left(\frac{1}{s}\right)\right]+\frac{2}{g}\left[h_1\left(p_{fi}+\frac{3}{4}p_b\right)+h_2\left(s+\frac{1}{4}p_b\right)\right]+\frac{g}{2}$	
Four-Bolt Flush Stiffened **Between** the Bolts	$Y=\frac{b_p}{2}\left[h_1\left(\frac{1}{p_{fi}}+\frac{1}{p_{so}}\right)+h_2\left(\frac{1}{p_{si}}+\frac{1}{s}\right)\right]+\frac{2}{g}\left[h_1\left(p_{fi}+p_{so}\right)+h_2\left(p_{si}+s\right)\right]$	
Four-Bolt Flush Stiffened **Below** the Bolts	$Y=\frac{b_p}{2}\left[h_1\left(\frac{1}{p_{fi}}\right)+h_2\left(\frac{1}{p_s}\right)\right]+\frac{2}{g}\left[h_1\left(p_{fi}+\frac{3}{4}p_b\right)+h_2\left(p_s+\frac{1}{4}p_b\right)\right]+\frac{g}{2}$	
Six-Bolt Flush Four Wide / Two Wide Unstiffened	$Y=\frac{b_p}{2}\left[h_1\left(\frac{1}{p_{fi}}\right)+h_2\left(\frac{1}{s}\right)\right]+\frac{2}{g}\left[h_1\left(p_{fi}+\frac{3}{4}p_b\right)+h_2\left(s+\frac{1}{4}p_b\right)\right]+\frac{g}{2}$	

Table 2-1b Summary of Yield Line Parameters for Extended End-Plate Configurations

Configuration	Yield Line Parameter	Notes
Four-bolt Extended Unstiffened	$Y=\frac{b_p}{2}\left[h_1\left(\frac{1}{p_{fo}}\right)+h_2\left(\frac{1}{p_{fi}}+\frac{1}{s}\right)-\frac{1}{2}\right]+\frac{2}{g}\left[h_2\left(p_{fi}+s\right)\right]$	
Four-bolt Extended Stiffened	$Y=\frac{b_p}{2}\left[h_1\left(\frac{1}{p_{fo}}+\frac{1}{2d_e}\right)+h_2\left(\frac{1}{p_{fi}}+\frac{1}{s}\right)\right]+\frac{2}{g}\left[h_1\left(p_{fo}+d_e\right)+h_2\left(p_{fi}+s\right)\right]$	Experimentally Validated
	$Y=\frac{b_p}{2}\left[h_1\left(\frac{1}{p_{fo}}\right)+h_2\left(\frac{1}{p_{fi}}+\frac{1}{s}\right)-\frac{1}{2}\right]+\frac{2}{g}\left[h_1\left(p_{fo}+d_e\right)+h_2\left(p_{fi}+s\right)\right]+\frac{g}{4}$	Alternate 1
	$Y=\left\{\frac{b_p}{2}\left[h_1\left(\frac{1}{p_{fo}}+\frac{1}{s}\right)+h_2\left(\frac{1}{p_{fi}}+\frac{1}{s}\right)\right]+\frac{2}{g}\left[h_1\left(p_{fo}+s\right)+h_2\left(p_{fi}+s\right)\right]\right\}$	Alternate 2
MRE 1/2 Unstiffened	$Y=\frac{b_p}{2}\left[h_1\left(\frac{1}{p_{fo}}\right)+h_2\left(\frac{1}{p_{fi}}\right)+h_3\left(\frac{1}{s}\right)-\frac{1}{2}\right]+\frac{2}{g}\left[h_2\left(p_{fi}+\frac{3p_b}{4}\right)+h_3\left(\frac{p_b}{4}+s\right)\right]+\frac{g}{2}$	
MRE 1/3 Unstiffened	$Y=\frac{b_p}{2}\left[h_1\left(\frac{1}{p_{fo}}\right)+h_2\left(\frac{1}{p_{fi}}\right)+h_4\left(\frac{1}{s}\right)-\frac{1}{2}\right]+\frac{2}{g}\left[h_2\left(p_{fi}+\frac{3p_b}{2}\right)+h_4\left(\frac{p_b}{2}+s\right)\right]+\frac{g}{2}$	
MRE 1/3 Stiffened	$Y=\frac{b_p}{2}\left[h_1\left(\frac{1}{p_{fo}}+\frac{1}{2d_e}\right)+h_2\left(\frac{1}{p_{fi}}\right)+h_4\left(\frac{1}{s}\right)\right]+\dots$ $\frac{2}{g}\left[h_1\left(p_{fo}+d_e\right)+h_2\left(p_{fi}+\frac{3}{2}p_b\right)+h_4\left(\frac{1}{2}p_b+s\right)\right]+\frac{g}{2}$	Experimentally Validated
	$Y=\left\{\begin{array}{l}\frac{b_p}{2}\left[h_1\left(\frac{1}{p_{fo}}\right)+h_2\left(\frac{1}{p_{fi}}\right)+h_4\left(\frac{1}{s}\right)-\frac{1}{2}\right]+.. \\ \frac{2}{g}\left[h_1\left(p_{fo}+d_e\right)+h_2\left(p_{fi}+\frac{3}{2}p_b\right)+h_4\left(\frac{1}{2}p_b+s\right)\right]+\frac{3g}{4}\end{array}\right\}$	Alternate
Eight-Bolt Extended Four Wide Unstiffened	$Y=\frac{b_p}{2}\left[h_1\left(\frac{1}{p_{fo}}\right)+h_2\left(\frac{1}{p_{fi}}+\frac{1}{s}\right)-\frac{1}{2}\right]+\frac{2}{g}\left[h_2\left(p_{fi}+s\right)\right]$	
Eight-Bolt Extended Stiffened	$Y=\frac{b_p}{2}\left[h_1\left(\frac{1}{2d_e}\right)+h_2\left(\frac{1}{p_{fo}}\right)+h_3\left(\frac{1}{p_{fi}}\right)+h_4\left(\frac{1}{s}\right)\right]+\dots$ $\frac{2}{g}\left[h_1\left(\frac{3p_b}{4}+d_e\right)+h_2\left(\frac{p_b}{4}+p_{fo}\right)+h_3\left(\frac{3p_b}{4}+p_{fi}\right)+h_4\left(\frac{p_b}{4}+s\right)\right]+g$	Experimentally Validated
	$Y=\frac{b_p}{2}\left[h_2\left(\frac{1}{p_{fo}}\right)+h_3\left(\frac{1}{p_{fi}}\right)+h_4\left(\frac{1}{s}\right)-\frac{1}{2}\right]+\dots$ $\frac{2}{g}\left[h_1\left(\frac{3p_b}{4}+d_e\right)+h_2\left(\frac{p_b}{4}+p_{fo}\right)+h_3\left(\frac{3p_b}{4}+p_{fi}\right)+h_4\left(\frac{p_b}{4}+s\right)\right]+\frac{5g}{4}$	Alternate
Twelve-Bolt MRE 1/3 Unstiffened	$Y=\frac{b_p}{2}\left[h_1\left(\frac{1}{p_{fo}}\right)+h_2\left(\frac{1}{p_{fi}}\right)+h_4\left(\frac{1}{s}\right)-\frac{1}{2}\right]+\frac{2}{g}\left[h_2\left(p_{fi}+\frac{3p_b}{2}\right)+h_4\left(\frac{p_b}{2}+s\right)\right]+\frac{g}{2}$	
Twelve-Bolt Extended Stiffened	$Y=\frac{b_p}{2}\left[h_2\left(\frac{1}{p_{fo}}\right)+h_3\left(\frac{1}{p_{fi}}\right)+h_4\left(\frac{1}{s}\right)-\frac{1}{2}\right]+\dots$ $\frac{2}{g}\left[h_1\left(\frac{3p_b}{4}+d_e\right)+h_2\left(\frac{p_b}{4}+p_{fo}\right)+h_3\left(\frac{3p_b}{4}+p_{fi}\right)+h_4\left(\frac{p_b}{4}+s\right)\right]+\frac{5g}{4}$	

Table 2-2 References for the Original Work on Each End-Plate Configuration

Configuration	References
Two-Bolt Flush Unstiffened	Boorse and Murray 1999, Jenner et al 1985, Kline et al 1995, Kukreti et al 1987, Srouji et al. 1983, Thompson and Murray 1975
Four-Bolt Flush Unstiffened	Italiano and Murray 2001, Jenner et al 1985, Kline et al 1995, Srouji et al. 1983, Sumner et al. 1995
Four-Bolt Flush Stiffened Between the Bolts	Hendrick et al 1984
Four-Bolt Flush Stiffened Below the Bolts	Hendrick et al 1984
Six-Bolt Flush Four Wide / Two Wide Unstiffened	Jain et al. 2015
Four-bolt Extended Unstiffened	Abel and Murray 1994, Blumenbaum and Murray 2004, Blumenbaum and Murray 2003, Borgsmiller et al. 1995, Curtis and Murray 1989, Eatherton et al. 2013, Eatherton et al. 2017, Jenner et al 1985, Kline et al 1995, Meng 1996, Murray 1989, Ryan and Murray 1999, Sumner and Murray 2002, Young and Murray 1997
Four-bolt Extended Stiffened	Blumenbaum and Murray 2004, Kline et al 1995, Meng 1996, Morrison et al 1985, Ryan and Murray 1999, Thompson and Murray 1975
MRE 1/2 Unstiffened	Abel and Murray 1992, Blumenbaum and Murray 2004, Borgsmiller et al. 1995, Jenner et al 1985, Sumner and Murray 2001a, Sumner et al. 1995
MRE 1/3 Unstiffened	Blumenbaum and Murray 2004, Borgsmiller et al. 1995, Kline et al 1995, Morrison et al 1986, Rodkey and Murray 1993b, Ryan and Murray 1999, Structural Engineers Inc 1984, Sumner et al. 1995
MRE 1/3 Stiffened	Blumenbaum and Murray 2004, Structural Engineers Inc 1984
Eight-Bolt Extended Four Wide Unstiffened	Meng 1996, Murray and Sumner 1999, Sumner et al 2000a, Sumner and Murray 2001b
Eight-Bolt Extended Stiffened	Curtis and Murray 1989, Eatherton et al. 2013, Jain et al. 2015, Ghassemieh et al 1983, Kukreti et al 1990, Seek and Murray 2008, Sumner and Murray 2002
Twelve-Bolt MRE 1/3 Unstiffened	Jain et al. 2015
Twelve-Bolt Extended Stiffened	Szabo et al. 2017

2.2 Two-Bolt Flush Unstiffened End-Plate

The yield line pattern is shown in Figure 2-1. The rotation of each facet (facets are labeled in Figure 2-1) is given in Table 2-3 and the internal work associated with rotation along each yield line is given in Table 2-4. The yield lines are identified by the adjacent facet numbers (e.g., yield line 1/2 separates facets 1 and 2). Variables associated with the geometry of the connection are shown in Figure 2-1. Variables associated with the virtual rotations, displacement, and end-plate moment strength per unit length are described in Chapter 1.

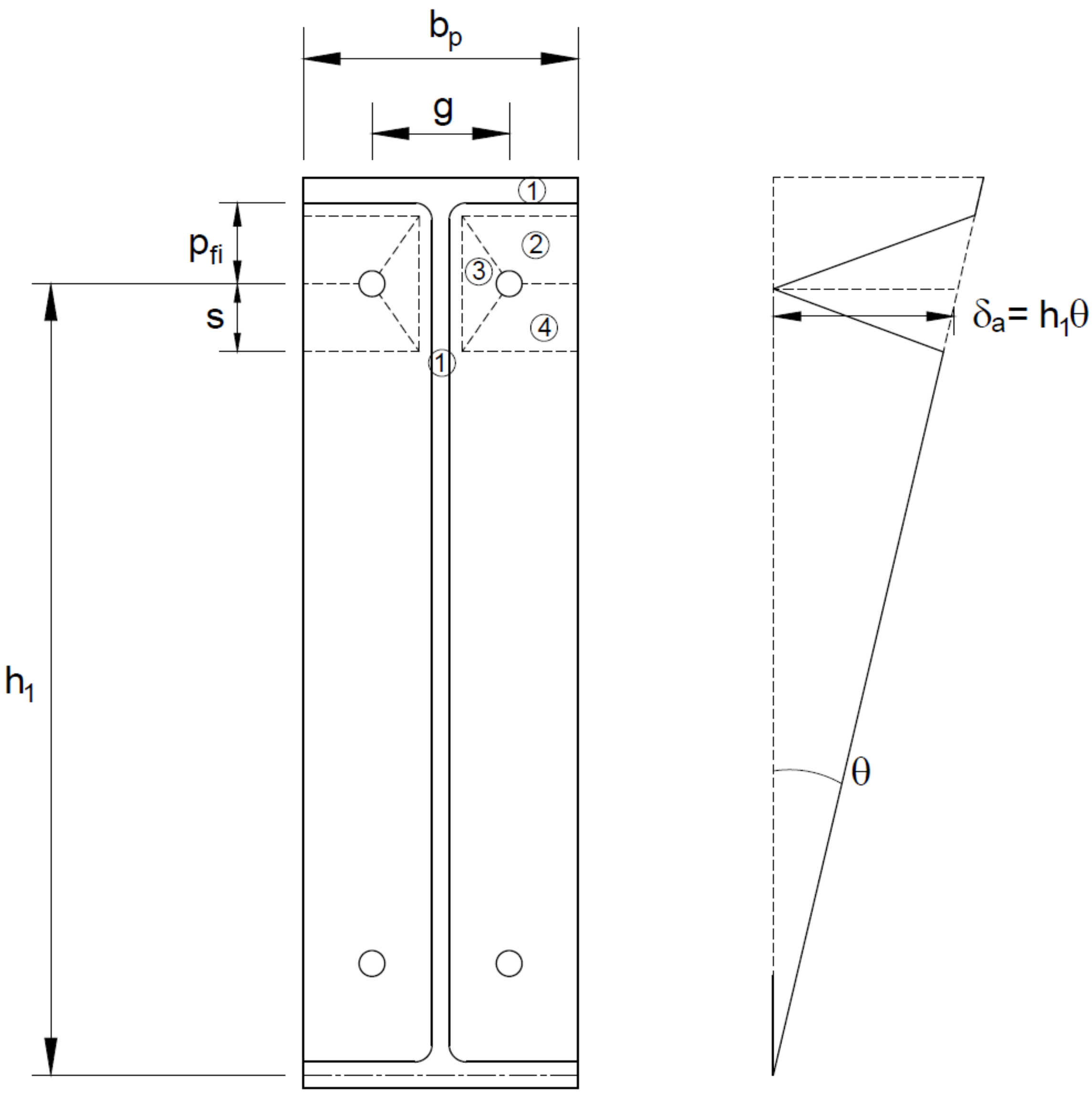

Figure 2-1 Yield Line Pattern for the Two Bolt Flush Unstiffened End Plate

Table 2-3 Rotation for Each Facet in the Two Bolt Flush Unstiffened End Plate

Facet	θ_x	θ_y
1	θ	0
2	$(\delta_a + p_{fi}\theta) / p_{fi}$	0
3	θ	$2\delta_a / g$
4	$-(\delta_a - s\theta)/s$	0

Table 2-4 Internal Work Associated with Each Yield Line in the Two Bolt Flush Unstiffened End Plate

Yield Line	Internal Work	Simplified Internal Work	Number of Lines
1/2	$m_p\left(\frac{b_p}{2}\right)\left(\frac{\delta_a + p_{fi}\theta}{p_{fi}} - \theta\right)$	$m_p\left(\frac{b_p}{2}\right)\left(\frac{\delta_a}{p_{fi}}\right)$	2
2/3	$m_p\left[\left(\frac{g}{2}\right)\left(\frac{\delta_a + p_{fi}\theta}{p_{fi}} - \theta\right) + p_{fi}\left(\frac{2\delta_a}{g}\right)\right]$	$m_p\left[\left(\frac{g}{2}\right)\frac{\delta_a}{p_{fi}} + \left(\frac{2}{g}\right)\delta_a p_{fi}\right]$	2
3/4	$m_p\left[\left(\frac{g}{2}\right)\left(\theta + \frac{\delta_a - s\theta}{s}\right) + s\left(\frac{2\delta_a}{g}\right)\right]$	$m_p\left[\left(\frac{g}{2}\right)\frac{\delta_a}{s} + \left(\frac{2}{g}\right)\delta_a s\right]$	2
2/4	$m_p\left[\left(\frac{b_p - g}{2}\right)\left(\frac{\delta_a + p_{fi}\theta}{p_{fi}} + \frac{\delta_a - s\theta}{s}\right)\right]$	$m_p\left(\frac{b_p - g}{2}\right)\delta_a\left(\frac{1}{p_{fi}} + \frac{1}{s}\right)$	2
1/3	$m_p\left[\left(p_{fi} + s\right)\left(\frac{2\delta_a}{g}\right)\right]$	$m_p\left(\frac{2}{g}\right)\delta_a\left(p_{fi} + s\right)$	2
1/4	$m_p\left[\left(\frac{b_p}{2}\right)\left(\theta + \frac{\delta_a - s\theta}{s}\right)\right]$	$m_p\left(\frac{b_p}{2}\right)\left(\frac{\delta_a}{s}\right)$	2

Summing up the internal work given in Table 2-4 and substituting $\delta_a = h_1 \theta$ results in the following equation for internal work:

$$W_I = 4m_p\theta\left\{\frac{b_p}{2}\left[h_1\left(\frac{1}{p_{fi}}+\frac{1}{s}\right)\right]+\frac{2}{g}\left[h_1\left(p_{fi}+s\right)\right]\right\} \tag{2-1}$$

The external work, W_E, is given by Eq. (2-2). Setting the internal work and external work equal results in Eq. (2-3).

$$W_E = M_{pl}\theta \tag{2-2}$$

$$M_{pl} = 4m_p\left\{\frac{b_p}{2}\left[h_1\left(\frac{1}{p_{fi}}+\frac{1}{s}\right)\right]+\frac{2}{g}\left[h_1\left(p_{fi}+s\right)\right]\right\} \tag{2-3}$$

This equation is further simplified into the form given in Eq. (2-4) by substituting the moment capacity per unit length, m_p, from Chapter 1, and defining the yield line parameter, Y, as given in Eq. (2-5).

$$M_{pl} = F_{yp}t_p{}^2Y \tag{2-4}$$

$$Y = \frac{b_p}{2}\left[h_1\left(\frac{1}{p_{fi}}+\frac{1}{s}\right)\right]+\frac{2}{g}\left[h_1\left(p_{fi}+s\right)\right] \tag{2-5}$$

Note: Use $p_{fi}=s$ if $p_{fi} > s$

To obtain an equation for the dimension s, the equation for moment strength, M_{pl}, is minimized. The derivative of Eq. (2-4), taken with respect to the variable s, is set equal to zero and solved for the variable s. The result is Eq. (2-6).

$$s = \frac{1}{2}\sqrt{b_p g} \tag{2-6}$$

2.3 Four-Bolt Unstiffened Flush End-Plate

The yield line pattern is shown in Figure 2-2. The rotation of each facet (facets are labeled in Figure 2-2) is given in Table 2-5 and the internal work associated with rotation along each yield line is given in Table 2-6. The yield lines are identified by the adjacent facet numbers (e.g., yield line 1/2 separates facets 1 and 2). Variables associated with the geometry of the connection are shown in Figure 2-2. Variables associated with the virtual rotations, displacement, and end-plate moment strength per unit length are described in Chapter 1. It is also noted that hatched areas represent facets that are not rotating.

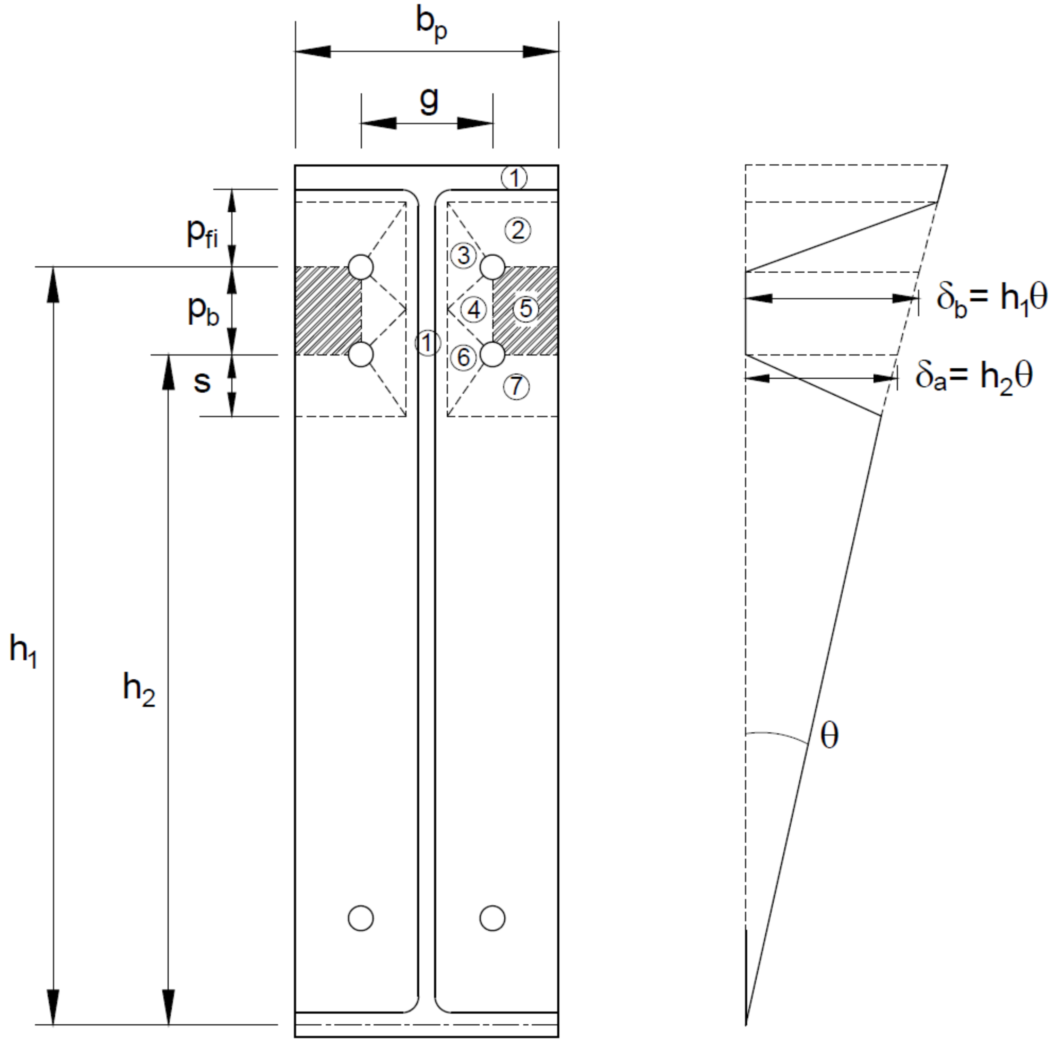

Figure 2-2 Yield Line Pattern for the Four-Bolt Unstiffened Flush End-Plate

Table 2-5 Rotation for Each Facet in the Four-Bolt Unstiffened Flush End-Plate

Facet	θ_x	θ_y
1	θ	0
2	$(\delta_b + p_{fi}\theta)/p_{fi}$	0
3	θ	$2\delta_b/g$
4	0	$(\delta_b+\delta_a)/g$
5	0	0
6	θ	$2\delta_a/g$
7	$-(\delta_a - s\theta)/s$	0

Table 2-6 Internal Work Associated with Each Yield Line in the Four-Bolt Unstiffened Flush End-Plate

Yield Line	Internal Work	Simplified Internal Work	Number of Lines
1/2	$m_p\left(\frac{b_p}{2}\right)\left(\frac{\delta_b+p_{fi}\theta}{p_{fi}}-\theta\right)$	$m_p\left(\frac{b_p}{2}\right)\left(\frac{\delta_b}{p_{fi}}\right)$	2
2/3	$m_p\left[\left(\frac{g}{2}\right)\left(\frac{\delta_b+p_{fi}\theta}{p_{fi}}-\theta\right)+p_{fi}\left(\frac{2\delta_b}{g}\right)\right]$	$m_p\left[\left(\frac{g}{2}\right)\frac{\delta_b}{p_{fi}}+\left(\frac{2}{g}\right)\delta_b p_{fi}\right]$	2
3/4	$m_p\left[\left(\frac{g}{2}\right)\theta+\frac{p_b}{2}\left(\frac{2\delta_b}{g}-\frac{\delta_b+\delta_a}{g}\right)\right]$	$m_p\left\{\left(\frac{g}{2}\right)\theta+\left(\frac{2}{g}\right)\left[p_b\left(\frac{\delta_b}{4}-\frac{\delta_a}{4}\right)\right]\right\}$	2
4/5	$m_p\left[p_b\left(\frac{\delta_b+\delta_a}{g}\right)\right]$	$m_p\left(\frac{2}{g}\right)\left[p_b\left(\frac{\delta_b+\delta_a}{2}\right)\right]$	2
4/6	$m_p\left[\left(\frac{g}{2}\right)\theta+\frac{p_b}{2}\left(\frac{\delta_b+\delta_a}{g}-\frac{2\delta_a}{g}\right)\right]$	$m_p\left\{\left(\frac{g}{2}\right)\theta+\left(\frac{2}{g}\right)\left[p_b\left(\frac{\delta_b}{4}-\frac{\delta_a}{4}\right)\right]\right\}$	2
6/7	$m_p\left[\left(\frac{g}{2}\right)\left(\theta+\frac{\delta_a-s\theta}{s}\right)+s\left(\frac{2\delta_a}{g}\right)\right]$	$m_p\left[\frac{g}{2}\left(\frac{\delta_a}{s}\right)+\frac{2}{g}(s\delta_a)\right]$	2
7/1	$m_p\left[\frac{b_p}{2}\left(\theta+\frac{\delta_a-s\theta}{s}\right)\right]$	$m_p\left[\frac{b_p}{2}\left(\frac{\delta_a}{s}\right)\right]$	2
6/1	$m_p\left[\left(s+\frac{p_b}{2}\right)\left(\frac{2\delta_a}{g}\right)\right]$	$m_p\left[\frac{2}{g}\left(\delta_a s+\frac{\delta_a p_b}{2}\right)\right]$	2
3/1	$m_p\left[\left(p_f+\frac{p_b}{2}\right)\left(\frac{2\delta_b}{g}\right)\right]$	$m_p\left[\frac{2}{g}\left(\delta_b p_f+\frac{\delta_b p_b}{2}\right)\right]$	2
2/5	$m_p\left[\left(\frac{b_p-g}{2}\right)\left(\frac{\delta_b+p_f\theta}{p_f}\right)\right]$	$m_p\left[\frac{b_p}{2}\left(\frac{\delta_b}{p_f}+\theta\right)-\frac{g}{2}\left(\frac{\delta_b}{p_f}+\theta\right)\right]$	2
5/7	$m_p\left[\left(\frac{b_p-g}{2}\right)\left(\frac{\delta_a-s\theta}{s}\right)\right]$	$m_p\left[\frac{b_p}{2}\left(\frac{\delta_a}{s}-\theta\right)-\frac{g}{2}\left(\frac{\delta_a}{s}-\theta\right)\right]$	2

Summing up the internal work given in Table 2-6 and substituting $\delta_a = h_2\,\theta$ and $\delta_b = h_1\,\theta$ results in the following equation for internal work:

$$W_I = 4m_p\theta\left\{\frac{b_p}{2}\left[h_1\left(\frac{1}{p_{fi}}\right)+h_2\left(\frac{1}{s}\right)\right]+\frac{2}{g}\left[h_1\left(p_{fi}+\frac{3}{4}p_b\right)+h_2\left(s+\frac{1}{4}p_b\right)\right]+\frac{g}{2}\right\} \tag{2-7}$$

The external work, W_E, is given by Eq. (2-8). Setting the internal work and external work equal results in Eq. (2-9).

$$W_E = M_{pl}\theta \tag{2-8}$$

$$M_{pl} = 4m_p\left\{\frac{b_p}{2}\left[h_1\left(\frac{1}{p_{fi}}\right)+h_2\left(\frac{1}{s}\right)\right]+\frac{2}{g}\left[h_1\left(p_{fi}+\frac{3}{4}p_b\right)+h_2\left(s+\frac{1}{4}p_b\right)\right]+\frac{g}{2}\right\} \tag{2-9}$$

This equation is further simplified into the form given in Eq. (2-10) by substituting the moment capacity per unit length, m_p, from Chapter 1, and defining the yield line parameter, Y, as given in Eq. (2-11).

$$M_{pl} = F_{yp}t_p^{\,2}Y \tag{2-10}$$

$$Y = \frac{b_p}{2}\left[h_1\left(\frac{1}{p_{fi}}\right)+h_2\left(\frac{1}{s}\right)\right]+\frac{2}{g}\left[h_1\left(p_{fi}+\frac{3}{4}p_b\right)+h_2\left(s+\frac{1}{4}p_b\right)\right]+\frac{g}{2} \tag{2-11}$$

Note: Use $p_{fi}=s$ if $p_{fi} > s$

To obtain an equation for the dimension s, the equation for moment strength, M_{pl}, is minimized. The derivative of Eq. (2-10), taken with respect to the variable s, is set equal to zero and solved for the variable s. The result is Eq. (2-12).

$$s = \frac{1}{2}\sqrt{b_p g} \tag{2-12}$$

2.4 Four-Bolt Flush End-Plate Stiffened Between the Bolt Lines

The yield line pattern is shown in Figure 2-3. The rotation of each facet (facets are labeled in Figure 2-3) is given in Table 2-7 and the internal work associated with rotation along each yield line is given in Table 2-8. The yield lines are identified by the adjacent facet numbers (e.g., yield line 1/2 separates facets 1 and 2). Variables associated with the geometry of the connection are shown in Figure 2-3. Variables associated with the virtual rotations, displacement, and end-plate moment strength per unit length are described in Chapter 1.

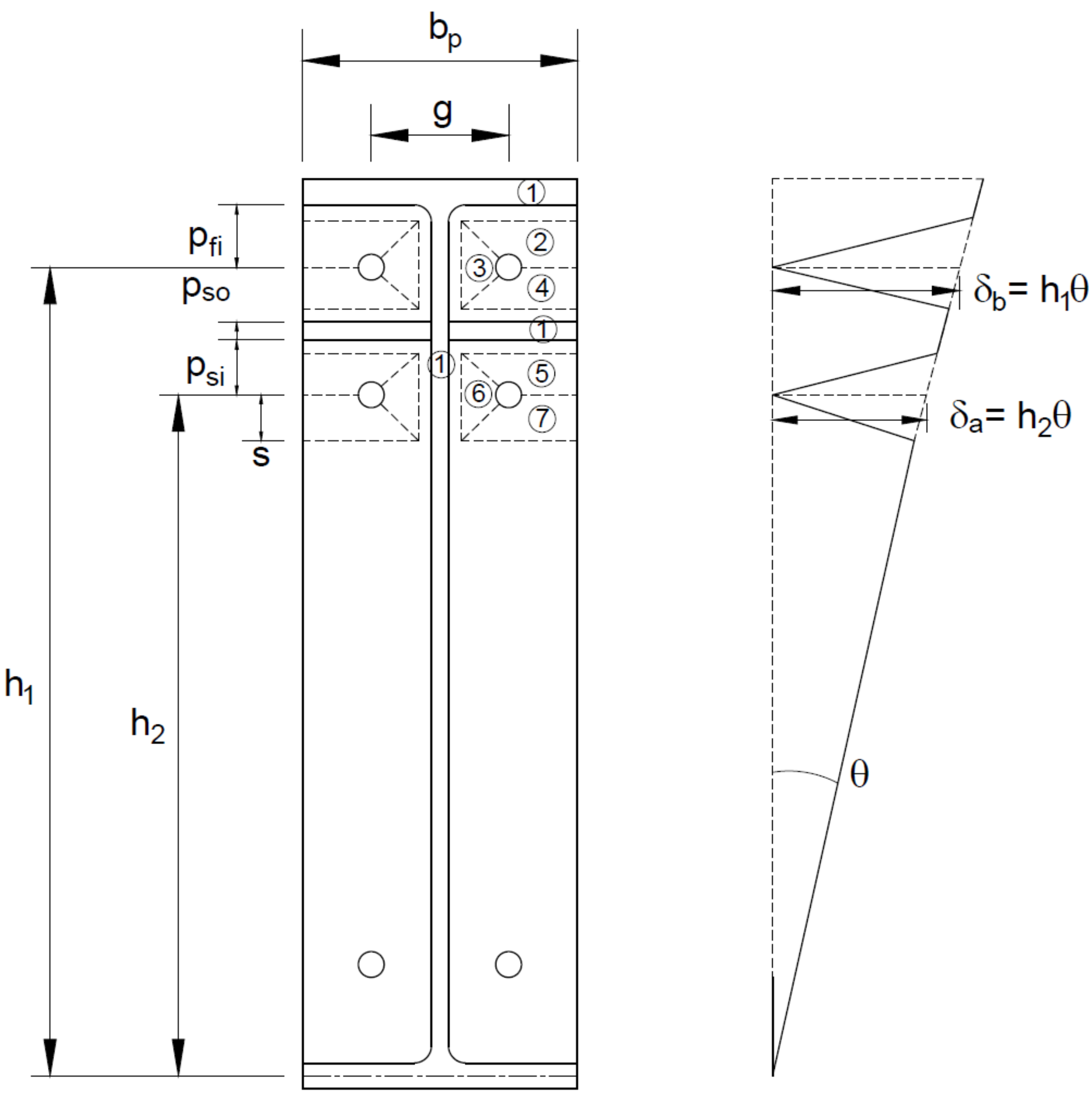

Figure 2-3 Yield Line Pattern for the Four-Bolt Flush End-Plate Stiffened Between the Bolt Lines

Table 2-7 Rotation for Each Facet in the Four-Bolt Flush End-Plate Stiffened Between the Bolt Lines

Facet	θ_x	θ_y
1	θ	0
2	$(\delta_b + p_{fi}\theta) / p_{fi}$	0
3	θ	$2\delta_b / g$
4	$-(\delta_b - p_{so}\theta) / p_{so}$	0
5	$(\delta_a + p_{si}\theta) / p_{si}$	0
6	θ	$2\delta_a / g$
7	$-(\delta_a - s\theta) / s$	0

Table 2-8 Internal Work Associated with Each Yield Line in the Four-Bolt Flush End-Plate Stiffened Between the Bolt Lines

Yield Line	Internal Work	Simplified Internal Work	Number of Lines
1/2	$m_p\left(\frac{b_p}{2}\right)\left(\frac{\delta_b + p_{fi}\theta}{p_{fi}} - \theta\right)$	$m_p\left(\frac{b_p}{2}\right)\left(\frac{\delta_b}{p_{fi}}\right)$	2
2/3	$m_p\left[\frac{g}{2}\left(\frac{\delta_b + p_{fi}\theta}{p_{fi}} - \theta\right) + p_{fi}\left(\frac{2\delta_b}{g}\right)\right]$	$m_p\left[\frac{g}{2}\left(\frac{\delta_b}{p_{fi}}\right) + \frac{2}{g}\left(p_{fi}\delta_b\right)\right]$	2
3/4	$m_p\left[\frac{g}{2}\left(\frac{\delta_b - p_{so}\theta}{p_{so}} + \theta\right) + p_{so}\left(\frac{2\delta_b}{g}\right)\right]$	$m_p\left[\frac{g}{2}\left(\frac{\delta_b}{p_{so}}\right) + \frac{2}{g}\left(p_{so}\delta_b\right)\right]$	2
2/4	$m_p\left[\frac{b_p - g}{2}\left(\frac{\delta_b + p_{fi}\theta}{p_{fi}} + \frac{\delta_b - p_{so}\theta}{p_{so}}\right)\right]$	$m_p\left[\frac{b_p - g}{2}\left(\frac{\delta_b}{p_{fi}} + \frac{\delta_b}{p_{so}}\right)\right]$	2
1/3	$m_p\left[\left(p_{fi} + p_{so}\right)\left(\frac{2\delta_b}{g}\right)\right]$	$m_p\left[\frac{2}{g}\left(\delta_b p_{fi} + \delta_b p_{so}\right)\right]$	2
1/4	$m_p\left[\frac{b_p}{2}\left(\frac{\delta_b - p_{so}\theta}{p_{so}} + \theta\right)\right]$	$m_p\left[\frac{b_p}{2}\left(\frac{\delta_b}{p_{so}}\right)\right]$	2
1/5	$m_p\left[\frac{b_p}{2}\left(\frac{\delta_a + p_{si}\theta}{p_{si}} - \theta\right)\right]$	$m_p\left[\frac{b_p}{2}\left(\frac{\delta_a}{p_{si}}\right)\right]$	2
5/6	$m_p\left[\frac{g}{2}\left(\frac{\delta_a + p_{si}\theta}{p_{si}} - \theta\right) + p_{si}\left(\frac{2\delta_a}{g}\right)\right]$	$m_p\left[\frac{g}{2}\left(\frac{\delta_a}{p_{si}}\right) + \frac{2}{g}\left(p_{si}\delta_a\right)\right]$	2
6/7	$m_p\left[\frac{g}{2}\left(\frac{\delta_a - s\theta}{s} + \theta\right) + s\left(\frac{2\delta_a}{g}\right)\right]$	$m_p\left[\frac{g}{2}\left(\frac{\delta_a}{s}\right) + \frac{2}{g}\left(s\delta_a\right)\right]$	2
1/6	$m_p\left[\left(p_{si} + s\right)\left(\frac{2\delta_a}{g}\right)\right]$	$m_p\left[\frac{2}{g}\left(\delta_a p_{si} + \delta_a s\right)\right]$	2
5/7	$m_p\left[\frac{b_p - g}{2}\left(\frac{\delta_a + p_{si}\theta}{p_{si}} + \frac{\delta_a - s\theta}{s}\right)\right]$	$m_p\left[\frac{b_p - g}{2}\left(\frac{\delta_a}{p_{si}} + \frac{\delta_a}{s}\right)\right]$	2
1/7	$m_p\left[\frac{b_p}{2}\left(\frac{\delta_a - s\theta}{s} + \theta\right)\right]$	$m_p\left[\frac{b_p}{2}\left(\frac{\delta_a}{s}\right)\right]$	2

Summing up the internal work given in Table 2-8 and substituting $\delta_a = h_2\,\theta$ and $\delta_b = h_1\,\theta$ results in the following equation for internal work:

$$W_I = 4m_p\theta\left\{\frac{b_p}{2}\left[h_1\left(\frac{1}{p_{fi}}+\frac{1}{p_{so}}\right)+h_2\left(\frac{1}{p_{si}}+\frac{1}{s}\right)\right]+\frac{2}{g}\left[h_1\left(p_{fi}+p_{so}\right)+h_2\left(p_{si}+s\right)\right]\right\} \qquad (2\text{-}13)$$

The external work, W_E, is given by Eq. (2-14). Setting the internal work and external work equal results in Eq. (2-15).

$$W_E = M_{pl}\theta \qquad (2\text{-}14)$$

$$M_{pl} = 4m_p\left\{\frac{b_p}{2}\left[h_1\left(\frac{1}{p_{fi}}+\frac{1}{p_{so}}\right)+h_2\left(\frac{1}{p_{si}}+\frac{1}{s}\right)\right]+\frac{2}{g}\left[h_1\left(p_{fi}+p_{so}\right)+h_2\left(p_{si}+s\right)\right]\right\} \qquad (2\text{-}15)$$

This equation is further simplified into the form given in Eq. (2-16) by substituting the moment capacity per unit length, m_p, from Chapter 1, and defining the yield line parameter, Y, as given in Eq. (2-17).

$$M_{pl} = F_{yp}t_p{}^2Y \qquad (2\text{-}16)$$

$$Y = \frac{b_p}{2}\left[h_1\left(\frac{1}{p_{fi}}+\frac{1}{p_{so}}\right)+h_2\left(\frac{1}{p_{si}}+\frac{1}{s}\right)\right]+\frac{2}{g}\left[h_1\left(p_{fi}+p_{so}\right)+h_2\left(p_{si}+s\right)\right] \qquad (2\text{-}17)$$

Note: Use $p_{fi}=s$ if $p_{fi} > s$ Use $p_{so}=s$ if $p_{so} > s$ Use $p_{si}=s$ if $p_{si} > s$

To obtain an equation for the dimension s, the equation for moment strength, M_{pl}, is minimized. The derivative of Eq. (2-16), taken with respect to the variable s, is set equal to zero and solved for the variable s. The result is Eq. (2-18).

$$s = \frac{1}{2}\sqrt{b_p g} \qquad (2\text{-}18)$$

2.5 Four-Bolt Flush End-Plate Stiffened Below the Bolt Lines

The yield line pattern is shown in Figure 2-4. The rotation of each facet (facets are labeled in Figure 2-4) is given in Table 2-9 and the internal work associated with rotation along each yield line is given in Table 2-10. The yield lines are identified by the adjacent facet numbers (e.g., yield line 1/2 separates facets 1 and 2). Variables associated with the geometry of the connection are shown in Figure 2-4. Variables associated with the virtual rotations, displacement, and end-plate moment strength per unit length are described in Chapter 1. It is noted that hatched areas represent facets that are not rotating.

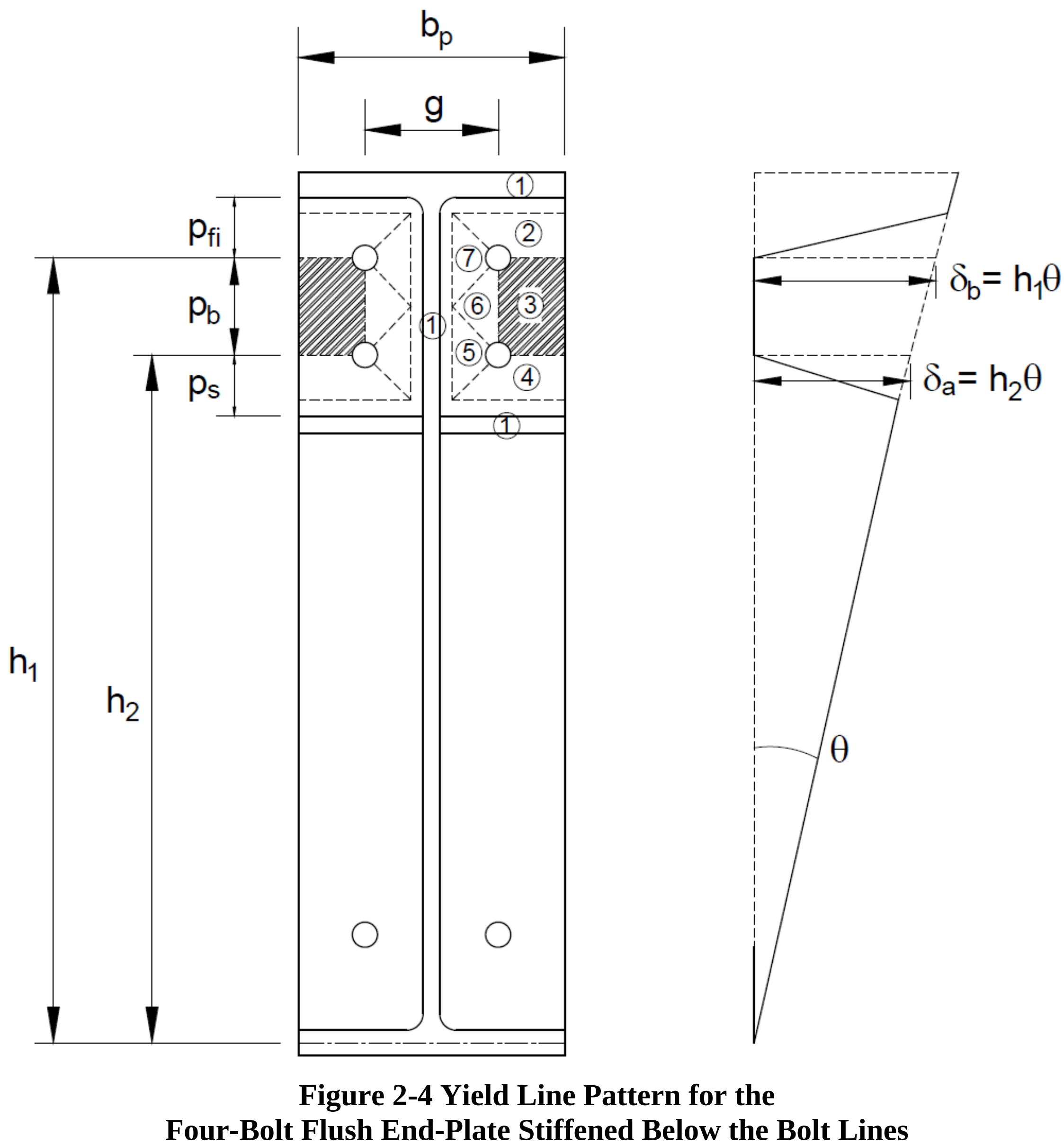

Figure 2-4 Yield Line Pattern for the Four-Bolt Flush End-Plate Stiffened Below the Bolt Lines

Table 2-9 Rotation for Each Facet in the Four-Bolt Flush End-Plate Stiffened Below the Bolt Lines

Facet	θ_x	θ_y
1	θ	0
2	$(\delta_b + p_{fi}\theta) / p_{fi}$	0
3	0	0
4	$-(\delta_a - p_s\theta) / s$	0
5	θ	$2\delta_a / g$
6	0	$(\delta_b + \delta_a) / g$
7	θ	$2\delta_b / g$

Table 2-10 Internal Work Associated with Each Yield Line in the Four-Bolt Flush End-Plate Stiffened Below the Bolt Lines

Yield Line	Internal Work	Simplified Internal Work	Number of Lines
1/2	$m_p\left[\frac{b_p}{2}\left(\frac{\delta_b + p_{fi}\theta}{p_{fi}} - \theta\right)\right]$	$m_p\left[\frac{b_p}{2}\left(\frac{\delta_b}{p_{fi}}\right)\right]$	2
2/7	$m_p\left[\frac{g}{2}\left(\frac{\delta_b + p_{fi}\theta}{p_{fi}} - \theta\right) + p_{fi}\left(\frac{2\delta_b}{g}\right)\right]$	$m_p\left[\frac{g}{2}\left(\frac{\delta_b}{p_{fi}}\right) + \frac{2}{g}\left(p_{fi}\delta_b\right)\right]$	2
1/7	$m_p\left[\left(p_{fi} + \frac{p_b}{2}\right)\left(\frac{2\delta_b}{g}\right)\right]$	$m_p\left[\frac{2}{g}\left(\delta_b p_{fi} + \frac{\delta_b p_b}{2}\right)\right]$	2
7/6	$m_p\left[\frac{g}{2}(\theta) + \frac{p_b}{2}\left(\frac{2\delta_b}{g} - \frac{\delta_b + \delta_a}{g}\right)\right]$	$m_p\left\{\frac{g}{2}(\theta) + \frac{2}{g}\left[\frac{p_b\left(\delta_b - \delta_a\right)}{4}\right]\right\}$	2
2/3	$m_p\left[\frac{b_p - g}{2}\left(\frac{\delta_b + p_{fi}\theta}{p_{fi}}\right)\right]$	$m_p\left[\frac{b_p}{2}\left(\frac{\delta_b}{p_{fi}} + \theta\right) - \frac{g}{2}\left(\frac{\delta_b}{p_{fi}} + \theta\right)\right]$	2
6/3	$m_p\left[p_b\left(\frac{\delta_b + \delta_a}{g}\right)\right]$	$m_p\left\{\frac{2}{g}\left[\frac{p_b\left(\delta_b + \delta_a\right)}{2}\right]\right\}$	2
6/5	$m_p\left[\frac{g}{2}(\theta) + \frac{p_b}{2}\left(\frac{\delta_b + \delta_a}{g} - \frac{2\delta_a}{g}\right)\right]$	$m_p\left\{\frac{g}{2}(\theta) + \frac{2}{g}\left[\frac{p_b\left(\delta_b - \delta_a\right)}{4}\right]\right\}$	2
1/5	$m_p\left[\left(p_s + \frac{p_b}{2}\right)\left(\frac{2\delta_a}{g}\right)\right]$	$m_p\left[\frac{2}{g}\left(\delta_a p_s + \frac{\delta_a p_b}{2}\right)\right]$	2
4/5	$m_p\left[\frac{g}{2}\left(\frac{\delta_a - p_s\theta}{p_s} + \theta\right) + p_s\left(\frac{2\delta_a}{g}\right)\right]$	$m_p\left[\frac{g}{2}\left(\frac{\delta_a}{p_s}\right) + \frac{2}{g}\left(p_s\delta_a\right)\right]$	2
3/4	$m_p\left[\frac{b_p - g}{2}\left(\frac{\delta_a - p_s\theta}{p_s}\right)\right]$	$m_p\left[\frac{b_p}{2}\left(\frac{\delta_a}{p_s} - \theta\right) - \frac{g}{2}\left(\frac{\delta_a}{p_s} - \theta\right)\right]$	2
4/1	$m_p\left[\frac{b_p}{2}\left(\frac{\delta_a - p_s\theta}{p_s} + \theta\right)\right]$	$m_p\left[\frac{b_p}{2}\left(\frac{\delta_a}{p_s}\right)\right]$	2

Summing up the internal work given in Table 2-10 and substituting $\delta_a = h_2\theta$ and $\delta_b = h_1\theta$ results in the following equation for internal work:

$$W_I = 4m_p\theta\left\{\frac{b_p}{2}\left[h_1\left(\frac{1}{p_{fi}}\right)+h_2\left(\frac{1}{p_s}\right)\right]+\frac{2}{g}\left[h_1\left(p_{fi}+\frac{3}{4}p_b\right)+h_2\left(p_s+\frac{1}{4}p_b\right)\right]+\frac{g}{2}\right\} \tag{2-19}$$

The external work, W_E, is given by Eq. (2-20). Setting the internal work and external work equal results in Eq. (2-21).

$$W_E = M_{pl}\theta \tag{2-20}$$

$$M_{pl} = 4m_p\left\{\frac{b_p}{2}\left[h_1\left(\frac{1}{p_{fi}}\right)+h_2\left(\frac{1}{p_s}\right)\right]+\frac{2}{g}\left[h_1\left(p_{fi}+\frac{3}{4}p_b\right)+h_2\left(p_s+\frac{1}{4}p_b\right)\right]+\frac{g}{2}\right\} \tag{2-21}$$

This equation is further simplified into the form given in Eq. (2-22) by substituting the moment capacity per unit length, m_p, from Chapter 1, and defining the yield line parameter, Y, as given in Eq. (2-23).

$$M_{pl} = F_{yp}t_p{}^2Y \tag{2-22}$$

$$Y = \frac{b_p}{2}\left[h_1\left(\frac{1}{p_{fi}}\right)+h_2\left(\frac{1}{p_s}\right)\right]+\frac{2}{g}\left[h_1\left(p_{fi}+\frac{3}{4}p_b\right)+h_2\left(p_s+\frac{1}{4}p_b\right)\right]+\frac{g}{2} \tag{2-23}$$

Note: Use $p_{fi}=s$ if $p_{fi} > s$ Use $p_s=s$ if $p_s > s$

2.6 Six-Bolt Flush End-Plate

The yield line pattern is shown in Figure 2-5. The rotation of each facet (facets are labeled in Figure 2-5) is given in Table 2-11 and the internal work associated with rotation along each yield line is given in Table 2-12. The yield lines are identified by the adjacent facet numbers (e.g., yield line 1/2 separates facets 1 and 2). Variables associated with the geometry of the connection are shown in Figure 2-5. Variables associated with the virtual rotations, displacement, and end-plate moment strength per unit length are described in Chapter 1.

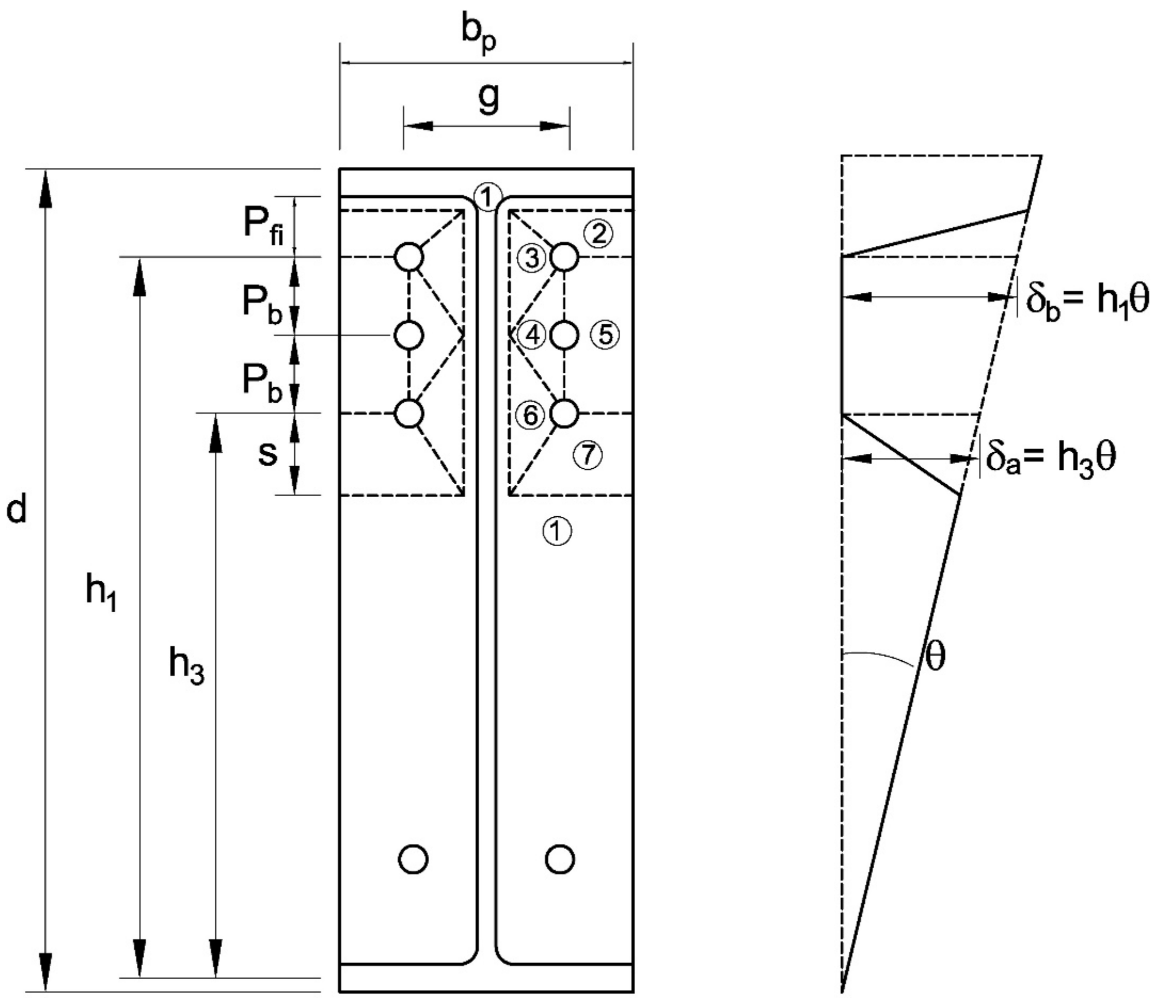

Figure 2-5 Yield Line Pattern for the Multiple Row Extended 1/3 Unstiffened End-Plate

Table 2-11 Rotation for Each Facet in the Multiple Row Extended 1/3 Unstiffened End-Plate

Facet	θ_x	θ_y
1	θ	0
2	$(\delta_b + p_{fi}\theta) / p_{fi}$	0
3	θ	$2\delta_b / g$
4	0	$(\delta_b + \delta_a) / g$
5	0	0
6	θ	$2\delta_a / g$
7	$-(\delta_a - s\theta) / s$	0

Table 2-12 Internal Work Associated with Each Yield Line in the Multiple Row Extended 1/3 Unstiffened End-Plate

Yield Line	Internal Work	Simplified Internal Work	Number of Lines
1/2	$m_p\left[\frac{b_p}{2}\left(\frac{\delta_b + p_{fi}\theta}{p_{fi}} - \theta\right)\right]$	$m_p\left[\frac{b_p}{2}\left(\frac{\delta_b}{p_{fi}}\right)\right]$	2
2/3	$m_p\left[\frac{g}{2}\left(\frac{\delta_b + p_{fi}\theta}{p_{fi}} - \theta\right) + p_{fi}\left(\frac{2\delta_b}{g}\right)\right]$	$m_p\left[\frac{g}{2}\left(\frac{\delta_b}{p_{fi}}\right) + \frac{2}{g}\left(p_{fi}\delta_b\right)\right]$	2
3/4	$m_p\left[\frac{g}{2}(\theta) + p_b\left(\frac{2\delta_b}{g} - \frac{\delta_b + \delta_a}{g}\right)\right]$	$m_p\left[\frac{g}{2}(\theta) + \frac{2}{g}\left(\frac{p_b\delta_b}{2} - \frac{p_b\delta_a}{2}\right)\right]$	2
4/6	$m_p\left[\frac{g}{2}(\theta) + p_b\left(\frac{\delta_b + \delta_a}{g} - \frac{2\delta_a}{g}\right)\right]$	$m_p\left[\frac{g}{2}(\theta) + \frac{2}{g}\left(\frac{p_b\delta_b}{2} - \frac{p_b\delta_a}{2}\right)\right]$	2
6/7	$m_p\left[\frac{g}{2}\left(\theta + \frac{\delta_a - s\theta}{s}\right) + s\left(\frac{2\delta_a}{g}\right)\right]$	$m_p\left[\frac{g}{2}\left(\frac{\delta_a}{s}\right) + \frac{2}{g}\left(s\delta_a\right)\right]$	2
1/3	$m_p\left[\left(p_{fi} + p_b\right)\left(\frac{2\delta_b}{g}\right)\right]$	$m_p\left[\frac{2}{g}\left(\delta_b p_{fi} + \delta_b p_b\right)\right]$	2
1/6	$m_p\left[\left(s + p_b\right)\left(\frac{2\delta_a}{g}\right)\right]$	$m_p\left[\frac{2}{g}\left(\delta_a s + \delta_a p_b\right)\right]$	2
2/5	$m_p\left[\left(\frac{b_p - g}{2}\right)\left(\frac{\delta_b + p_{fi}\theta}{p_{fi}}\right)\right]$	$m_p\left[\frac{b_p}{2}\left(\frac{\delta_b + p_{fi}\theta}{p_{fi}}\right) - \frac{g}{2}\left(\frac{\delta_b + p_{fi}\theta}{p_{fi}}\right)\right]$	2
4/5	$m_p\left[2p_b\left(\frac{\delta_b + \delta_a}{g}\right)\right]$	$m_p\left[\frac{2}{g}\left(p_b\delta_b + p_b\delta_a\right)\right]$	2
5/7	$m_p\left[\left(\frac{b_p - g}{2}\right)\left(\frac{\delta_a - s\theta}{s}\right)\right]$	$m_p\left[\frac{b_p}{2}\left(\frac{\delta_a - s\theta}{s}\right) - \frac{g}{2}\left(\frac{\delta_a - s\theta}{s}\right)\right]$	2
1/7	$m_p\left[\frac{b_p}{2}\left(\theta + \frac{\delta_a - s\theta}{s}\right)\right]$	$m_p\left[\frac{b_p}{2}\left(\frac{\delta_a}{s}\right)\right]$	2

Summing up the internal work given in Table 2-12 and substituting $\delta_a = h_3\theta$ and $\delta_b = h_1 \theta$, results in the following equation for internal work:

$$W_I = 4m_p\theta\left\{\frac{b_p}{2}\left[h_1\left(\frac{1}{p_{fi}}\right)+h_3\left(\frac{1}{s}\right)\right]+\frac{2}{g}\left[h_1\left(p_{fi}+\frac{3p_b}{2}\right)+h_3\left(\frac{p_b}{2}+s\right)\right]+\frac{g}{2}\right\} \qquad (2\text{-}24)$$

The external work, W_E, is given by Eq. (2-25). Setting the internal work and external work equal results in Eq. (2-26).

$$W_E = M_{pl}\theta \qquad (2\text{-}25)$$

$$M_{pl} = 4m_p\left\{\frac{b_p}{2}\left[h_1\left(\frac{1}{p_{fi}}\right)+h_3\left(\frac{1}{s}\right)\right]+\frac{2}{g}\left[h_1\left(p_{fi}+\frac{3p_b}{2}\right)+h_3\left(\frac{p_b}{2}+s\right)\right]+\frac{g}{2}\right\} \qquad (2\text{-}26)$$

This equation is further simplified into the form given in Eq. (2-27) by substituting the moment capacity per unit length, m_p, from Chapter 1, and defining the yield line parameter, Y, as given in Eq. (2-28).

$$M_{pl} = F_{yp}t_p{}^2Y \qquad (2\text{-}27)$$

$$Y = \frac{b_p}{2}\left[h_1\left(\frac{1}{p_{fi}}\right)+h_3\left(\frac{1}{s}\right)\right]+\frac{2}{g}\left[h_1\left(p_{fi}+\frac{3p_b}{2}\right)+h_3\left(\frac{p_b}{2}+s\right)\right]+\frac{g}{2} \qquad (2\text{-}28)$$

Note: Use $p_{fi}=s$ if $p_{fi} > s$

To obtain an equation for the dimension s, the equation for moment strength, M_{pl}, is minimized. The derivative of Eq. (2-28), taken with respect to the variable s, is set equal to zero and solved for the variable s. The result is Eq. (2-29).

$$s = \frac{1}{2}\sqrt{b_p g} \qquad (2\text{-}29)$$

2.7 Six-Bolt Flush Four Wide / Two Wide Unstiffened End-Plate

The yield line pattern is shown in Figure 2-6. The rotation of each facet (facets are labeled in Figure 2-6) is given in Table 2-13 and the internal work associated with rotation along each yield line is given in Table 2-14. The yield lines are identified by the adjacent facet numbers (e.g., yield line 1/2 separates facets 1 and 2). Variables associated with the geometry of the connection are shown in Figure 2-6. Variables associated with the virtual rotations, displacement, and end-plate moment strength per unit length are described in Chapter 1. It is noted that hatched areas represent facets that are not rotating.

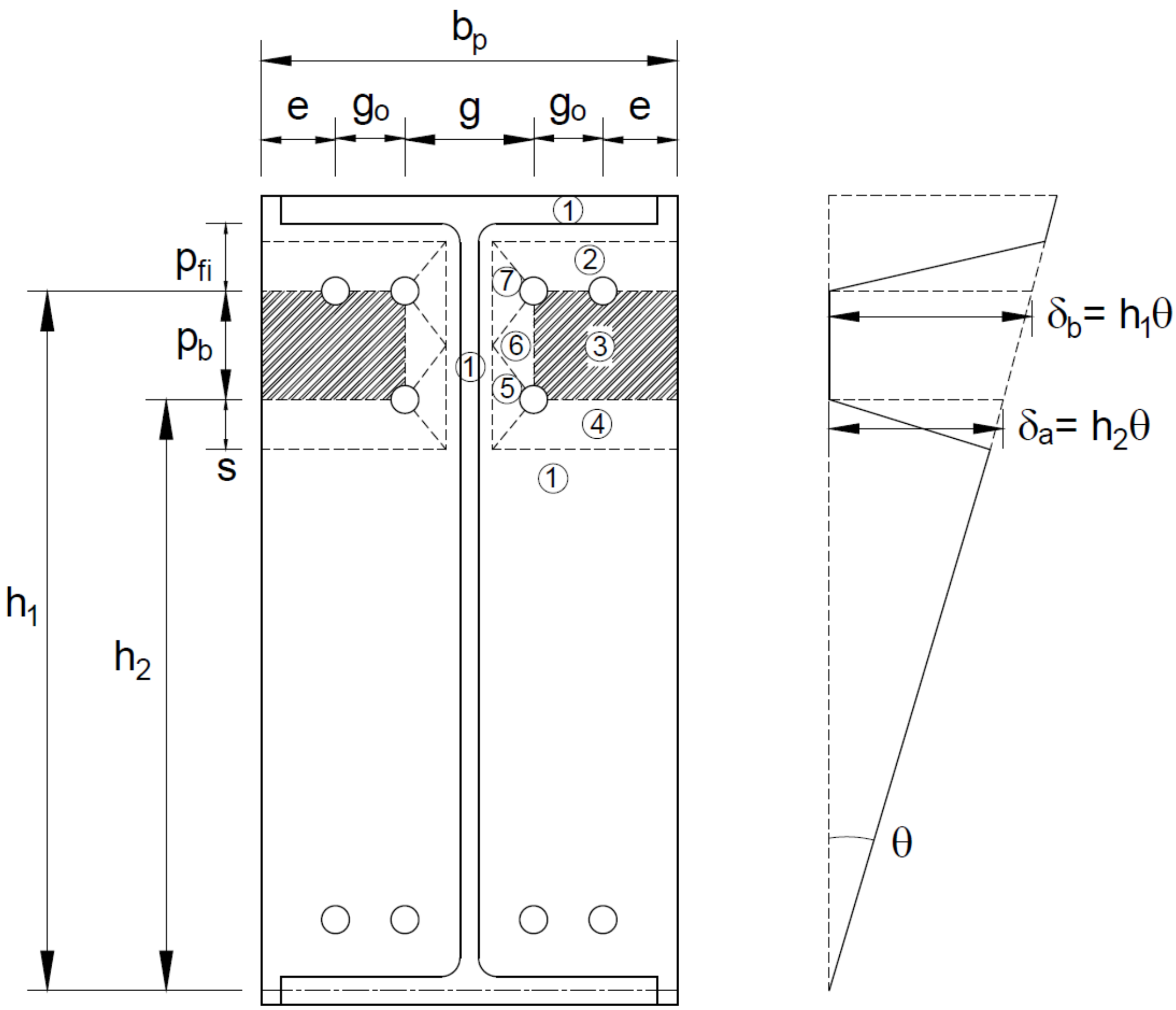

Figure 2-6 Yield Line Pattern for the
Six Bolt Flush Four Wide / Two Wide Unstiffened End-Plate

Table 2-13 Rotation for Each Facet in the Six Bolt Flush Four Wide / Two Wide Unstiffened End-Plate

Facet	θ_x	θ_y
1	θ	0
2	$(\delta_b + p_{fi}\theta)/p_{fi}$	0
3	0	0
4	$-(\delta_a - s\theta)/s$	0
5	θ	$2\delta_a / g$
6	0	$(\delta_b + \delta_a)/g$
7	θ	$2\delta_b / g$

Table 2-14 Internal Work Associated with Each Yield Line in the Six Bolt Flush Four Wide / Two Wide Unstiffened End-Plate

Yield Line	Internal Work	Simplified Internal Work	Number of Lines
1/2	$m_p\left[\frac{b_p}{2}\left(\frac{\delta_b + p_{fi}\theta}{p_{fi}} - \theta\right)\right]$	$m_p\left[\frac{b_p}{2}\left(\frac{\delta_b}{p_{fi}}\right)\right]$	2
2/7	$m_p\left[\frac{g}{2}\left(\frac{\delta_b + p_{fi}\theta}{p_{fi}} - \theta\right) + p_{fi}\left(\frac{2\delta_b}{g}\right)\right]$	$m_p\left[\frac{g}{2}\left(\frac{\delta_b}{p_{fi}}\right) + \frac{2}{g}\left(p_{fi}\delta_b\right)\right]$	2
1/7	$m_p\left[\left(p_{fi} + \frac{p_b}{2}\right)\left(\frac{2\delta_b}{g}\right)\right]$	$m_p\left[\frac{2}{g}\left(\delta_b p_{fi} + \frac{\delta_b p_b}{2}\right)\right]$	2
7/6	$m_p\left[\frac{g}{2}(\theta) + \frac{p_b}{2}\left(\frac{2\delta_b}{g} - \frac{\delta_b + \delta_a}{g}\right)\right]$	$m_p\left\{\frac{g}{2}(\theta) + \frac{2}{g}\left[\frac{p_b\left(\delta_b - \delta_a\right)}{4}\right]\right\}$	2
2/3	$m_p\left[\frac{b_p - g}{2}\left(\frac{\delta_b + p_{fi}\theta}{p_{fi}}\right)\right]$	$m_p\left[\frac{b_p}{2}\left(\frac{\delta_b}{p_{fi}} + \theta\right) - \frac{g}{2}\left(\frac{\delta_b}{p_{fi}} + \theta\right)\right]$	2
6/3	$m_p\left[p_b\left(\frac{\delta_b + \delta_a}{g}\right)\right]$	$m_p\left\{\frac{2}{g}\left[\frac{p_b\left(\delta_b + \delta_a\right)}{2}\right]\right\}$	2
6/5	$m_p\left[\frac{g}{2}(\theta) + \frac{p_b}{2}\left(\frac{\delta_b + \delta_a}{g} - \frac{2\delta_a}{g}\right)\right]$	$m_p\left\{\frac{g}{2}(\theta) + \frac{2}{g}\left[\frac{p_b\left(\delta_b - \delta_a\right)}{4}\right]\right\}$	2
1/5	$m_p\left[\left(s + \frac{p_b}{2}\right)\left(\frac{2\delta_a}{g}\right)\right]$	$m_p\left[\frac{2}{g}\left(\delta_a s + \frac{\delta_a p_b}{2}\right)\right]$	2
4/5	$m_p\left[\frac{g}{2}\left(\frac{\delta_a - s\theta}{s} + \theta\right) + s\left(\frac{2\delta_a}{g}\right)\right]$	$m_p\left[\frac{g}{2}\left(\frac{\delta_a}{s}\right) + \frac{2}{g}\left(s\delta_a\right)\right]$	2
3/4	$m_p\left[\frac{b_p - g}{2}\left(\frac{\delta_a - s\theta}{s}\right)\right]$	$m_p\left[\frac{b_p}{2}\left(\frac{\delta_a}{s} - \theta\right) - \frac{g}{2}\left(\frac{\delta_a}{s} - \theta\right)\right]$	2
4/1	$m_p\left[\frac{b_p}{2}\left(\frac{\delta_a - s\theta}{s} + \theta\right)\right]$	$m_p\left[\frac{b_p}{2}\left(\frac{\delta_a}{s}\right)\right]$	2

Summing up the internal work given in Table 2-14 and substituting $\delta_a = h_2\theta$ and $\delta_b = h_1\theta$ results in the following equation for internal work:

$$W_I = 4m_p\theta\left\{\frac{b_p}{2}\left[h_1\left(\frac{1}{p_{fi}}\right)+h_2\left(\frac{1}{s}\right)\right]+\frac{2}{g}\left[h_1\left(p_{fi}+\frac{3}{4}p_b\right)+h_2\left(s+\frac{1}{4}p_b\right)\right]+\frac{g}{2}\right\} \tag{2-30}$$

The external work, W_E, is given by Eq. (2-31). Setting the internal work and external work equal results in Eq. (2-32).

$$W_E = M_{pl}\theta \tag{2-31}$$

$$M_{pl} = 4m_p\left\{\frac{b_p}{2}\left[h_1\left(\frac{1}{p_{fi}}\right)+h_2\left(\frac{1}{s}\right)\right]+\frac{2}{g}\left[h_1\left(p_{fi}+\frac{3}{4}p_b\right)+h_2\left(s+\frac{1}{4}p_b\right)\right]+\frac{g}{2}\right\} \tag{2-32}$$

This equation is further simplified into the form given in Eq. (2-33) by substituting the moment capacity per unit length, m_p, from Chapter 1, and defining the yield line parameter, Y, as given in Eq. (2-34).

$$M_{pl} = F_{yp}t_p^{\,2}Y \tag{2-33}$$

$$Y = \frac{b_p}{2}\left[h_1\left(\frac{1}{p_{fi}}\right)+h_2\left(\frac{1}{s}\right)\right]+\frac{2}{g}\left[h_1\left(p_{fi}+\frac{3}{4}p_b\right)+h_2\left(s+\frac{1}{4}p_b\right)\right]+\frac{g}{2} \tag{2-34}$$

Note: Use $p_{fi}=s$ if $p_{fi} > s$

To obtain an equation for the dimension s, the equation for moment strength, M_{pl}, is minimized. The derivative of Eq. (2-33), taken with respect to the variable s, is set equal to zero and solved for the variable s. The result is Eq. (2-35).

$$s = \frac{1}{2}\sqrt{b_p g} \tag{2-35}$$

2.8 Four-Bolt Extended Unstiffened End-Plate

The yield line pattern is shown in Figure 2-7. The rotation of each facet (facets are labeled in Figure 2-7) is given in Table 2-15 and the internal work associated with rotation along each yield line is given in Table 2-16. The yield lines are identified by the adjacent facet numbers (e.g., yield line 1/2 separates facets 1 and 2). Variables associated with the geometry of the connection are shown in Figure 2-7. Variables associated with the virtual rotations, displacement, and end-plate moment strength per unit length are described in Chapter 1. It is noted that hatched areas represent facets that are not rotating.

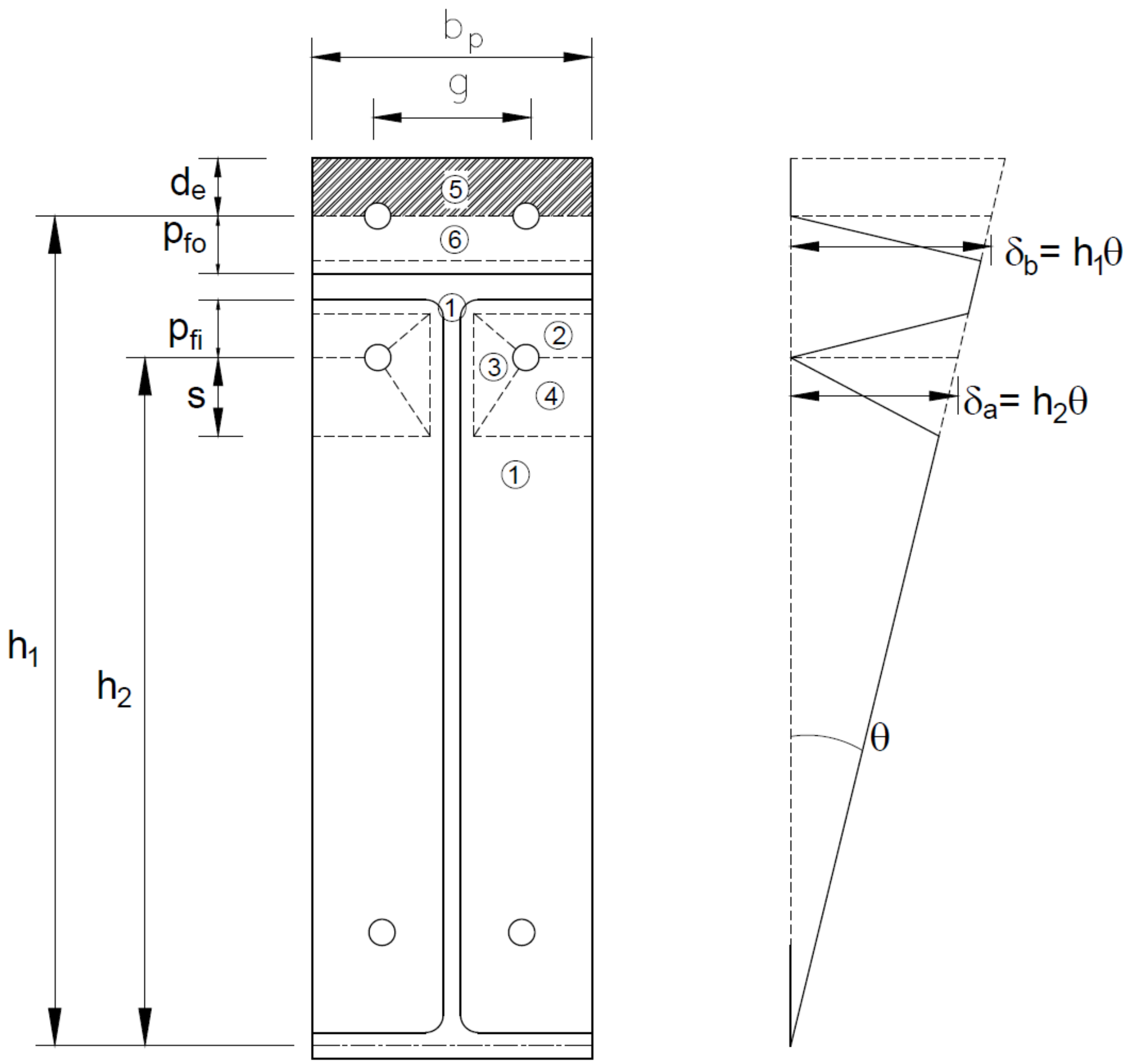

Figure 2-7 Yield Line Pattern for the Four-Bolt Extended Unstiffened End-Plate

Table 2-15 Rotation for Each Facet in the Four-Bolt Extended Unstiffened End-Plate

Facet	θ_x	θ_y
1	θ	0
2	$\left(\delta_a + p_{fi}\theta\right)/p_{fi}$	0
3	θ	$2\delta_a/g$
4	$-\left(\delta_a - s\theta\right)/s$	0
5	0	0
6	$-\left(\delta_b - p_{fo}\theta\right)/p_{fo}$	0

Table 2-16 Internal Work Associated with Each Yield Line in the Four-Bolt Extended Unstiffened End-Plate

Yield Line	Internal Work	Simplified Internal Work	Number of Lines
1/2	$m_p\left(\frac{b_p}{2}\right)\left(\frac{\delta_a + p_{fi}\theta}{p_{fi}} - \theta\right)$	$m_p\left[\left(\frac{b_p}{2}\right)\frac{\delta_a}{p_{fi}}\right]$	2
2/3	$m_p\left[\frac{g}{2}\left(\frac{\delta_a + p_{fi}\theta}{p_{fi}} - \theta\right) + p_{fi}\frac{2\delta_a}{g}\right]$	$m_p\left[\left(\frac{g}{2}\right)\frac{\delta_a}{p_{fi}} + \left(\frac{2}{g}\right)\delta_a p_{fi}\right]$	2
3/4	$m_p\left[\frac{g}{2}\left(\frac{\delta_a - s\theta}{s} + \theta\right) + s\frac{2\delta_a}{g}\right]$	$m_p\left[\left(\frac{g}{2}\right)\frac{\delta_a}{s} + \left(\frac{2}{g}\right)\delta_a s\right]$	2
2/4	$m_p\left(\frac{b_p - g}{2}\right)\left[\left(\frac{\delta_a + p_{fi}\theta}{p_{fi}}\right) + \left(\frac{\delta_a - s\theta}{s}\right)\right]$	$m_p\left(\frac{b_p}{2} - \frac{g}{2}\right)\left(\frac{\delta_a}{p_{fi}} + \frac{\delta_a}{s}\right)$	2
4/1	$m_p\left(\frac{b_p}{2}\right)\left(\frac{\delta_a - s\theta}{s} + \theta\right)$	$m_p\left(\frac{b_p}{2}\right)\left(\frac{\delta_a}{s}\right)$	2
1/6	$m_p\left(b_p\right)\left(\frac{\delta_b - p_{fo}\theta}{p_{fo}} + \theta\right)$	$m_p\left(\frac{b_p}{2}\right)\left(\frac{2\delta_b}{p_{fo}}\right)$	1
6/5	$m_p\left(b_p\right)\left(\frac{\delta_b - p_{fo}\theta}{p_{fo}}\right)$	$m_p\left(\frac{b_p}{2}\right)\left(\frac{2\delta_b}{p_{fo}} - 2\theta\right)$	1
1/3	$m_p\left(p_{fi} + s\right)\left(\frac{2\delta_a}{g}\right)$	$m_p\left(\frac{2}{g}\right)\left(\delta_a p_{fi} + \delta_a s\right)$	2

Summing up the internal work given in Table 2-16 and substituting $\delta_a = h_2\,\theta$ and $\delta_b = h_1\,\theta$ results in the following equation for internal work:

$$W_I = 4m_p\theta\left\{\frac{b_p}{2}\left[h_1\left(\frac{1}{p_{fo}}\right)+h_2\left(\frac{1}{p_{fi}}+\frac{1}{s}\right)-\frac{1}{2}\right]+\frac{2}{g}\left[h_2\left(p_{fi}+s\right)\right]\right\} \tag{2-36}$$

The external work, W_E, is given by Eq. (2-37). Setting the internal work and external work equal results in Eq. (2-38).

$$W_E = M_{pl}\theta \tag{2-37}$$

$$M_{pl} = 4m_p\left\{\frac{b_p}{2}\left[h_1\left(\frac{1}{p_{fo}}\right)+h_2\left(\frac{1}{p_{fi}}+\frac{1}{s}\right)-\frac{1}{2}\right]+\frac{2}{g}\left[h_2\left(p_{fi}+s\right)\right]\right\} \tag{2-38}$$

This equation is further simplified into the form given in Eq. (2-39) by substituting the moment capacity per unit length, m_p, from Chapter 1, and defining the yield line parameter, Y, as given in Eq. (2-40).

$$M_{pl} = F_{yp}t_p^{\,2}Y \tag{2-39}$$

$$Y = \frac{b_p}{2}\left[h_1\left(\frac{1}{p_{fo}}\right)+h_2\left(\frac{1}{p_{fi}}+\frac{1}{s}\right)-\frac{1}{2}\right]+\frac{2}{g}\left[h_2\left(p_{fi}+s\right)\right] \tag{2-40}$$

Note: Use $p_{fi}=s$ if $p_{fi} > s$

To obtain an equation for the dimension s, the equation for moment strength, M_{pl}, is minimized. The derivative of Eq. (2-39), taken with respect to the variable s, is set equal to zero and solved for the variable s. The result is Eq. (2-41).

$$s = \frac{1}{2}\sqrt{b_p g} \tag{2-41}$$

2.9 Four-Bolt Extended Stiffened End-Plate

The yield line pattern is shown in Figure 2-8. The rotation of each facet (facets are labeled in Figure 2-8) is given in Table 2-17 and the internal work associated with rotation along each yield line is given in Table 2-18. The yield lines are identified by the adjacent facet numbers (e.g., yield line 1/2 separates facets 1 and 2). Variables associated with the geometry of the connection are shown in Figure 2-8. Variables associated with the virtual rotations, displacement, and end-plate moment strength per unit length are described in Chapter 1.

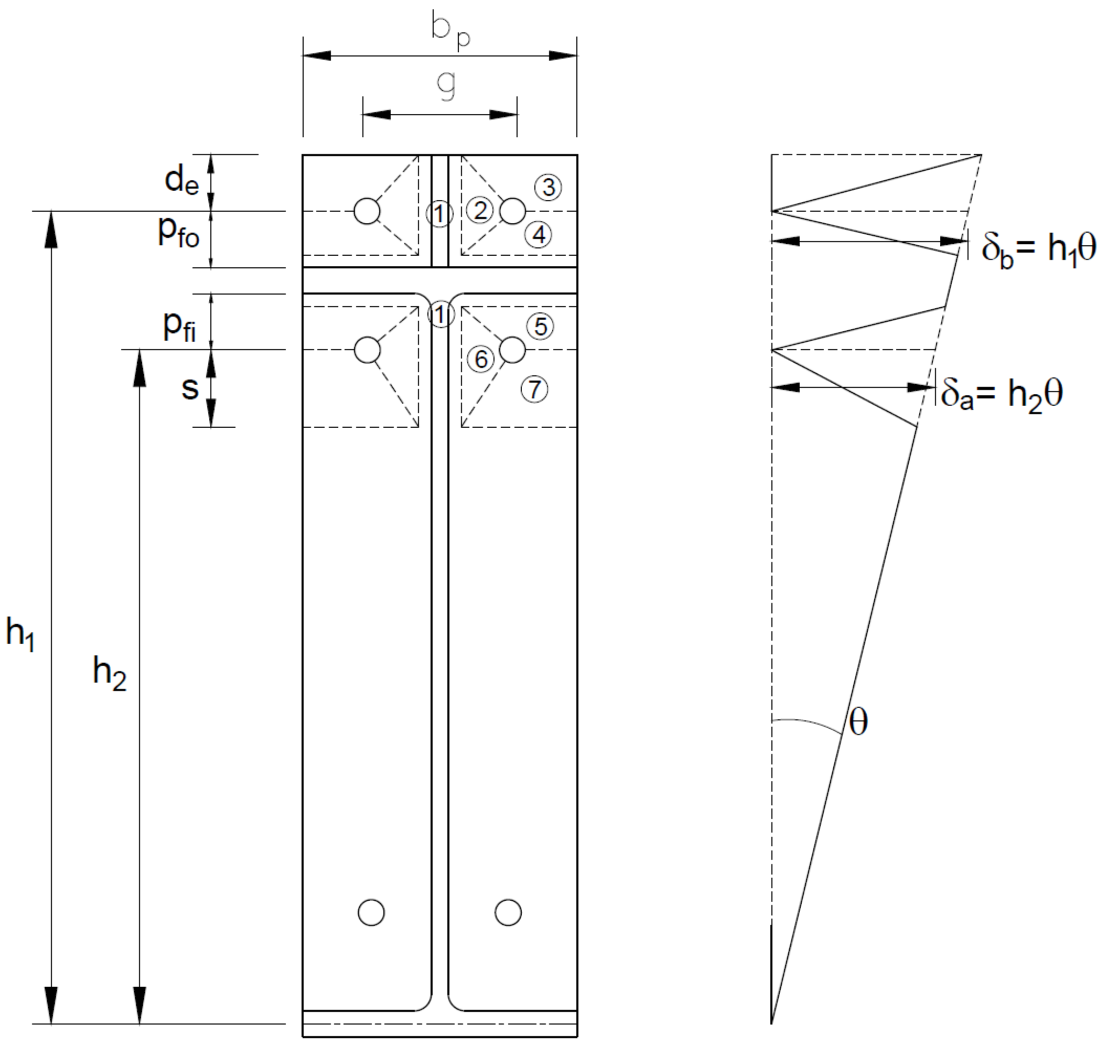

Figure 2-8 Yield Line Pattern for the Four-Bolt Extended Stiffened End-Plate

Table 2-17 Rotation for Each Facet in the Four-Bolt Extended Stiffened End-Plate

Facet	θ_x	θ_y
1	θ	0
2	θ	$2\delta_b / g$
3	$(\delta_b + d_e\theta) / d_e$	0
4	$-(\delta_b - p_{fo}\theta) / p_{fo}$	0
5	$(\delta_a + p_{fi}\theta) / p_{fi}$	0
6	θ	$2\delta_a / g$
7	$-(\delta_s - s\theta) / s$	0

Table 2-18 Internal Work Associated with Each Yield Line in the Four-Bolt Extended Stiffened End-Plate

Yield Line	Internal Work	Simplified Internal Work	Number of Lines
1/2	$m_p\left[\left(d_e + p_{fo}\right)\left(\frac{2\delta_b}{g}\right)\right]$	$m_p\left\{\frac{2}{g}\left[\delta_b\left(d_e + p_{fo}\right)\right]\right\}$	2
2/3	$m_p\left[\frac{g}{2}(\frac{\delta_b + d_e\theta}{d_e} - \theta) + d_e\left(\frac{2\delta_b}{g}\right)\right]$	$m_p\left[\frac{g}{2}(\frac{\delta_b}{d_e}) + \frac{2}{g}(d_e\delta_b)\right]$	2
2/4	$m_p\left[\frac{g}{2}\left(\theta + \frac{\delta_b - p_{fo}\theta}{p_{fo}}\right) + p_{fo}\left(\frac{2\delta_b}{g}\right)\right]$	$m_p\left[\frac{g}{2}\left(\frac{\delta_b}{p_{fo}}\right) + \frac{2}{g}\left(p_{fo}\delta_b\right)\right]$	2
3/4	$m_p\left[\frac{b_p - g}{2}\left(\frac{\delta_b + d_e\theta}{d_e} + \frac{\delta_b - p_{fo}\theta}{p_{fo}}\right)\right]$	$m_p\left\{\frac{b_p}{2}\left[\delta_b\left(\frac{1}{d_e} + \frac{1}{p_{fo}}\right)\right] - \frac{g}{2}\left[\delta_b\frac{1}{d_e} + \frac{1}{p_{fo}}\right]\right\}$	2
1/4	$m_p\left[\frac{b_p}{2}\left(\theta + \frac{\delta_b - p_{fo}\theta}{p_{fo}}\right)\right]$	$m_p\left[\frac{b_p}{2}\left(\frac{\delta_b}{p_{fo}}\right)\right]$	2
1/5	$m_p\left[\frac{b_p}{2}\left(\frac{\delta_a + p_{fi}\theta}{p_{fi}} - \theta\right)\right]$	$m_p\left[\frac{b_p}{2}\left(\frac{\delta_a}{p_{fi}}\right)\right]$	2
5/6	$m_p\left[\frac{g}{2}\left(\frac{\delta_a + p_{fi}\theta}{p_{fi}} - \theta\right) + p_{fi}\left(\frac{2\delta_a}{g}\right)\right]$	$m_p\left[\frac{g}{2}\left(\frac{\delta_a}{p_{fi}}\right) + \frac{2}{g}\left(p_{fi}\delta_a\right)\right]$	2
1/6	$m_p\left[\left(p_{fi} + s\right)\left(\frac{2\delta_a}{g}\right)\right]$	$m_p\left\{\frac{2}{g}\left[\delta_a\left(p_{fi} + s\right)\right]\right\}$	2
6/7	$m_p\left[\frac{g}{2}\left(\theta + \frac{\delta_a - s\theta}{s}\right) + s\left(\frac{2\delta_a}{g}\right)\right]$	$m_p\left[\frac{g}{2}\left(\frac{\delta_a}{s}\right) + \frac{2}{g}(\delta_a s)\right]$	2
5/7	$m_p\left[\left(\frac{b_p - g}{2}\right)\left(\frac{\delta_a + p_{fi}\theta}{p_{fi}} + \frac{\delta_a - s\theta}{s}\right)\right]$	$m_p\left\{\frac{b_p}{2}\left[\delta_a\left(\frac{1}{p_{fi}} + \frac{1}{s}\right)\right] - \frac{g}{2}\left[\delta_a\left(\frac{1}{p_{fi}} + \frac{1}{s}\right)\right]\right\}$	2
1/7	$m_p\left[\frac{b_p}{2}\left(\theta + \frac{\delta_a - s\theta}{s}\right)\right]$	$m_p\left[\frac{b_p}{2}\left(\frac{\delta_a}{s}\right)\right]$	2

Summing up the internal work given in Table 2-18 and substituting $\delta_a = h_2\,\theta$ and $\delta_b = h_1\,\theta$ results in the following equation for internal work:

$$W_I = 4m_p\theta\left\{\frac{b_p}{2}\left[h_1\left(\frac{1}{p_{fo}}+\frac{1}{2d_e}\right)+h_2\left(\frac{1}{p_{fi}}+\frac{1}{s}\right)\right]+\frac{2}{g}\left[h_1\left(p_{fo}+d_e\right)+h_2\left(p_{fi}+s\right)\right]\right\} \tag{2-42}$$

The external work, W_E, is given by Eq. (2-43). Setting the internal work and external work equal results in Eq. (2-44).

$$W_E = M_{pl}\theta \tag{2-43}$$

$$M_{pl} = 4m_p\left\{\frac{b_p}{2}\left[h_1\left(\frac{1}{p_{fo}}+\frac{1}{2d_e}\right)+h_2\left(\frac{1}{p_{fi}}+\frac{1}{s}\right)\right]+\frac{2}{g}\left[h_1\left(p_{fo}+d_e\right)+h_2\left(p_{fi}+s\right)\right]\right\} \tag{2-44}$$

This equation is further simplified into the form given in Eq. (2-45) by substituting the moment capacity per unit length, m_p, from Chapter 1, and defining the yield line parameter, Y, as given in Eq. (2-46).

$$M_{pl} = F_{yp}t_p^{\,2}Y \tag{2-45}$$

$$Y = \frac{b_p}{2}\left[h_1\left(\frac{1}{p_{fo}}+\frac{1}{2d_e}\right)+h_2\left(\frac{1}{p_{fi}}+\frac{1}{s}\right)\right]+\frac{2}{g}\left[h_1\left(p_{fo}+d_e\right)+h_2\left(p_{fi}+s\right)\right] \tag{2-46}$$

Note: Use $p_{fi}=s$ if $p_{fi} > s$ Use $p_{fo}=s$ if $p_{fo} > s$

To obtain an equation for the dimension s, the equation for moment strength, M_{pl}, is minimized. The derivative of Eq. (2-45), taken with respect to the variable s, is set equal to zero and solved for the variable s. The result is Eq. (2-47).

$$s = \frac{1}{2}\sqrt{b_p g} \tag{2-47}$$

The equation for the yield line parameter given by Eq. (2-46) has been validated against experiments and is therefore used in design.

2.9.1 Alternate Yield Line Pattern 1

An alternate yield line pattern which produces a smaller yield line parameter for the four-bolt extended stiffened end-plate is shown in Figure 2-9. The rotation of each facet (facets are labeled in Figure 2-9) is given in Table 2-19 and the internal work associated with rotation along each yield line is given in Table 2-20. The yield lines are identified by the adjacent facet numbers (e.g., yield line 1/2 separates facets 1 and 2). Variables associated with the geometry of the connection are shown in Figure 2-9. Variables associated with the virtual rotations, displacement, and end-plate moment strength per unit length are described in Chapter 1. It is noted that hatched areas represent facets that are not rotating.

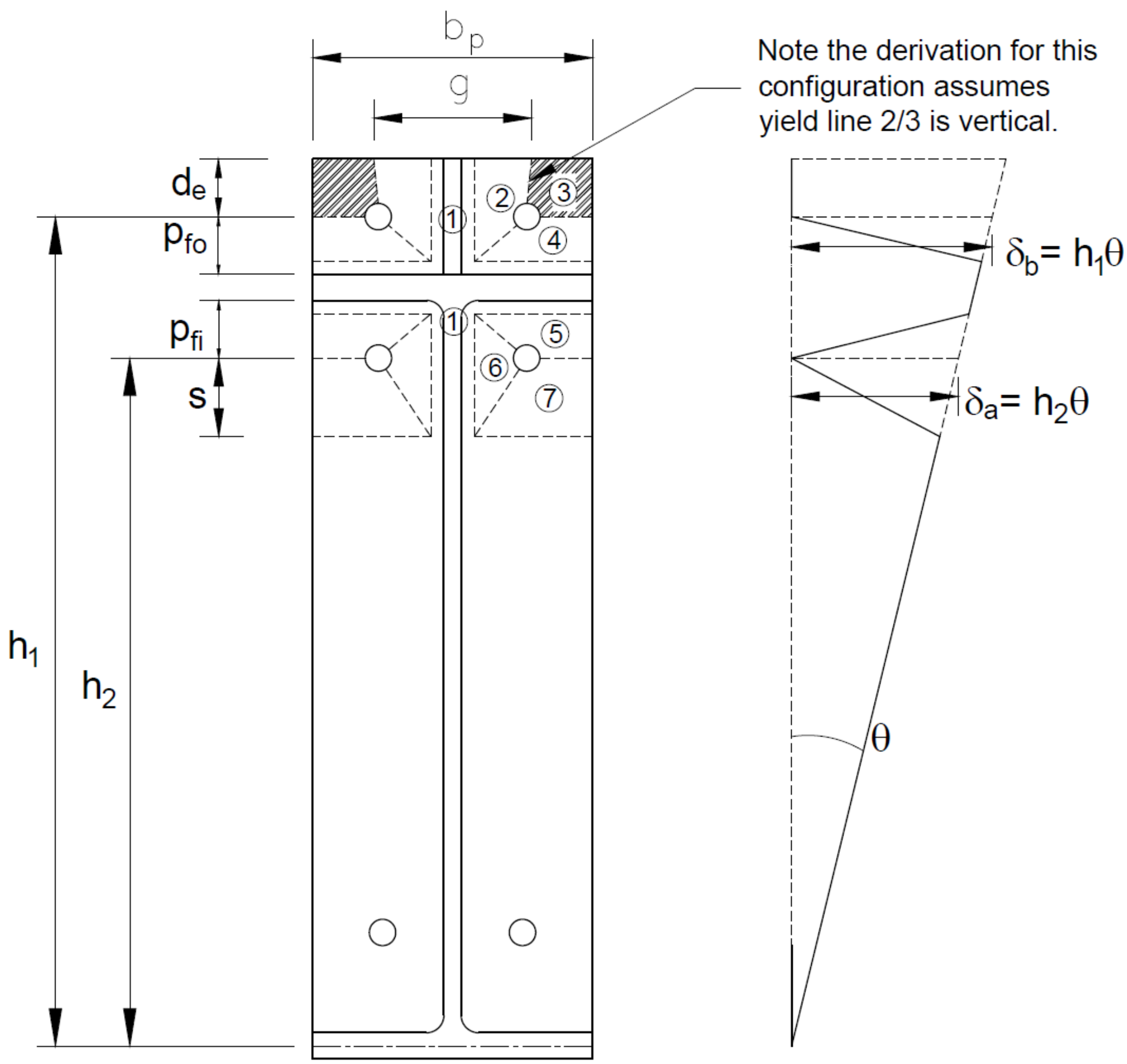

Figure 2-9 Alternative Yield Line Pattern 1 for the Four-Bolt Extended Stiffened End-Plate

Table 2-19 Rotation for Each Facet in the Four-Bolt Extended Stiffened End-Plate

Facet	θ_x	θ_y
1	θ	0
2	θ	$2\delta_b / g$
3	0	0
4	$-(\delta_b - p_{fo}\theta) / p_{fo}$	0
5	$(\delta_a + p_{fi}\theta) / p_{fi}$	0
6	θ	$2\delta_a / g$
7	$-(\delta_a - s\theta) / s$	0

Table 2-20 Internal Work Associated with Each Yield Line in the Four-Bolt Extended Stiffened End-Plate

Yield Line	Internal Work	Simplified Internal Work	Number of Lines
1/2	$m_p\left[\left(d_e + p_{fo}\right)\left(\frac{2\delta_b}{g}\right)\right]$	$m_p\left\{\frac{2}{g}\left[\delta_b\left(d_e + p_{fo}\right)\right]\right\}$	2
2/3	$m_p\left[d_e\left(\frac{2\delta_b}{g}\right)\right]$	$m_p\left[\frac{2}{g}\left(\delta_b d_e\right)\right]$	2
2/4	$m_p\left[\frac{g}{2}\left(\theta + \frac{\delta_b - p_{fo}\theta}{p_{fo}}\right) + p_{fo}\left(\frac{2\delta_b}{g}\right)\right]$	$m_p\left[\frac{g}{2}\left(\frac{\delta_b}{p_{fo}}\right) + \frac{2}{g}\left(p_{fo}\delta_b\right)\right]$	2
3/4	$m_p\left[\frac{b_p - g}{2}\left(\frac{\delta_b - p_{fo}\theta}{p_{fo}}\right)\right]$	$m_p\left[\frac{b_p}{2}\left(\frac{\delta_b}{p_{fo}} - \theta\right) - \frac{g}{2}\left(\frac{\delta_b}{p_{fo}} - \theta\right)\right]$	2
1/4	$m_p\left[\frac{b_p}{2}\left(\theta + \frac{\delta_b - p_{fo}\theta}{p_{fo}}\right)\right]$	$m_p\left[\frac{b_p}{2}\left(\frac{\delta_b}{p_{fo}}\right)\right]$	2
1/5	$m_p\left[\frac{b_p}{2}\left(\frac{\delta_a + p_{fi}\theta}{p_{fi}} - \theta\right)\right]$	$m_p\left[\frac{b_p}{2}\left(\frac{\delta_a}{P_{fi}}\right)\right]$	2
5/6	$m_p\left[\frac{g}{2}\left(\frac{\delta_a + p_{fi}\theta}{p_{fi}} - \theta\right) + p_{fi}\left(\frac{2\delta_a}{g}\right)\right]$	$m_p\left[\frac{g}{2}\left(\frac{\delta_a}{p_{fi}}\right) + \frac{2}{g}\left(p_{fi}\delta_a\right)\right]$	2
1/6	$m_p\left[\left(p_{fi} + s\right)\left(\frac{2\delta_a}{g}\right)\right]$	$m_p\left\{\frac{2}{g}\left[\delta_a\left(p_{fi} + s\right)\right]\right\}$	2
6/7	$m_p\left[\frac{g}{2}\left(\theta + \frac{\delta_a - s\theta}{s}\right) + s\left(\frac{2\delta_a}{g}\right)\right]$	$m_p\left[\frac{g}{2}\left(\frac{\delta_a}{s}\right) + \frac{2}{g}\left(\delta_a s\right)\right]$	2
5/7	$m_p\left[\left(\frac{b_p - g}{2}\right)\left(\frac{\delta_a + p_{fi}\theta}{p_{fi}} + \frac{\delta_a - s\theta}{s}\right)\right]$	$m_p\left\{\frac{b_p}{2}\left[\delta_a\left(\frac{1}{p_{fi}} + \frac{1}{s}\right)\right] - \frac{g}{2}\left[\delta_a\left(\frac{1}{p_{fi}} + \frac{1}{s}\right)\right]\right\}$	2
1/7	$m_p\left[\frac{b_p}{2}\left(\theta + \frac{\delta_a - s\theta}{s}\right)\right]$	$m_p\left[\frac{b_p}{2}\left(\frac{\delta_a}{s}\right)\right]$	2

Summing up the internal work given in Table 2-20 and substituting $\delta_a = h_2\theta$ and $\delta_b = h_1\theta$ results in the following equation for internal work:

$$W_I = 4m_p\theta\left\{\frac{b_p}{2}\left[h_1\left(\frac{1}{p_{fo}}\right)+h_2\left(\frac{1}{p_{fi}}+\frac{1}{s}\right)-\frac{1}{2}\right]+\frac{2}{g}\left[h_1\left(p_{fo}+d_e\right)+h_2\left(p_{fi}+s\right)\right]+\frac{g}{4}\right\} \tag{2-48}$$

The external work, W_E, is given by Eq. (2-49). Setting the internal work and external work equal results in Eq. (2-50).

$$W_E = M_{pl}\theta \tag{2-49}$$

$$M_{pl} = 4m_p\left\{\frac{b_p}{2}\left[h_1\left(\frac{1}{p_{fo}}\right)+h_2\left(\frac{1}{p_{fi}}+\frac{1}{s}\right)-\frac{1}{2}\right]+\frac{2}{g}\left[h_1\left(p_{fo}+d_e\right)+h_2\left(p_{fi}+s\right)\right]+\frac{g}{4}\right\} \tag{2-50}$$

This equation is further simplified into the form given in Eq. (2-51) by substituting the moment capacity per unit length, m_p, from Chapter 1, and defining the yield line parameter, Y, as given in Eq. (2-52).

$$M_{pl} = F_{yp}t_p^{\,2}Y \tag{2-51}$$

$$Y = \frac{b_p}{2}\left[h_1\left(\frac{1}{p_{fo}}\right)+h_2\left(\frac{1}{p_{fi}}+\frac{1}{s}\right)-\frac{1}{2}\right]+\frac{2}{g}\left[h_1\left(p_{fo}+d_e\right)+h_2\left(p_{fi}+s\right)\right]+\frac{g}{4} \tag{2-52}$$

Note: Use $p_{fi}=s$ if $p_{fi} > s$ Use $p_{fo}=s$ if $p_{fo} > s$

To obtain an equation for the dimension s, the equation for moment strength, M_{pl}, is minimized. The derivative of Eq. (2-52), taken with respect to the variable s, is set equal to zero and solved for the variable s. The result is Eq. (2-53).

$$s = \frac{1}{2}\sqrt{b_p g} \tag{2-53}$$

2.9.2 Alternate Yield Line Pattern 2

An alternate yield line pattern 2 associated with the case $d_e > s$ for the four-bolt extended stiffened end-plate is shown in Figure 2-10. The rotation of each facet (facets are labeled in Figure 2-10) is given in Table 2-21 and the internal work associated with rotation along each yield line is given in Table 2-22. The yield lines are identified by the adjacent facet numbers (e.g., yield line 1/2 separates facets 1 and 2). Variables associated with the geometry of the connection are shown in Figure 2-10. Variables associated with the virtual rotations, displacement, and end-plate moment strength per unit length are described in Chapter 1.

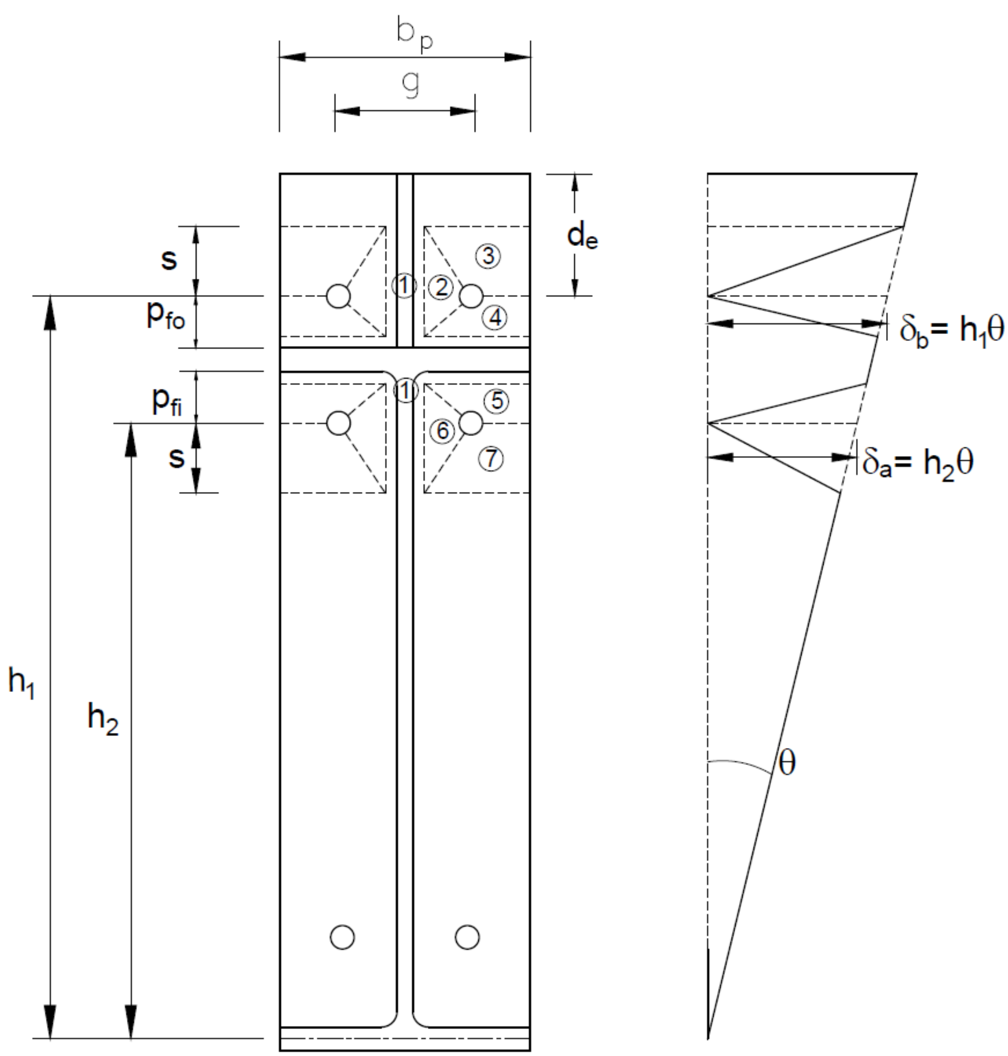

Figure 2-10 Alternative Yield Line Pattern 2 for the Four-Bolt Extended Stiffened End-Plate

Table 2-21 Rotation for Each Facet in the Four-Bolt Extended Stiffened End-Plate

Facet	θ_x	θ_y
1	θ	0
2	θ	$2\delta_b / g$
3	$(\delta_b + s\theta) / s$	0
4	$-(\delta_b - p_{fo}\theta) / p_{fo}$	0
5	$(\delta_a + p_{fi}\theta) / p_{fi}$	0
6	θ	$2\delta_a / g$
7	$-(\delta_s - s\theta) / s$	0

Table 2-22 Internal Work Associated with Each Yield Line in the Four-Bolt Extended Stiffened End-Plate

Yield Line	Internal Work	Simplified Internal Work	Number of Lines
1/2	$m_p\left[\left(s + p_{fo}\right)\left(\frac{2\delta_b}{g}\right)\right]$	$m_p\left\{\frac{2}{g}\left[\delta_b\left(s + p_{fo}\right)\right]\right\}$	2
1/3	$m_p\left[\frac{b_p}{2}\left(\frac{\delta_b + s\theta}{s} - \theta\right)\right]$	$m_p\left[\frac{b_p}{2}\left(\frac{\delta_b}{s}\right)\right]$	2
2/3	$m_p\left[\frac{g}{2}(\frac{\delta_b + s\theta}{s} - \theta) + s\left(\frac{2\delta_b}{g}\right)\right]$	$m_p\left[\frac{g}{2}(\frac{\delta_b}{s}) + \frac{2}{g}(s\delta_b)\right]$	2
2/4	$m_p\left[\frac{g}{2}\left(\theta + \frac{\delta_b - p_{fo}\theta}{p_{fo}}\right) + p_{fo}\left(\frac{2\delta_b}{g}\right)\right]$	$m_p\left[\frac{g}{2}\left(\frac{\delta_b}{p_{fo}}\right) + \frac{2}{g}\left(p_{fo}\delta_b\right)\right]$	2
3/4	$m_p\left[\frac{b_p - g}{2}\left(\frac{\delta_b + s\theta}{s} + \frac{\delta_b - p_{fo}\theta}{p_{fo}}\right)\right]$	$m_p\left\{\frac{b_p}{2}\left[\delta_b\left(\frac{1}{s} + \frac{1}{p_{fo}}\right)\right] - \frac{g}{2}\left[\delta_b \frac{1}{s} + \frac{1}{p_{fo}}\right]\right\}$	2
1/4	$m_p\left[\frac{b_p}{2}\left(\theta + \frac{\delta_b - p_{fo}\theta}{p_{fo}}\right)\right]$	$m_p\left[\frac{b_p}{2}\left(\frac{\delta_b}{p_{fo}}\right)\right]$	2
1/5	$m_p\left[\frac{b_p}{2}\left(\frac{\delta_a + p_{fi}\theta}{p_{fi}} - \theta\right)\right]$	$m_p\left[\frac{b_p}{2}\left(\frac{\delta_a}{p_{fi}}\right)\right]$	2
5/6	$m_p\left[\frac{g}{2}\left(\frac{\delta_a + p_{fi}\theta}{p_{fi}} - \theta\right) + p_{fi}\left(\frac{2\delta_a}{g}\right)\right]$	$m_p\left[\frac{g}{2}\left(\frac{\delta_a}{p_{fi}}\right) + \frac{2}{g}\left(p_{fi}\delta_a\right)\right]$	2
1/6	$m_p\left[\left(p_{fi} + s\right)\left(\frac{2\delta_a}{g}\right)\right]$	$m_p\left\{\frac{2}{g}\left[\delta_a\left(p_{fi} + s\right)\right]\right\}$	2
6/7	$m_p\left[\frac{g}{2}\left(\theta + \frac{\delta_a - s\theta}{s}\right) + s\left(\frac{2\delta_a}{g}\right)\right]$	$m_p\left[\frac{g}{2}\left(\frac{\delta_a}{s}\right) + \frac{2}{g}\left(\delta_a s\right)\right]$	2
5/7	$m_p\left[\left(\frac{b_p - g}{2}\right)\left(\frac{\delta_a + p_{fi}\theta}{p_{fi}} + \frac{\delta_a - s\theta}{s}\right)\right]$	$m_p\left\{\frac{b_p}{2}\left[\delta_a\left(\frac{1}{p_{fi}} + \frac{1}{s}\right)\right] - \frac{g}{2}\left[\delta_a\left(\frac{1}{p_{fi}} + \frac{1}{s}\right)\right]\right\}$	2
1/7	$m_p\left[\frac{b_p}{2}\left(\theta + \frac{\delta_a - s\theta}{s}\right)\right]$	$m_p\left[\frac{b_p}{2}\left(\frac{\delta_a}{s}\right)\right]$	2

Summing up the internal work given in Table 2-22 and substituting $\delta_a = h_2\,\theta$ and $\delta_b = h_1\,\theta$ results in the following equation for internal work:

$$W_I = 4m_p\theta\left\{\frac{b_p}{2}\left[h_1\left(\frac{1}{p_{fo}}+\frac{1}{s}\right)+h_2\left(\frac{1}{p_{fi}}+\frac{1}{s}\right)\right]+\frac{2}{g}\left[h_1\left(p_{fo}+s\right)+h_2\left(p_{fi}+s\right)\right]\right\} \tag{2-54}$$

The external work, W_E, is given by Eq. (2-55). Setting the internal work and external work equal results in Eq. (2-56).

$$W_E = M_{pl}\theta \tag{2-55}$$

$$M_{pl} = 4m_p\left\{\frac{b_p}{2}\left[h_1\left(\frac{1}{p_{fo}}+\frac{1}{s}\right)+h_2\left(\frac{1}{p_{fi}}+\frac{1}{s}\right)\right]+\frac{2}{g}\left[h_1\left(p_{fo}+s\right)+h_2\left(p_{fi}+s\right)\right]\right\} \tag{2-56}$$

This equation is further simplified into the form given in Eq. (2-57) by substituting the moment capacity per unit length, m_p, from Chapter 1, and defining the yield line parameter, Y, as given in Eq. (2-58).

$$M_{pl} = F_{yp}t_p^{\,2}Y \tag{2-57}$$

$$Y = \left\{\frac{b_p}{2}\left[h_1\left(\frac{1}{p_{fo}}+\frac{1}{s}\right)+h_2\left(\frac{1}{p_{fi}}+\frac{1}{s}\right)\right]+\frac{2}{g}\left[h_1\left(p_{fo}+s\right)+h_2\left(p_{fi}+s\right)\right]\right\} \tag{2-58}$$

Note: Use p_{fi}=s if $p_{fi} > s$ Use p_{fo}=s if $p_{fo}> s$

To obtain an equation for the dimension s, the equation for moment strength, M_{pl}, is minimized. The derivative of Eq. (2-57), taken with respect to the variable s, is set equal to zero and solved for the variable s. The result is Eq. (2-59).

$$s = \frac{1}{2}\sqrt{b_p g} \tag{2-59}$$

2.9.3 Comparison for an Example Connection

The effect of end-plate extensions, d_e, on Yield Line Parameter is further investigated in this section using an example connection. Example 5.3-2 in AISC Design Guide 4+16 is selected to compare yield line parameter, Y, values associated with three yield line patterns discussed above. Figure 2-11 shows the geometry and details for this example connection and dimensions are summarized in Table 2-23. Table 2-24 summarizes the yield line parameters associated with the three patterns discussed in this section. Figure 2-12 shows how the yield line parameters vary with the end-plate extension past the outermost bolt, d_e.

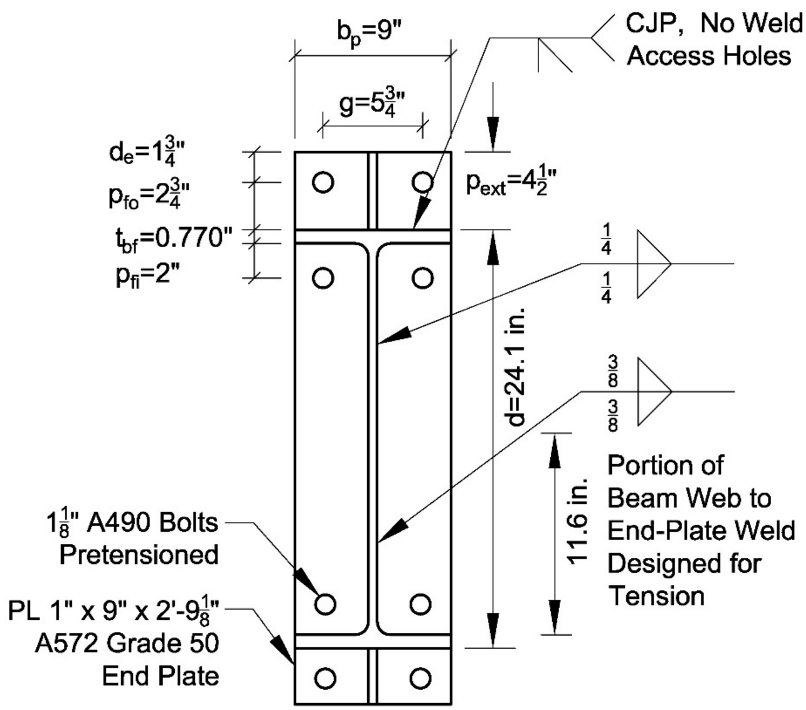

Figure 2-11 Four-Bolt Extended Stiffened End Plate (from example 5.3-2 Design Guide 4+16)

Table 2-23. Summary of Dimensions

Width of the plate	$b_p = 9\ in.$
Extension of End Plate Above Flange	$p_{ext} = 4.5\ in.$
End Plate Above Top Bolt Line	$d_e = 1.75\ in.$
End Plate Thickness	$t_p = 1\ in.$
Gage	$g = 5.75\ in.$
Exterior Distance to Bolt Row	$p_{fo} = 2.75\ in.$
Interior Distance to Bolt Row	$p_{fi} = 2\ in.$
Depth of Beam at End Plate	$d = 24.1\ in.$
Beam Flange Width	$b_{bf} = 9.02\ in.$
Beam Flange Thickness	$t_{bf} = 0.77\ in.$
Beam Web Thickness	$t_{bw} = 0.47\ in.$
Distance from centroid of compression flange to first row	$h_2 = 20.9\ in.$
Distance from centroid of compression flange to second row	$h_1 = 26.5\ in.$
Distance to Yield Line	$s = \frac{1}{2}\sqrt{b_p g} = 3.6\ in.$

Table 2-24 Summary of Yield Line Parameters for Four-Bolt Extended Stiffened End Plate

	Pattern	Yield Line Parameter
A	Equation derived at beginning of Section 2.8. Also, AISC 358-18 Table 6.3 Case 1 for $d_e \leq s$.	$Y=\frac{b_p}{2}\left[h_1\left(\frac{1}{p_{fo}}+\frac{1}{2d_e}\right)+h_2\left(\frac{1}{p_{fi}}+\frac{1}{s}\right)\right]+\frac{2}{g}\left[h_1\left(p_{fo}+d_e\right)+h_2\left(p_{fi}+s\right)\right]$
B	Equation derived in Section 2.8.1.	$Y=\frac{b_p}{2}\left[h_1\left(\frac{1}{p_{fo}}\right)+h_2\left(\frac{1}{p_{fi}}+\frac{1}{s}\right)-\frac{1}{2}\right]+\frac{2}{g}\left[h_1\left(p_{fo}+d_e\right)+h_2\left(p_{fi}+s\right)\right]+\frac{g}{4}$
C	Equation derived in Section 2.8.3. Also, AISC 358-18 Table 6.3 Case 2 for $d_e > s$.	$Y=\left\{\frac{b_p}{2}\left[h_1\left(\frac{1}{p_{fo}}+\frac{1}{s}\right)+h_2\left(\frac{1}{p_{fi}}+\frac{1}{s}\right)\right]+\frac{2}{g}\left[h_1\left(p_{fo}+s\right)+h_2\left(p_{fi}+s\right)\right]\right\}$

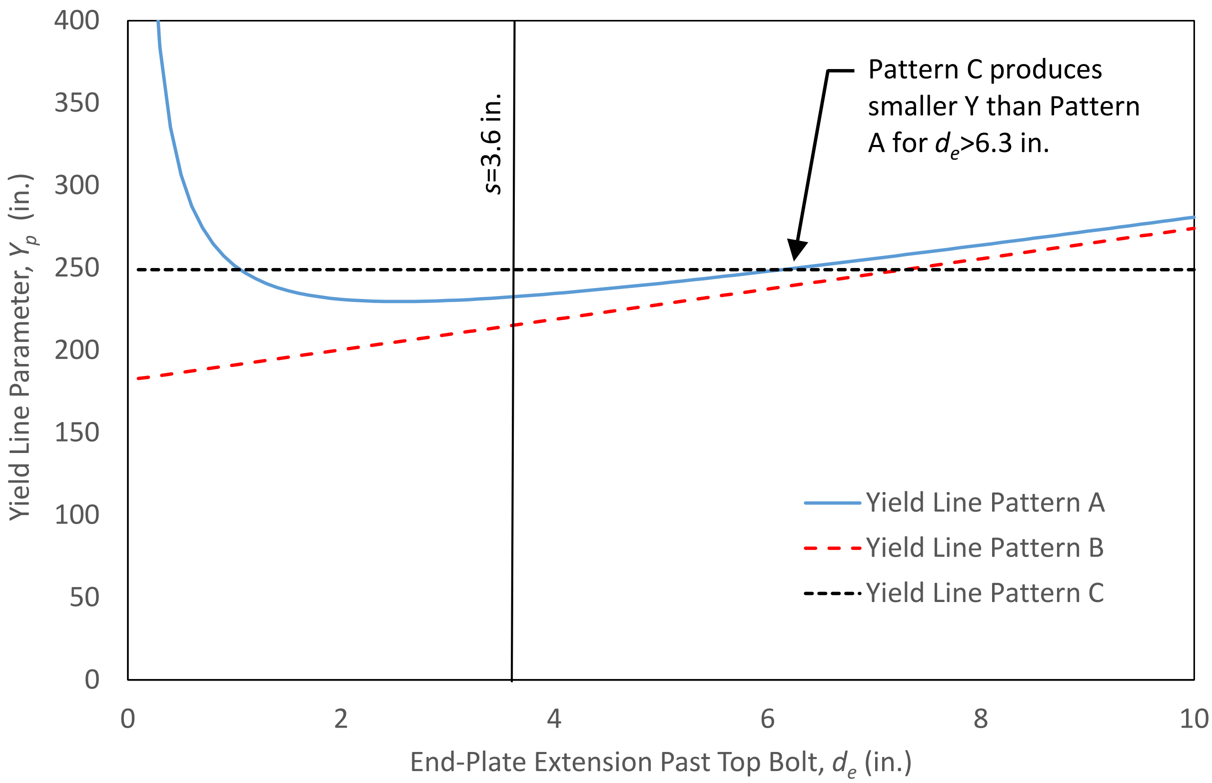

Figure 2-12. The effect of End-Plate Extension on Yield Line Parameter

AISC 358 specifies that Pattern A shall be used for $d_e \leq s$ and Pattern C shall be used for $d_e > s$. However, Figure 2-12, shows that for this example where s=3.6 in., the yield line parameter, Y, associated with Pattern A is smaller than the value for Pattern C until the end-plate dimension exceeds d_e>6.3 in. This is because Pattern C includes additional yield lines along the top of the yield line pattern (see Figure 2-10) which will only control when the end-plate extension past the outermost bolt, d_e, is especially large. For typical end-plate connection geometries, Pattern C will not control.

Figure 2-12 also demonstrates the difference between Pattern A which has been validated against experiments and Pattern B which produces a small yield line pattern. For the value of d_e=1.75 in. corresponding to the end-plate geometry in the example shown in Figure 2-12, the yield line parameter for Pattern B is 85% of the yield line parameter for Pattern A. Regardless of this difference, Pattern A has been shown to produce end-plate moment strength, M_{pl}, that matches experimental results reasonably well (Abel and Murray 1994, Blumenbaum and Murray 2004, Blumenbaum and Murray 2003, Borgsmiller et al. 1995, Curtis and Murray 1989, Eatherton et al. 2013, Eatherton et al. 2017, Jenner et al 1985, Kline et al 1995, Meng 1996, Murray 1989, Ryan and Murray 1999, Sumner and Murray 2002, Young and Murray 1997). For that reason, Pattern A is recommended for use in design over Pattern B.

It is noted that these same issues associated with different yield line parameters exists for all stiffened extended configurations including the multiple row extended 1/3 stiffened, eight-bolt extended stiffened, and twelve-bolt extended stiffened configurations. These yield line parameter comparisons are only conducted for the four-bolt extended stiffened, but the observations made here are expected to be similar for the other extended stiffened end-plate configurations.

2.10 Multiple Row Extended 1/2 Unstiffened End-Plate

The yield line pattern is shown in Figure 2-13. The rotation of each facet (facets are labeled in Figure 2-13) is given in Table 2-25 and the internal work associated with rotation along each yield line is given in Table 2-26. The yield lines are identified by the adjacent facet numbers (e.g., yield line 1/2 separates facets 1 and 2). Variables associated with the geometry of the connection are shown in Figure 2-13. Variables associated with the virtual rotations, displacement, and end-plate moment strength per unit length are described in Chapter 1. It is noted that hatched areas represent facets that are not rotating.

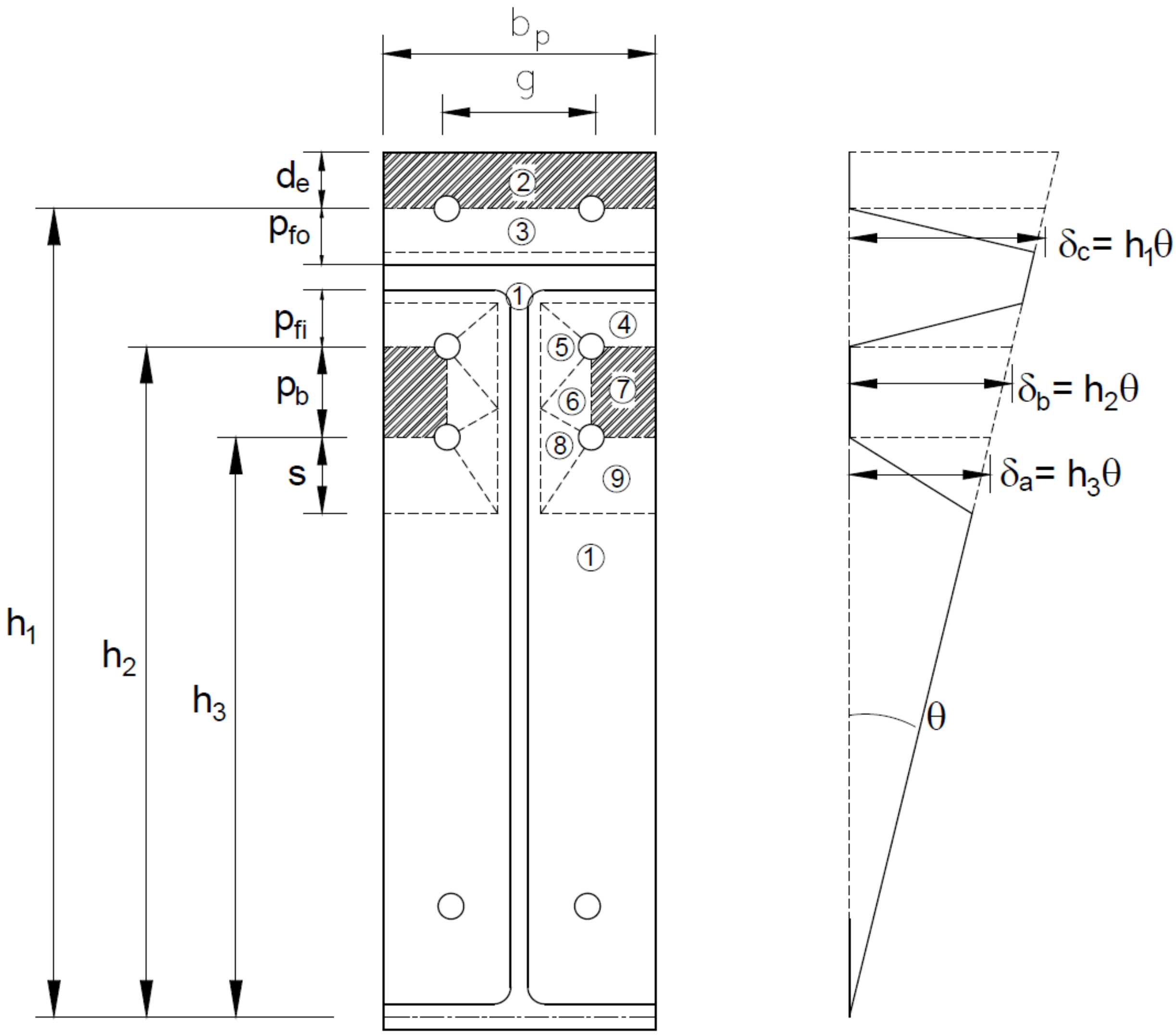

Figure 2-13 Yield Line Pattern for the Multiple Row Extended 1/2 Unstiffened End-Plate

Table 2-25 Rotation for Each Facet in the Multiple Row Extended 1/2 Unstiffened End-Plate

Facet	θ_x	θ_y
1	θ	0
2	0	0
3	$-(\delta_c - p_{fo}\theta)/p_{fo}$	0
4	$(\delta_b + p_{fi}\theta)/p_{fi}$	0
5	θ	$2\delta_b/g$
6	0	$(\delta_b + \delta_a)/g$
7	0	0
8	θ	$2\delta_a/g$
9	$-(\delta_a - s\theta)/s$	0

Table 2-26 Internal Work Associated with Each Yield Line in the Multiple Row Extended 1/2 Unstiffened End-Plate (Part 1 of 2)

Yield Line	Internal Work	Simplified Internal Work	Number of Lines
2/3	$m_p\left[b_p\left(\frac{\delta_c - p_{fo}\theta}{p_{fo}}\right)\right]$	$m_p\left[\frac{b_p}{2}\left(\frac{2\delta_c}{p_{fo}} - 2\theta\right)\right]$	1
1/3	$m_p\left[b_p\left(\theta + \frac{\delta_c - p_{fo}\theta}{p_{fo}}\right)\right]$	$m_p\left[\frac{b_p}{2}\left(\frac{2\delta_c}{p_{fo}}\right)\right]$	1
1/4	$m_p\left[\frac{b_p}{2}\left(\frac{\delta_b + p_{fi}\theta}{p_{fi}} - \theta\right)\right]$	$m_p\left[\frac{b_p}{2}\left(\frac{\delta_b}{p_{fi}}\right)\right]$	2
4/5	$m_p\left[\frac{g}{2}\left(\frac{\delta_b + p_{fi}\theta}{p_{fi}} - \theta\right) + p_{fi}\left(\frac{2\delta_b}{g}\right)\right]$	$m_p\left[\frac{g}{2}\left(\frac{\delta_b}{p_{fi}}\right) + \frac{2}{g}\left(p_{fi}\delta_b\right)\right]$	2
5/6	$m_p\left[\frac{g}{2}(\theta) + \frac{p_b}{2}\left(\frac{2\delta_b}{g} - \frac{\delta_b + \delta_a}{g}\right)\right]$	$m_p\left[\frac{g}{2}(\theta) + \frac{2}{g}\left(\frac{p_b\delta_b}{4} - \frac{p_b\delta_a}{4}\right)\right]$	2
6/8	$m_p\left[\frac{g}{2}(\theta) + \frac{p_b}{2}\left(\frac{\delta_b + \delta_a}{g} - \frac{2\delta_a}{g}\right)\right]$	$m_p\left[\frac{g}{2}(\theta) + \frac{2}{g}\left(\frac{p_b\delta_b}{4} - \frac{p_b\delta_a}{4}\right)\right]$	2
8/9	$m_p\left[\frac{g}{2}\left(\theta + \frac{\delta_a - s\theta}{s}\right) + s\left(\frac{2\delta_a}{g}\right)\right]$	$m_p\left[\frac{g}{2}\left(\frac{\delta_a}{s}\right) + \frac{2}{g}\left(s\delta_a\right)\right]$	2
1/5	$m_p\left[\left(p_{fi} + \frac{p_b}{2}\right)\left(\frac{2\delta_b}{g}\right)\right]$	$m_p\left[\frac{2}{g}\left(\delta_b p_{fi} + \frac{\delta_b p_b}{2}\right)\right]$	2
1/8	$m_p\left[\left(s + \frac{p_b}{2}\right)\left(\frac{2\delta_a}{g}\right)\right]$	$m_p\left[\frac{2}{g}\left(\delta_a s + \frac{\delta_a p_b}{2}\right)\right]$	2
4/7	$m_p\left[\left(\frac{b_p - g}{2}\right)\left(\frac{\delta_b + p_{fi}\theta}{p_{fi}}\right)\right]$	$m_p\left[\frac{b_p}{2}\left(\frac{\delta_b + p_{fi}\theta}{p_{fi}}\right) - \frac{g}{2}\left(\frac{\delta_b + p_{fi}\theta}{p_{fi}}\right)\right]$	2

Table 2-26 Internal Work Associated with Each Yield Line in the Multiple Row Extended 1/2 Unstiffened End-Plate (Part 2 of 2)

6/7	$m_p\left[p_b\left(\frac{\delta_b+\delta_a}{g}\right)\right]$	$m_p\left[\frac{2}{g}\left(\frac{p_b\delta_b+p_b\delta_a}{2}\right)\right]$	2
7/9	$m_p\left[\left(\frac{b_p-g}{2}\right)\left(\frac{\delta_a-s\theta}{s}\right)\right]$	$m_p\left[\frac{b_p}{2}\left(\frac{\delta_a-s\theta}{s}\right)-\frac{g}{2}\left(\frac{\delta_a-s\theta}{s}\right)\right]$	2
1/9	$m_p\left[\frac{b_p}{2}\left(\theta+\frac{\delta_a-s\theta}{s}\right)\right]$	$m_p\left[\frac{b_p}{2}\left(\frac{\delta_a}{s}\right)\right]$	2

Summing up the internal work given in Table 2-26 and substituting $\delta_a = h_3\,\theta$, $\delta_b = h_2\,\theta$, *and* $\delta_c = h_1\,\theta$ results in the following equation for internal work:

$$W_I = 4m_p\theta\left\{\frac{b_p}{2}\left[h_1\left(\frac{1}{p_{fo}}\right)+h_2\left(\frac{1}{p_{fi}}\right)+h_3\left(\frac{1}{s}\right)-\frac{1}{2}\right]+\frac{2}{g}\left[h_2\left(p_{fi}+\frac{3p_b}{4}\right)+h_3\left(\frac{p_b}{4}+s\right)\right]+\frac{g}{2}\right\} \qquad (2\text{-}60)$$

The external work, W_E, is given by Eq. (2-61). Setting the internal work and external work equal results in Eq. (2-62).

$$W_E = M_{pl}\theta \qquad (2\text{-}61)$$

$$M_{pl} = 4m_p\left\{\frac{b_p}{2}\left[h_1\left(\frac{1}{p_{fo}}\right)+h_2\left(\frac{1}{p_{fi}}\right)+h_3\left(\frac{1}{s}\right)-\frac{1}{2}\right]+\frac{2}{g}\left[h_2\left(p_{fi}+\frac{3p_b}{4}\right)+h_3\left(\frac{p_b}{4}+s\right)\right]+\frac{g}{2}\right\} \qquad (2\text{-}62)$$

This equation is further simplified into the form given in Eq. (2-63) by substituting the moment capacity per unit length, m_p, from Chapter 1, and defining the yield line parameter, Y, as given in Eq. (2-64).

$$M_{pl} = F_{yp}t_p^{\,2}Y \qquad (2\text{-}63)$$

$$Y = \frac{b_p}{2}\left[h_1\left(\frac{1}{p_{fo}}\right)+h_2\left(\frac{1}{p_{fi}}\right)+h_3\left(\frac{1}{s}\right)-\frac{1}{2}\right]+\frac{2}{g}\left[h_2\left(p_{fi}+\frac{3p_b}{4}\right)+h_3\left(\frac{p_b}{4}+s\right)\right]+\frac{g}{2} \qquad (2\text{-}64)$$

Note: Use $p_{fi}=s$ if $p_{fi} > s$

To obtain an equation for the dimension s, the equation for moment strength, M_{pl}, is minimized. The derivative of Eq. (2-63), taken with respect to the variable s, is set equal to zero and solved for the variable s. The result is Eq. (2-65).

$$s = \frac{1}{2}\sqrt{b_p g} \qquad (2\text{-}65)$$

2.11 Multiple Row Extended 1/3 Unstiffened End-Plate

The yield line pattern is shown in Figure 2-14. The rotation of each facet (facets are labeled in Figure 2-14) is given in Table 2-27 and the internal work associated with rotation along each yield line is given in Table 2-28. The yield lines are identified by the adjacent facet numbers (e.g., yield line 1/2 separates facets 1 and 2). Variables associated with the geometry of the connection are shown in Figure 2-14. Variables associated with the virtual rotations, displacement, and end-plate moment strength per unit length are described in Chapter 1. It is noted that hatched areas represent facets that are not rotating.

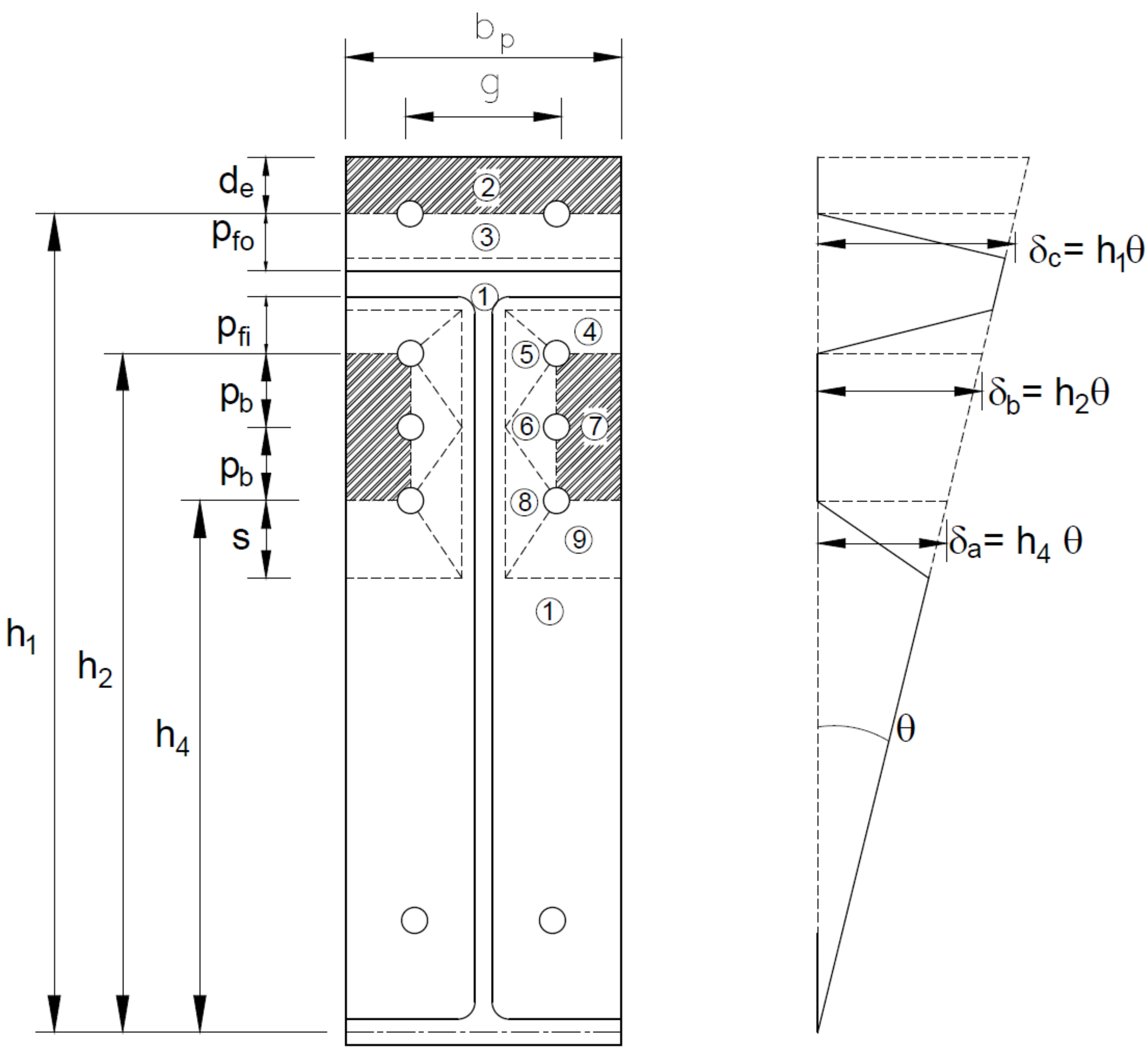

Figure 2-14 Yield Line Pattern for the Multiple Row Extended 1/3 Unstiffened End-Plate

Table 2-27 Rotation for Each Facet in the Multiple Row Extended 1/3 Unstiffened End-Plate

Facet	θ_x	θ_y
1	θ	0
2	0	0
3	$-(\delta_c - p_{fo}\theta)/p_{fo}$	0
4	$(\delta_b + p_{fi}\theta)/p_{fi}$	0
5	θ	$2\delta_b / g$
6	0	$(\delta_b + \delta_a)/g$
7	0	0
8	θ	$2\delta_a / g$
9	$-(\delta_a - s\theta)/s$	0

Table 2-28 Internal Work Associated with Each Yield Line in the Multiple Row Extended 1/3 Unstiffened End-Plate (Part 1 of 2)

Yield Line	Internal Work	Simplified Internal Work	Number of Lines
2/3	$m_p\left[b_p\left(\frac{\delta_c - p_{fo}\theta}{p_{fo}}\right)\right]$	$m_p\left[\frac{b_p}{2}\left(\frac{2\delta_c - 2p_{fo}\theta}{p_{fo}}\right)\right]$	1
1/3	$m_p\left[b_p\left(\theta + \frac{\delta_c - p_{fo}\theta}{p_{fo}}\right)\right]$	$m_p\left[\frac{b_p}{2}\left(\frac{2\delta_c}{p_{fo}}\right)\right]$	1
1/4	$m_p\left[\frac{b_p}{2}\left(\frac{\delta_b + p_{fi}\theta}{p_{fi}} - \theta\right)\right]$	$m_p\left[\frac{b_p}{2}\left(\frac{\delta_b}{p_{fi}}\right)\right]$	2
4/5	$m_p\left[\frac{g}{2}\left(\frac{\delta_b + p_{fi}\theta}{p_{fi}} - \theta\right) + p_{fi}\left(\frac{2\delta_b}{g}\right)\right]$	$m_p\left[\frac{g}{2}\left(\frac{\delta_b}{p_{fi}}\right) + \frac{2}{g}\left(p_{fi}\delta_b\right)\right]$	2
5/6	$m_p\left[\frac{g}{2}(\theta) + p_b\left(\frac{2\delta_b}{g} - \frac{\delta_b + \delta_a}{g}\right)\right]$	$m_p\left[\frac{g}{2}(\theta) + \frac{2}{g}\left(\frac{p_b\delta_b}{2} - \frac{p_b\delta_a}{2}\right)\right]$	2
6/8	$m_p\left[\frac{g}{2}(\theta) + p_b\left(\frac{\delta_b + \delta_a}{g} - \frac{2\delta_a}{g}\right)\right]$	$m_p\left[\frac{g}{2}(\theta) + \frac{2}{g}\left(\frac{p_b\delta_b}{2} - \frac{p_b\delta_a}{2}\right)\right]$	2
8/9	$m_p\left[\frac{g}{2}\left(\theta + \frac{\delta_a - s\theta}{s}\right) + s\left(\frac{2\delta_a}{g}\right)\right]$	$m_p\left[\frac{g}{2}\left(\frac{\delta_a}{s}\right) + \frac{2}{g}(s\delta_a)\right]$	2
1/5	$m_p\left[\left(p_{fi} + p_b\right)\left(\frac{2\delta_b}{g}\right)\right]$	$m_p\left[\frac{2}{g}\left(\delta_b p_{fi} + \delta_b p_b\right)\right]$	2
1/8	$m_p\left[\left(s + p_b\right)\left(\frac{2\delta_a}{g}\right)\right]$	$m_p\left[\frac{2}{g}\left(\delta_a s + \delta_a p_b\right)\right]$	2
4/7	$m_p\left[\left(\frac{b_p - g}{2}\right)\left(\frac{\delta_b + p_{fi}\theta}{p_{fi}}\right)\right]$	$m_p\left[\frac{b_p}{2}\left(\frac{\delta_b + p_{fi}\theta}{p_{fi}}\right) - \frac{g}{2}\left(\frac{\delta_b + p_{fi}\theta}{p_{fi}}\right)\right]$	2

Table 2-28 Internal Work Associated with Each Yield Line in the Multiple Row Extended 1/3 Unstiffened End-Plate (Part 2 of 2)

6/7	$m_p\left[2p_b\left(\frac{\delta_b+\delta_a}{g}\right)\right]$	$m_p\left[\frac{2}{g}(p_b\delta_b+p_b\delta_a)\right]$	2
7/9	$m_p\left[\left(\frac{b_p-g}{2}\right)\left(\frac{\delta_a-s\theta}{s}\right)\right]$	$m_p\left[\frac{b_p}{2}\left(\frac{\delta_a-s\theta}{s}\right)-\frac{g}{2}\left(\frac{\delta_a-s\theta}{s}\right)\right]$	2
1/9	$m_p\left[\frac{b_p}{2}\left(\theta+\frac{\delta_a-s\theta}{s}\right)\right]$	$m_p\left[\frac{b_p}{2}\left(\frac{\delta_a}{s}\right)\right]$	2

Summing up the internal work given in Table 2-28 and substituting $\delta_a = h_4\theta$, $\delta_b = h_2\theta$, *and* $\delta_c = h_1\theta$ results in the following equation for internal work:

$$W_I = 4m_p\theta\left\{\frac{b_p}{2}\left[h_1\left(\frac{1}{p_{fo}}\right)+h_2\left(\frac{1}{p_{fi}}\right)+h_4\left(\frac{1}{s}\right)-\frac{1}{2}\right]+\frac{2}{g}\left[h_2\left(p_{fi}+\frac{3p_b}{2}\right)+h_4\left(\frac{p_b}{2}+s\right)\right]+\frac{g}{2}\right\} \tag{2-66}$$

The external work, W_E, is given by Eq. (2-67). Setting the internal work and external work equal results in Eq. (2-68).

$$W_E = M_{pl}\theta \tag{2-67}$$

$$M_{pl} = 4m_p\left\{\frac{b_p}{2}\left[h_1\left(\frac{1}{p_{fo}}\right)+h_2\left(\frac{1}{p_{fi}}\right)+h_4\left(\frac{1}{s}\right)-\frac{1}{2}\right]+\frac{2}{g}\left[h_2\left(p_{fi}+\frac{3p_b}{2}\right)+h_4\left(\frac{p_b}{2}+s\right)\right]+\frac{g}{2}\right\} \tag{2-68}$$

This equation is further simplified into the form given in Eq. (2-69) by substituting the moment capacity per unit length, m_p, from Chapter 1, and defining the yield line parameter, Y, as given in Eq. (2-70).

$$M_{pl} = F_{yp}t_p{}^2Y \tag{2-69}$$

$$Y = \frac{b_p}{2}\left[h_1\left(\frac{1}{p_{fo}}\right)+h_2\left(\frac{1}{p_{fi}}\right)+h_4\left(\frac{1}{s}\right)-\frac{1}{2}\right]+\frac{2}{g}\left[h_2\left(p_{fi}+\frac{3p_b}{2}\right)+h_4\left(\frac{p_b}{2}+s\right)\right]+\frac{g}{2} \tag{2-70}$$

Note: Use $p_{fi}=s$ if $p_{fi} > s$

To obtain an equation for the dimension s, the equation for moment strength, M_{pl}, is minimized. The derivative of Eq. (2-69), taken with respect to the variable s, is set equal to zero and solved for the variable s. The result is Eq. (2-71).

$$s = \frac{1}{2}\sqrt{b_p g} \tag{2-71}$$

2.12 Multiple Row Extended 1/3 Stiffened End-Plate

The yield line pattern is shown in Figure 2-15. The rotation of each facet (facets are labeled in Figure 2-15) is given in Table 2-29 and the internal work associated with rotation along each yield line is given in Table 2-30. The yield lines are identified by the adjacent facet numbers (e.g., yield line 1/2 separates facets 1 and 2). Variables associated with the geometry of the connection are shown in Figure 2-15. Variables associated with the virtual rotations, displacement, and end-plate moment strength per unit length are described in Chapter 1. It is noted that hatched areas represent facets that are not rotating.

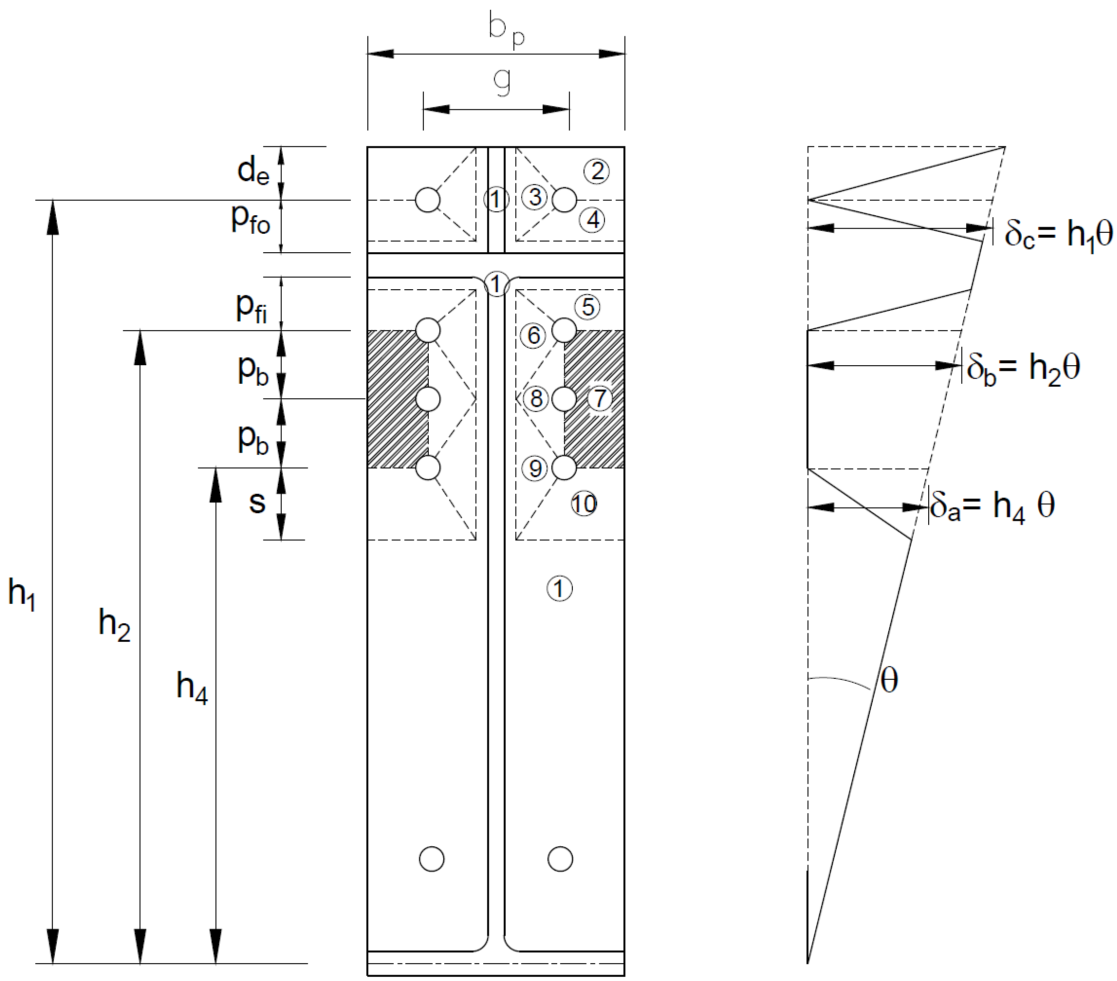

Figure 2-15 Yield Line Pattern for the Multiple Row Extended 1/3 Stiffened End-Plate

Table 2-29 Rotation for Each Facet in the Multiple Row Extended 1/3 Stiffened End-Plate

Facet	θ_x	θ_y
1	θ	0
2	$(\delta_c + d_e\theta)/d_e$	0
3	θ	$2\delta_c / g$
4	$-(\delta_c - p_{fo}\theta)/p_{fo}$	0
5	$(\delta_b + p_{fi}\theta)/p_{fi}$	0
6	θ	$2\delta_b / g$
7	0	0
8	0	$(\delta_a + \delta_b)/g$
9	θ	$2\delta_a / g$
10	$-(\delta_a - s\theta)/s$	0

Table 2-30 Internal Work Associated with Each Yield Line in the Multiple Row Extended 1/3 Stiffened End-Plate (Part 1 of 2)

Yield Line	Internal Work	Simplified Internal Work	Number of Lines
1/3	$m_p\left[\left(d_e + p_{fo}\right)\left(\frac{2\delta_c}{g}\right)\right]$	$m_p\left[\frac{2}{g}\left(\delta_c d_e + \delta_c P_{fo}\right)\right]$	2
2/3	$m_p\left[\frac{g}{2}(\frac{\delta_c + d_e\theta}{d_e} - \theta) + d_e\left(\frac{2\delta_c}{g}\right)\right]$	$m_p\left[\frac{g}{2}(\frac{\delta_c}{d_e}) + \frac{2}{g}\left(\delta_c d_e\right)\right]$	2
2/4	$m_p\left[\frac{b_p - g}{2}\left(\frac{\delta_c + d_e\theta}{d_e} + \frac{\delta_c - p_{fo}\theta}{p_{fo}}\right)\right]$	$m_p\left[\frac{b_p}{2}\delta_c\left(\frac{1}{d_e} + \frac{1}{p_{fo}}\right) - \frac{g}{2}\delta_c\left(\frac{1}{d_e} + \frac{1}{p_{fo}}\right)\right]$	2
3/4	$m_p\left[\frac{g}{2}\left(\theta + \frac{\delta_c - p_{fo}\theta}{p_{fo}}\right) + p_{fo}\left(\frac{2\delta_c}{g}\right)\right]$	$m_p\left[\frac{g}{2}\left(\frac{\delta_c}{p_{fo}}\right) + \frac{2}{g}\left(\delta_c p_{fo}\right)\right]$	2
1/4	$m_p\left[\frac{b_p}{2}\left(\theta + \frac{\delta_c - p_{fo}\theta}{p_{fo}}\right)\right]$	$m_p\left[\frac{b_p}{2}\left(\frac{\delta_c}{p_{fo}}\right)\right]$	2
1/5	$m_p\left[\frac{b_p}{2}\left(\frac{\delta_b + p_{fi}\theta}{p_{fi}} - \theta\right)\right]$	$m_p\left[\frac{b_p}{2}\left(\frac{\delta_b}{p_{fi}}\right)\right]$	2
1/6	$m_p\left[\left(p_b + p_{fi}\right)\left(\frac{2\delta_b}{g}\right)\right]$	$m_p\left[\frac{2}{g}\left(\delta_b p_b + \delta_b p_{fi}\right)\right]$	2
5/6	$m_p\left[\frac{g}{2}\left(\frac{\delta_b + p_{fi}\theta}{p_{fi}} - \theta\right) + p_{fi}\left(\frac{2\delta_b}{g}\right)\right]$	$m_p\left[\frac{g}{2}\left(\frac{\delta_b}{p_{fi}}\right) + \frac{2}{g}\left(\delta_b p_{fi}\right)\right]$	2
5/7	$m_p\left[\frac{b_p - g}{2}\left(\frac{\delta_b + p_{fi}\theta}{p_{fi}}\right)\right]$	$m_p\left[\frac{b_p}{2}\left(\frac{\delta_b}{p_{fi}} + \theta\right) - \frac{g}{2}\left(\frac{\delta_b}{p_{fi}} + \theta\right)\right]$	2
6/8	$m_p\left[\frac{g}{2}(\theta) + p_b\left(\frac{2\delta_b}{g} - \frac{\delta_a + \delta_b}{g}\right)\right]$	$m_p\left\{\frac{g}{2}(\theta) + \frac{2}{g}\left[p_b\left(\frac{\delta_b - \delta_a}{2}\right)\right]\right\}$	2

Table 2-30 Internal Work Associated with Each Yield Line in the Multiple Row Extended 1/3 Stiffened End-Plate (Part 2 of 2)

7/8	$m_p\left[2p_b\left(\frac{\delta_a+\delta_b}{g}\right)\right]$	$m_p\left\{\frac{2}{g}\left[p_b\left(\delta_a+\delta_b\right)\right]\right\}$	2
8/9	$m_p\left[\frac{g}{2}(\theta)+p_b\left(\frac{\delta_a+\delta_b}{g}-\frac{2\delta_a}{g}\right)\right]$	$m_p\left\{\frac{g}{2}(\theta)+\frac{2}{g}\left[p_b\left(\frac{\delta_b-\delta_a}{2}\right)\right]\right\}$	2
7/10	$m_p\left[\frac{b_p-g}{2}\left(\frac{\delta_a-s\theta}{s}\right)\right]$	$m_p\left[\frac{b_p}{2}\left(\frac{\delta_a}{s}-\theta\right)-\frac{g}{2}\left(\frac{\delta_a}{s}-\theta\right)\right]$	2
1/9	$m_p\left[\left(p_b+s\right)\left(\frac{2\delta_a}{g}\right)\right]$	$m_p\left[\frac{2}{g}\left(\delta_a p_b+\delta_a s\right)\right]$	2
9/10	$m_p\left[\frac{g}{2}\left(\theta+\frac{\delta_a-s\theta}{s}\right)+s\left(\frac{2\delta_a}{g}\right)\right]$	$m_p\left[\frac{g}{2}\left(\frac{\delta_a}{s}\right)+\frac{2}{g}\left(\delta_a s\right)\right]$	2
1/10	$m_p\left[\frac{b_p}{2}\left(\theta+\frac{\delta_a-s\theta}{s}\right)\right]$	$m_p\left[\frac{b_p}{2}\left(\frac{\delta_a}{s}\right)\right]$	2

Summing up the internal work given in Table 2-30 and substituting $\delta_a = h_4\,\theta$, $\delta_b = h_2\,\theta$, *and* $\delta_c = h_1\,\theta$ results in the following equation for internal work:

$$W_I = 4m_p\theta\left\{\begin{array}{l}\frac{b_p}{2}\left[h_1\left(\frac{1}{p_{fo}}+\frac{1}{2d_e}\right)+h_2\left(\frac{1}{p_{fi}}\right)+h_4\left(\frac{1}{s}\right)\right]+\ldots\\ \frac{2}{g}\left[h_1\left(p_{fo}+d_e\right)+h_2\left(p_{fi}+\frac{3}{2}p_b\right)+h_4\left(s+\frac{1}{2}p_b\right)\right]+\frac{g}{2}\end{array}\right\} \quad (2\text{-}72)$$

The external work, W_E, is given by Eq. (2-73). Setting the internal work and external work equal results in Eq. (2-74).

$$W_E = M_{pl}\theta \quad (2\text{-}73)$$

$$M_{pl} = 4m_p\left\{\begin{array}{l}\frac{b_p}{2}\left[h_1\left(\frac{1}{p_{fo}}+\frac{1}{2d_e}\right)+h_2\left(\frac{1}{p_{fi}}\right)+h_4\left(\frac{1}{s}\right)\right]+\ldots\\ \frac{2}{g}\left[h_1\left(p_{fo}+d_e\right)+h_2\left(p_{fi}+\frac{3}{2}p_b\right)+h_4\left(s+\frac{1}{2}p_b\right)\right]+\frac{g}{2}\end{array}\right\} \quad (2\text{-}74)$$

This equation is further simplified into the form given in Eq. (2-75) by substituting the moment capacity per unit length, m_p, from Chapter 1, and defining the yield line parameter, Y, as given in Eq. (2-76).

$$M_{pl} = F_{yp}t_p{}^2Y \quad (2\text{-}75)$$

$$Y = \left\{ \begin{array}{l} \frac{b_p}{2}\left[h_1\left(\frac{1}{p_{fo}} + \frac{1}{2d_e} \right) + h_2\left(\frac{1}{p_{fi}} \right) + h_4\left(\frac{1}{s} \right) \right] + \ldots \\ \frac{2}{g}\left[h_1\left(p_{fo} + d_e \right) + h_2\left(p_{fi} + \frac{3}{2}p_b \right) + h_4\left(\frac{1}{2}p_b + s \right) \right] + \frac{g}{2} \end{array} \right\} \tag{2-76}$$

Note: Use $p_{fi}=s$ if $p_{fi} > s$ Use $p_{fo}=s$ if $p_{fo} > s$

To obtain an equation for the dimension s, the equation for moment strength, M_{pl}, is minimized. The derivative of Eq. (2-75), taken with respect to the variable s, is set equal to zero and solved for the variable s. The result is Eq. (2-77).

$$s = \frac{1}{2}\sqrt{b_p g} \tag{2-77}$$

2.12.1 Alternate Yield Line Pattern

The yield line pattern is shown in Figure 2-16. The rotation of each facet (facets are labeled in Figure 2-16) is given in Table 2-31 and the internal work associated with rotation along each yield line is given in Table 2-32. The yield lines are identified by the adjacent facet numbers (e.g., yield line 1/2 separates facets 1 and 2). Variables associated with the geometry of the connection are shown in Figure 2-16. Variables associated with the virtual rotations, displacement, and end-plate moment strength per unit length are described in Chapter 1. It is noted that hatched areas represent facets that are not rotating.

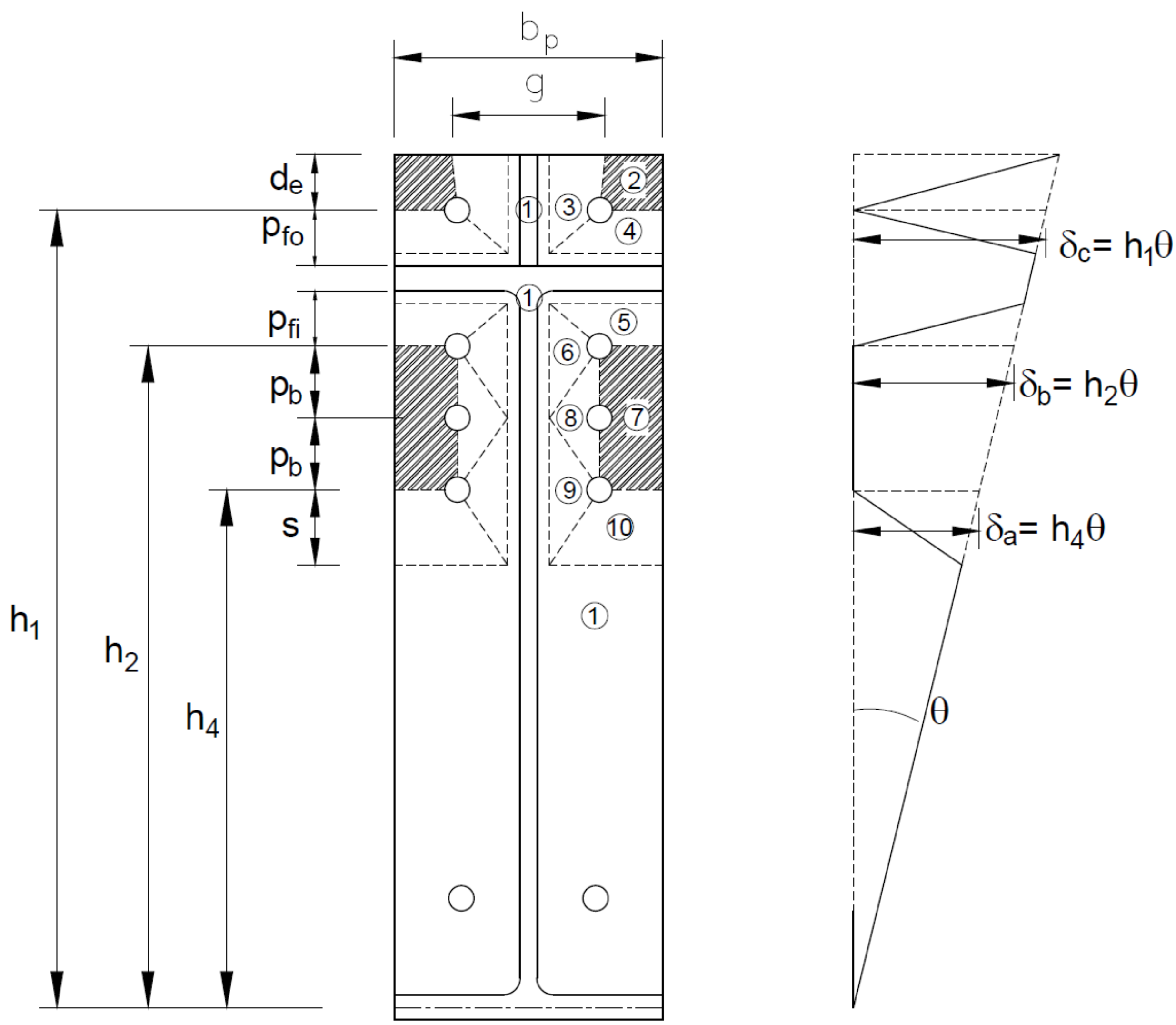

Figure 2-16 Alternative Yield Line Pattern for the Multiple Row Extended 1/3 Stiffened End-Plate

Table 2-31 Rotation for Each Facet in the Multiple Row Extended 1/3 Stiffened End-Plate

Facet	θ_x	θ_y
1	θ	0
2	0	0
3	θ	$2\delta_c / g$
4	$-(\delta_c - p_{fo}\theta)/p_{fo}$	0
5	$(\delta_b + p_{fi}\theta)/p_{fi}$	0
6	θ	$2\delta_b / g$
7	0	0
8	0	$(\delta_a + \delta_b)/g$
9	θ	$2\delta_a / g$
10	$-(\delta_a - s\theta)/s$	0

Table 2-32 Internal Work Associated with Each Yield Line in the Multiple Row Extended 1/3 Stiffened End-Plate (Part 1 of 2)

Yield Line	Internal Work	Simplified Internal Work	Number of Lines
1/3	$m_p\left[\left(d_e + p_{fo}\right)\left(\frac{2\delta_c}{g}\right)\right]$	$m_p\left[\frac{2}{g}\left(\delta_c d_e + \delta_c p_{fo}\right)\right]$	2
2/3	$m_p\left[d_e\left(\frac{2\delta_c}{g}\right)\right]$	$m_p\left[\frac{2}{g}\left(\delta_c d_e\right)\right]$	2
2/4	$m_p\left[\frac{b_p - g}{2}\left(\frac{\delta_c - p_{fo}\theta}{p_{fo}}\right)\right]$	$m_p\left[\frac{b_p}{2}\left(\frac{\delta_c}{p_{fo}} - \theta\right) - \frac{g}{2}\left(\frac{\delta_c}{p_{fo}} - \theta\right)\right]$	2
3/4	$m_p\left[\frac{g}{2}\left(\theta + \frac{\delta_c - p_{fo}\theta}{p_{fo}}\right) + p_{fo}\left(\frac{2\delta_c}{g}\right)\right]$	$m_p\left[\frac{g}{2}\left(\frac{\delta_c}{p_{fo}}\right) + \frac{2}{g}\left(\delta_c p_{fo}\right)\right]$	2
1/4	$m_p\left[\frac{b_p}{2}\left(\theta + \frac{\delta_c - p_{fo}\theta}{p_{fo}}\right)\right]$	$m_p\left[\frac{b_p}{2}\left(\frac{\delta_c}{p_{fo}}\right)\right]$	2
1/5	$m_p\left[\frac{b_p}{2}\left(\frac{\delta_b + p_{fi}\theta}{p_{fi}} - \theta\right)\right]$	$m_p\left[\frac{b_p}{2}\left(\frac{\delta_b}{p_{fi}}\right)\right]$	2
1/6	$m_p\left[\left(p_b + p_{fi}\right)\left(\frac{2\delta_b}{g}\right)\right]$	$m_p\left[\frac{2}{g}\left(\delta_b p_b + \delta_b p_{fi}\right)\right]$	2
5/6	$m_p\left[\frac{g}{2}\left(\frac{\delta_b + p_{fi}\theta}{p_{fi}} - \theta\right) + p_{fi}\left(\frac{2\delta_b}{g}\right)\right]$	$m_p\left[\frac{g}{2}\left(\frac{\delta_b}{p_{fi}}\right) + \frac{2}{g}\left(\delta_b p_{fi}\right)\right]$	2
5/7	$m_p\left[\frac{b_p - g}{2}\left(\frac{\delta_b + p_{fi}\theta}{p_{fi}}\right)\right]$	$m_p\left[\frac{b_p}{2}\left(\frac{\delta_b}{p_{fi}} + \theta\right) - \frac{g}{2}\left(\frac{\delta_b}{p_{fi}} + \theta\right)\right]$	2

Table 2-32 Internal Work Associated with Each Yield Line in the Multiple Row Extended 1/3 Stiffened End-Plate (Part 2 of 2)

6/8	$m_p\left[\frac{g}{2}(\theta)+p_b\left(\frac{2\delta_b}{g}-\frac{\delta_a+\delta_b}{g}\right)\right]$	$m_p\left\{\frac{g}{2}(\theta)+\frac{2}{g}\left[p_b\left(\frac{\delta_b-\delta_a}{2}\right)\right]\right\}$	2
7/8	$m_p\left[2p_b\left(\frac{\delta_a+\delta_b}{g}\right)\right]$	$m_p\left\{\frac{2}{g}\left[p_b\left(\delta_a+\delta_b\right)\right]\right\}$	2
8/9	$m_p\left[\frac{g}{2}(\theta)+p_b\left(\frac{\delta_a+\delta_b}{g}-\frac{2\delta_a}{g}\right)\right]$	$m_p\left\{\frac{g}{2}(\theta)+\frac{2}{g}\left[p_b\left(\frac{\delta_b-\delta_a}{2}\right)\right]\right\}$	2
7/10	$m_p\left[\frac{b_p-g}{2}\left(\frac{\delta_a-s\theta}{s}\right)\right]$	$m_p\left[\frac{b_p}{2}\left(\frac{\delta_a}{s}-\theta\right)-\frac{g}{2}\left(\frac{\delta_a}{s}-\theta\right)\right]$	2
1/9	$m_p\left[\left(p_b+s\right)\left(\frac{2\delta_a}{g}\right)\right]$	$m_p\left[\frac{2}{g}\left(\delta_a p_b+\delta_a s\right)\right]$	2
9/10	$m_p\left[\frac{g}{2}\left(\theta+\frac{\delta_a-s\theta}{s}\right)+s\left(\frac{2\delta_a}{g}\right)\right]$	$m_p\left[\frac{g}{2}\left(\frac{\delta_a}{s}\right)+\frac{2}{g}\left(\delta_a s\right)\right]$	2
1/10	$m_p\left[\frac{b_p}{2}\left(\theta+\frac{\delta_a-s\theta}{s}\right)\right]$	$m_p\left[\frac{b_p}{2}\left(\frac{\delta_a}{s}\right)\right]$	2

Summing up the internal work given in Table 2-32 and substituting $\delta_a = h_4\,\theta$, $\delta_b = h_2\,\theta$, *and* $\delta_c = h_1\,\theta$ results in the following equation for internal work:

$$W_I = 4m_p\theta\left\{\begin{array}{l}\frac{b_p}{2}\left[h_1\left(\frac{1}{p_{fo}}\right)+h_2\left(\frac{1}{p_{fi}}\right)+h_4\left(\frac{1}{s}\right)-\frac{1}{2}\right]+..\\ \frac{2}{g}\left[h_1\left(p_{fo}+d_e\right)+h_2\left(p_{fi}+\frac{3}{2}p_b\right)+h_4\left(\frac{1}{2}p_b+s\right)\right]+\frac{3g}{4}\end{array}\right\} \tag{2-78}$$

The external work, W_E, is given by Eq. (2-79). Setting the internal work and external work equal results in Eq. (2-80).

$$W_E = M_{pl}\theta \tag{2-79}$$

$$M_{pl} = 4m_p\left\{\begin{array}{l}\frac{b_p}{2}\left[h_1\left(\frac{1}{p_{fo}}\right)+h_2\left(\frac{1}{p_{fi}}\right)+h_4\left(\frac{1}{s}\right)-\frac{1}{2}\right]+..\\ \frac{2}{g}\left[h_1\left(p_{fo}+d_e\right)+h_2\left(p_{fi}+\frac{3}{2}p_b\right)+h_4\left(\frac{1}{2}p_b+s\right)\right]+\frac{3g}{4}\end{array}\right\} \tag{2-80}$$

This equation is further simplified into the form given in Eq. (2-81) by substituting the moment capacity per unit length, m_p, from Chapter 1, and defining the yield line parameter, Y, as given in Eq. (2-82).

$$M_{pl} = F_{yp}t_p{}^2Y \tag{2-81}$$

$$Y = \begin{Bmatrix} \frac{b_p}{2}\left[h_1\left(\frac{1}{p_{fo}}\right)+h_2\left(\frac{1}{p_{fi}}\right)+h_4\left(\frac{1}{s}\right)-\frac{1}{2}\right]+.. \\ \frac{2}{g}\left[h_1\left(p_{fo}+d_e\right)+h_2\left(p_{fi}+\frac{3}{2}p_b\right)+h_4\left(\frac{1}{2}p_b+s\right)\right]+\frac{3g}{4} \end{Bmatrix} \tag{2-82}$$

To obtain an equation for the dimension *s*, the equation for moment strength, M_{pl}, is minimized. The derivative of Eq. (2-81), taken with respect to the variable *s,* is set equal to zero and solved for the variable s. The result is Eq. (2-83).

$$s = \frac{1}{2}\sqrt{b_p g} \tag{2-83}$$

2.13 Eight Bolt Extended Four Wide Unstiffened End-Plate

The yield line pattern is shown in Figure 2-17. The rotation of each facet (facets are labeled in Figure 2-17) is given in Table 2-33 and the internal work associated with rotation along each yield line is given in Table 2-34. The yield lines are identified by the adjacent facet numbers (e.g., yield line 1/2 separates facets 1 and 2). Variables associated with the geometry of the connection are shown in Figure 2-17. Variables associated with the virtual rotations, displacement, and end-plate moment strength per unit length are described in Chapter 1. It is noted that hatched areas represent facets that are not rotating.

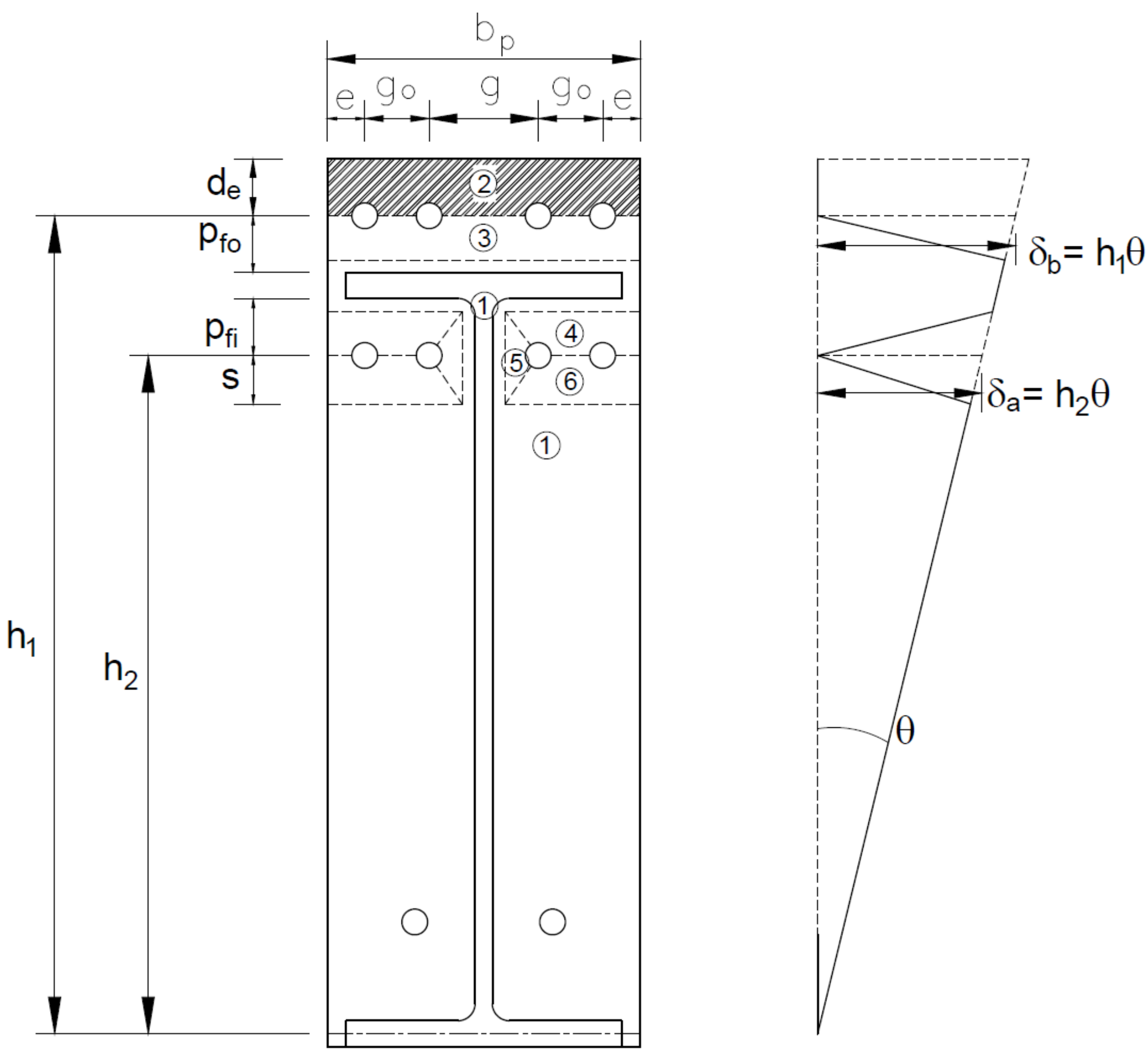

Figure 2-17 Yield Line Pattern for the Eight Bolt Extended Four Wide Unstiffened End-Plate

Table 2-33 Rotation for Each Facet in the Eight Bolt Extended Four Wide Unstiffened End-Plate

Facet	θ_x	θ_y
1	θ	0
2	0	0
3	$-(\delta_b - p_{fo}\theta)/p_{fo}$	0
4	$(\delta_a + p_{fi}\theta)/p_{fi}$	0
5	θ	$2\delta_a / g$
6	$-(\delta_a - s\theta)/s$	0

Table 2-34 Internal Work Associated with Each Yield Line in the Eight Bolt Extended Four Wide Unstiffened End-Plate

Yield Line	Internal Work	Simplified Internal Work	Number of Lines
2/3	$m_p\left[b_p\left(\frac{\delta_b - p_{fo}\theta}{p_{fo}}\right)\right]$	$m_p\left[\frac{b_p}{2}\left(\frac{2\delta_b}{p_{fo}} - 2\theta\right)\right]$	1
1/3	$m_p\left[b_p\left(\theta + \frac{\delta_b - p_{fo}\theta}{p_{fo}}\right)\right]$	$m_p\left[\frac{b_p}{2}\left(\frac{2\delta_b}{p_{fo}}\right)\right]$	1
1/4	$m_p\left[\frac{b_p}{2}\left(\frac{\delta_a + p_{fi}\theta}{p_{fi}} - \theta\right)\right]$	$m_p\left[\frac{b_p}{2}\left(\frac{\delta_a}{p_{fi}}\right)\right]$	2
4/5	$m_p\left[\frac{g}{2}\left(\frac{\delta_a + p_{fi}\theta}{p_{fi}} - \theta\right) + p_{fi}\left(\frac{2\delta_a}{g}\right)\right]$	$m_p\left[\frac{g}{2}\left(\frac{\delta_a}{p_{fi}}\right) + \frac{2}{g}\left(p_{fi}\delta_a\right)\right]$	2
5/6	$m_p\left[\frac{g}{2}\left(\theta + \frac{\delta_a - s\theta}{s}\right) + s\left(\frac{2\delta_a}{g}\right)\right]$	$m_p\left[\frac{g}{2}\left(\frac{\delta_a}{s}\right) + \frac{2}{g}\left(s\delta_a\right)\right]$	2
1/5	$m_p\left[\left(p_{fi} + s\right)\left(\frac{2\delta_a}{g}\right)\right]$	$m_p\left[\frac{2}{g}\left(\delta_a p_{fi} + \delta_a s\right)\right]$	2
4/6	$m_p\left[\frac{b_p - g}{2}\left(\frac{\delta_a + p_{fi}\theta}{p_{fi}} + \frac{\delta_a - s\theta}{s}\right)\right]$	$m_p\left[\frac{b_p}{2}\left(\frac{\delta_a}{p_{fi}} + \frac{\delta_a}{s}\right) - \frac{g}{2}\left(\frac{\delta_a}{p_{fi}} + \frac{\delta_a}{s}\right)\right]$	2
1/6	$m_p\left[\frac{b_p}{2}\left(\theta + \frac{\delta_a - s\theta}{s}\right)\right]$	$m_p\left[\frac{b_p}{2}\left(\frac{\delta_a}{s}\right)\right]$	2

Summing up the internal work given in Table 2-34 and substituting $\delta_a = h_2\,\theta$ and $\delta_b = h_1\,\theta$ results in the following equation for internal work:

$$W_I = 4m_p\theta\left\{\frac{b_p}{2}\left[h_1\left(\frac{1}{p_{fo}}\right)+h_2\left(\frac{1}{p_{fi}}+\frac{1}{s}\right)-\frac{1}{2}\right]+\frac{2}{g}\left[h_2\left(p_{fi}+s\right)\right]\right\} \tag{2-84}$$

The external work, W_E, is given by Eq. (2-85). Setting the internal work and external work equal results in Eq. (2-86).

$$W_E = M_{pl}\theta \tag{2-85}$$

$$M_{pl} = 4m_p\left\{\frac{b_p}{2}\left[h_1\left(\frac{1}{p_{fo}}\right)+h_2\left(\frac{1}{p_{fi}}+\frac{1}{s}\right)-\frac{1}{2}\right]+\frac{2}{g}\left[h_2\left(p_{fi}+s\right)\right]\right\} \tag{2-86}$$

This equation is further simplified into the form given in Eq. (2-87) by substituting the moment capacity per unit length, m_p, from Chapter 1, and defining the yield line parameter, Y, as given in Eq. (2-88).

$$M_{pl} = F_{yp}t_p{}^2Y \tag{2-87}$$

$$Y = \frac{b_p}{2}\left[h_1\left(\frac{1}{p_{fo}}\right)+h_2\left(\frac{1}{p_{fi}}+\frac{1}{s}\right)-\frac{1}{2}\right]+\frac{2}{g}\left[h_2\left(p_{fi}+s\right)\right] \tag{2-88}$$

Note: Use p_{fi}=s if $p_{fi} > s$

To obtain an equation for the dimension s, the equation for moment strength, M_{pl}, is minimized. The derivative of Eq. (2-87), taken with respect to the variable s, is set equal to zero and solved for the variable s. The result is Eq. (2-89).

$$s = \frac{1}{2}\sqrt{b_p g} \tag{2-89}$$

2.14 Eight Bolt Extended Stiffened End-Plate

The yield line pattern is shown in Figure 2-18. The rotation of each facet (facets are labeled in Figure 2-18) is given in Table 2-35 and the internal work associated with rotation along each yield line is given in Table 2-36. The yield lines are identified by the adjacent facet numbers (e.g., yield line 1/2 separates facets 1 and 2). Variables associated with the geometry of the connection are shown in Figure 2-18. Variables associated with the virtual rotations, displacement, and end-plate moment strength per unit length are described in Chapter 1. It is noted that hatched areas represent facets that are not rotating.

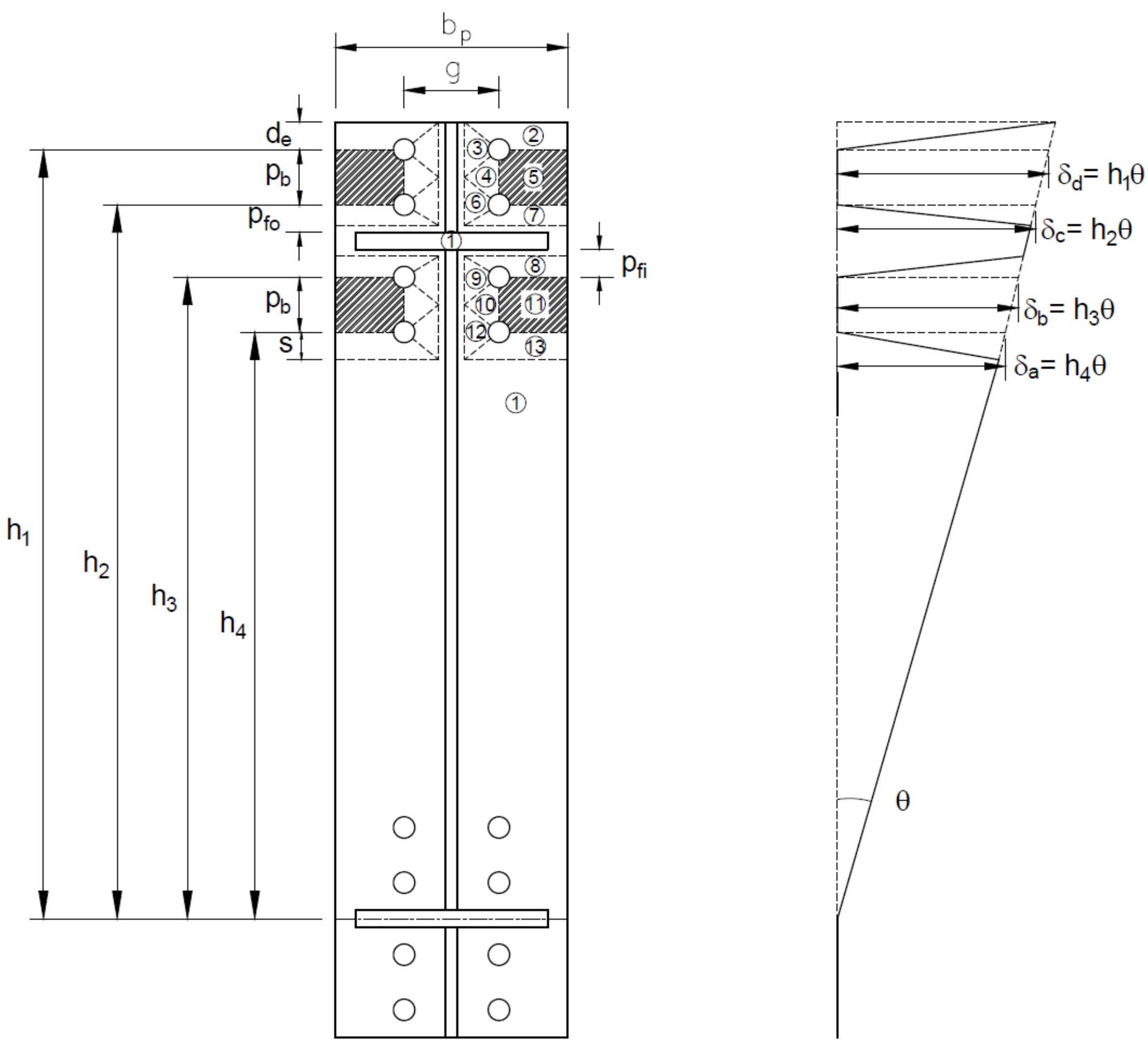

Figure 2-18 Yield Line Pattern for the Eight Bolt Extended Stiffened End-Plate

Table 2-35 Rotation for Each Facet in the Eight Bolt Extended Stiffened End-Plate

Facet	θ_x	θ_y
1	θ	0
2	$(\delta_d + d_e\theta)/d_e$	0
3	θ	$2\delta_d/g$
4	0	$(\delta_c+\delta_d)/g$
5	0	0
6	0	$2\delta_c/g$
7	$-(\delta_c - p_{fo}\theta)/p_{fo}$	0
8	$(\delta_b + p_{fi}\theta)/p_{fi}$	0
9	θ	$2\delta_b/g$
10	0	$(\delta_a+\delta_b)/g$
11	0	0
12	θ	$2\delta_a/g$
13	$-(\delta_a - s\theta)/s$	0

Table 2-36 Internal Work Associated with Each Yield Line in the Eight Bolt Extended Stiffened End-Plate (Part 1 of 2)

Yield Line	Internal Work	Simplified Internal Work	Number of Lines
2/3	$m_p[\frac{g}{2}(\frac{\delta_d + d_e\theta}{d_e} - \theta) + d_e\frac{2\delta_d}{g}]$	$m_p[\frac{g}{2}(\frac{\delta_d}{d_e}) + \frac{2}{g}(\delta_d d_e)]$	2
2/5	$m_p[\frac{b_p - g}{2}(\frac{\delta_d + d_e\theta}{d_e})]$	$m_p[\frac{b_p}{2}(\frac{\delta_d}{d_e}+\theta) - \frac{g}{2}(\frac{\delta_d}{d_e}+\theta)]$	2
1/3	$m_p[(d_e + \frac{p_b}{2})\frac{2\delta_d}{g}]$	$m_p[\frac{2}{g}\delta_d(d_e + \frac{p_b}{2})]$	2
3/4	$m_p[\frac{g}{2}\theta + \frac{p_b}{2}(\frac{2\delta_d}{g} - \frac{\delta_c+\delta_d}{g})]$	$m_p\left\{\frac{g}{2}(\theta) + \frac{2}{g}\left[\frac{p_b(\delta_d - \delta_c)}{4}\right]\right\}$	2
4/5	$m_p\left[p_b\left(\frac{\delta_c+\delta_d}{g}\right)\right]$	$m_p\left[\frac{2}{g}\left(\frac{p_b\delta_c + p_b\delta_d}{2}\right)\right]$	2
4/6	$m_p\left[\frac{g}{2}(\theta) + \frac{p_b}{2}\left(\frac{\delta_c+\delta_d}{g} - \frac{2\delta_c}{g}\right)\right]$	$m_p\left[\frac{g}{2}(\theta) + \frac{2}{g}\left(\frac{p_b(\delta_c+\delta_d)}{4} - \frac{p_b\delta_c}{2}\right)\right]$	2

Table 2-36 Internal Work Associated with Each Yield Line in the Eight Bolt Extended Stiffened End-Plate (Part 2 of 2)

Yield Line	Internal Work	Simplified Internal Work	Number of Lines
1/6	$m_p\left[\left(p_{fo}+\frac{p_b}{2}\right)\left(\frac{2\delta_c}{g}\right)\right]$	$m_p\left[\frac{2}{g}\left(\delta_c p_{fo}+\frac{\delta_c p_b}{2}\right)\right]$	2
6/7	$m_p\left[\frac{g}{2}\left(\theta+\frac{\delta_c-p_{fo}\theta}{p_{fo}}\right)+p_{fo}\left(\frac{2\delta_c}{g}\right)\right]$	$m_p\left[\frac{g}{2}\left(\frac{\delta_c}{p_{fo}}\right)+\frac{2}{g}\left(\delta_c p_{fo}\right)\right]$	2
5/7	$m_p\left[\frac{b_p-g}{2}\left(\frac{\delta_c-p_{fo}\theta}{p_{fo}}\right)\right]$	$m_p\left[\frac{b_p}{2}\left(\frac{\delta_c}{p_{fo}}-\theta\right)-\frac{g}{2}\left(\frac{\delta_c}{p_{fo}}-\theta\right)\right]$	2
1/7	$m_p\left[\frac{b_p}{2}\left(\theta+\frac{\delta_c-p_{fo}\theta}{p_{fo}}\right)\right]$	$m_p\left[\frac{b_p}{2}\left(\frac{\delta_c}{p_{fo}}\right)\right]$	2
1/8	$m_p\left[\frac{b_p}{2}\left(\frac{\delta_b+p_{fi}\theta}{p_{fi}}-\theta\right)\right]$	$m_p\left[\frac{b_p}{2}\left(\frac{\delta_b}{p_{fi}}\right)\right]$	2
8/9	$m_p\left[\frac{g}{2}\left(\frac{\delta_b+p_{fi}\theta}{p_{fi}}-\theta\right)+p_{fi}\left(\frac{2\delta_b}{g}\right)\right]$	$m_p\left[\frac{g}{2}\left(\frac{\delta_b}{p_{fi}}\right)+\frac{2}{g}\left(p_{fi}\delta_b\right)\right]$	2
8/11	$m_p\left[\frac{b_p-g}{2}\left(\frac{\delta_b+p_{fi}\theta}{p_{fi}}\right)\right]$	$m_p\left[\frac{b_p}{2}\left(\frac{\delta_b}{p_{fi}}+\theta\right)-\frac{g}{2}\left(\frac{\delta_b}{p_{fi}}+\theta\right)\right]$	2
1/9	$m_p\left[\left(p_{fi}+\frac{p_b}{2}\right)\left(\frac{2\delta_b}{g}\right)\right]$	$m_p\left[\frac{2}{g}\left(\delta_b p_{fi}+\frac{\delta_b p_b}{2}\right)\right]$	2
9/10	$m_p\left[\frac{g}{2}(\theta)+\frac{p_b}{2}\left(\frac{2\delta_b}{g}-\frac{\delta_a+\delta_b}{g}\right)\right]$	$m_p\left\{\frac{g}{2}(\theta)+\frac{2}{g}\left[\frac{p_b\left(\delta_b-\delta_a\right)}{4}\right]\right\}$	2
10/11	$m_p\left[p_b\left(\frac{\delta_a+\delta_b}{g}\right)\right]$	$m_p\left\{\frac{2}{g}\left[\frac{p_b\left(\delta_a+\delta_b\right)}{2}\right]\right\}$	2
10/12	$m_p\left[\frac{g}{2}(\theta)+\frac{p_b}{2}\left(\frac{\delta_a+\delta_b}{g}-\frac{2\delta_a}{g}\right)\right]$	$m_p\left\{\frac{g}{2}(\theta)+\frac{2}{g}\left[\frac{p_b\left(\delta_b-\delta_a\right)}{4}\right]\right\}$	2
11/13	$m_p\left[\frac{b_p-g}{2}\left(\frac{\delta_a-s\theta}{s}\right)\right]$	$m_p\left[\frac{b_p}{2}\left(\frac{\delta_a}{s}-\theta\right)-\frac{g}{2}\left(\frac{\delta_a}{s}-\theta\right)\right]$	2
12/13	$m_p\left[\frac{g}{2}\left(\theta+\frac{\delta_a-s\theta}{s}\right)+s\left(\frac{2\delta_a}{g}\right)\right]$	$m_p\left[\frac{g}{2}\left(\frac{\delta_a}{s}\right)+\frac{2}{g}\left(s\delta_a\right)\right]$	2
1/12	$m_p\left[\left(s+\frac{p_b}{2}\right)\left(\frac{2\delta_a}{g}\right)\right]$	$m_p\left[\frac{2}{g}\left(\delta_a s+\frac{\delta_a p_b}{2}\right)\right]$	2
1/13	$m_p\left[\frac{b_p}{2}\left(\theta+\frac{\delta_a-s\theta}{s}\right)\right]$	$m_p\left[\frac{b_p}{2}\left(\frac{\delta_a}{s}\right)\right]$	2

Summing up the internal work given in Table 2-36 and substituting $\delta_a = h_4\,\theta$, $\delta_b = h_3\,\theta$, $\delta_c = h_2\,\theta$, and $\delta_d = h_1\,\theta$ results in the following equation for internal work:

$$W_I = 4m_p\theta\left\{\begin{aligned}&\frac{b_p}{2}\left[h_1\left(\frac{1}{2d_e}\right)+h_2\left(\frac{1}{p_{fo}}\right)+h_3\left(\frac{1}{p_{fi}}\right)+h_4\left(\frac{1}{s}\right)\right]+...\\&\frac{2}{g}\left[h_1\left(\frac{3p_b}{4}+d_e\right)+h_2\left(\frac{p_b}{4}+p_{fo}\right)+h_3\left(\frac{3p_b}{4}+p_{fi}\right)+h_4\left(\frac{p_b}{4}+s\right)\right]+g\end{aligned}\right\} \tag{2-90}$$

The external work, W_E, is given by Eq. (2-91). Setting the internal work and external work equal results in Eq. (2-92).

$$W_E = M_{pl}\theta \tag{2-91}$$

$$M_{pl} = 4m_p\left\{\begin{aligned}&\frac{b_p}{2}\left[h_1\left(\frac{1}{2d_e}\right)+h_2\left(\frac{1}{p_{fo}}\right)+h_3\left(\frac{1}{p_{fi}}\right)+h_4\left(\frac{1}{s}\right)\right]+...\\&\frac{2}{g}\left[h_1\left(\frac{3p_b}{4}+d_e\right)+h_2\left(\frac{p_b}{4}+p_{fo}\right)+h_3\left(\frac{3p_b}{4}+p_{fi}\right)+h_4\left(\frac{p_b}{4}+s\right)\right]+g\end{aligned}\right\} \tag{2-92}$$

This equation is further simplified into the form given in Eq. (2-93) by substituting the moment capacity per unit length, m_p, from Chapter 1, and defining the yield line parameter, Y, as given in Eq. (2-94).

$$M_{pl} = F_{yp}t_p^{\,2}Y \tag{2-93}$$

$$Y = \left\{\begin{aligned}&\frac{b_p}{2}\left[h_1\left(\frac{1}{2d_e}\right)+h_2\left(\frac{1}{p_{fo}}\right)+h_3\left(\frac{1}{p_{fi}}\right)+h_4\left(\frac{1}{s}\right)\right]+...\\&\frac{2}{g}\left[h_1\left(\frac{3p_b}{4}+d_e\right)+h_2\left(\frac{p_b}{4}+p_{fo}\right)+h_3\left(\frac{3p_b}{4}+p_{fi}\right)+h_4\left(\frac{p_b}{4}+s\right)\right]+g\end{aligned}\right\} \tag{2-94}$$

Note: Use $p_{fi}=s$ if $p_{fi} > s$ Use $p_{fo}=s$ if $p_{fo} > s$

To obtain an equation for the dimension s, the equation for moment strength, M_{pl}, is minimized. The derivative of Eq. (2-93), taken with respect to the variable s, is set equal to zero and solved for the variable s. The result is Eq. (2-95).

$$s = \frac{1}{2}\sqrt{b_p g} \tag{2-95}$$

Equation (2-88) is the yield line pattern used in **AISC Design Guide 4** (Murray and Sumner 2004) and **AISC 358-18**. It has been validated against experiments in past research and therefore is used in design.

2.14.1 Alternate Yield Line Pattern

An alternate yield line pattern which produces a smaller yield line parameter for the Eight-Bolt Extended Stiffened End-Plate is shown in Figure 2-19. The rotation of each facet (facets are labeled in Figure 2-19) is given in Table 2-37 and the internal work associated with rotation along each yield line is given in Table 2-38. The yield lines are identified by the adjacent facet numbers (e.g., yield line 1/2 separates facets 1 and 2 Variables associated with the geometry of the connection are shown in Figure 2-19. Variables associated with the virtual rotations, displacement, and end-plate moment strength per unit length are described in Chapter 1). It is noted that hatched areas represent facets that are not rotating.

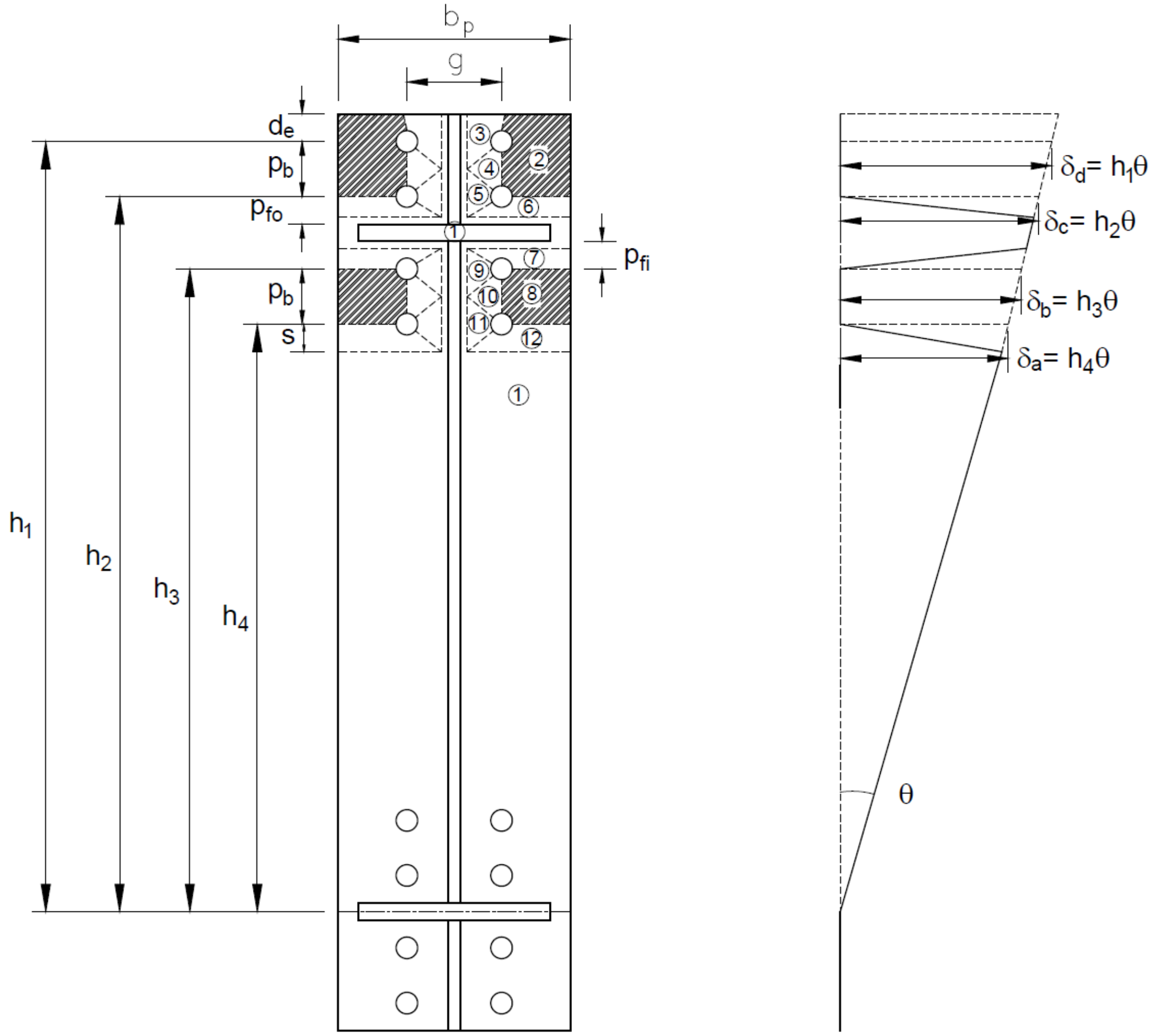

Figure 2-19 Alternative Yield Line Pattern for the Eight Bolt Extended Stiffened End-Plate

Table 2-37 Rotation for Each Facet in the Eight Bolt Extended Stiffened End-Plate

Facet	θ_x	θ_y
1	θ	0
2	0	0
3	θ	$2\delta_d / g$
4	0	$(\delta_c + \delta_d) / g$
5	θ	$2\delta_c / g$
6	$-(\delta_c - p_{fo}\theta) / p_{fo}$	0
7	$(\delta_b + p_{fi}\theta) / p_{fi}$	0
8	0	0
9	θ	$2\delta_b / g$
10	0	$(\delta_a + \delta_b) / g$
11	θ	$2\delta_a / g$
12	$-(\delta_a - s\theta) / s$	0

Table 2-38 Internal Work Associated with Each Yield Line in the Eight Bolt Extended Stiffened End-Plate (Part 1 of 2)

Yield Line	Internal Work	Simplified Internal Work	Number of Lines
1/3	$m_p\left[\left(d_e + \frac{p_b}{2}\right)\left(\frac{2\delta_d}{g}\right)\right]$	$m_p\left[\frac{2}{g}\left(\delta_d d_e + \frac{\delta_d p_b}{2}\right)\right]$	2
1/5	$m_p\left[\left(P_{fo} + \frac{p_b}{2}\right)\left(\frac{2\delta_c}{g}\right)\right]$	$m_p\left[\frac{2}{g}\left(\delta_c p_{fo} + \frac{\delta_c p_b}{2}\right)\right]$	2
2/3	$m_p\left[d_e\left(\frac{2\delta_d}{g}\right)\right]$	$m_p\left[\frac{2}{g}(d_e\delta_d)\right]$	2
3/4	$m_p\left[\frac{g}{2}(\theta) + \frac{p_b}{2}\left(\frac{2\delta_d}{g} - \frac{\delta_c + \delta_d}{g}\right)\right]$	$m_p\left[\frac{g}{2}(\theta) + \frac{2}{g}\left(\frac{p_b\delta_d}{2} - \frac{p_b(\delta_c + \delta_d)}{4}\right)\right]$	2
4/5	$m_p\left[\frac{g}{2}(\theta) + \frac{p_b}{2}\left(\frac{\delta_c + \delta_d}{g} - \frac{2\delta_c}{g}\right)\right]$	$m_p\left[\frac{g}{2}(\theta) + \frac{2}{g}\left(\frac{p_b(\delta_c + \delta_d)}{4} - \frac{p_b\delta_c}{2}\right)\right]$	2
5/6	$m_p\left[\frac{g}{2}\left(\theta + \frac{\delta_c - p_{fo}\theta}{p_{fo}}\right) + p_{fo}\left(\frac{2\delta_c}{g}\right)\right]$	$m_p\left[\frac{g}{2}\left(\frac{\delta_c}{p_{fo}}\right) + \frac{2}{g}(\delta_c p_{fo})\right]$	2

Table 2-38 Internal Work Associated with Each Yield Line in the Eight Bolt Extended Stiffened End-Plate (Part 2 of 2)

Yield Line	Internal Work	Simplified Internal Work	Number of Lines
4/2	$m_p\left[p_b\left(\frac{\delta_c+\delta_d}{g}\right)\right]$	$m_p\left[\frac{2}{g}\left(\frac{p_b\delta_c+p_b\delta_d}{2}\right)\right]$	2
2/6	$m_p\left[\frac{b_p-g}{2}\left(\frac{\delta_c-p_{fo}\theta}{p_{fo}}\right)\right]$	$m_p\left[\frac{b_p}{2}\left(\frac{\delta_c}{p_{fo}}-\theta\right)-\frac{g}{2}\left(\frac{\delta_c}{p_{fo}}-\theta\right)\right]$	2
1/6	$m_p\left[\frac{b_p}{2}\left(\theta+\frac{\delta_c-p_{fo}\theta}{p_{fo}}\right)\right]$	$m_p\left[\frac{b_p}{2}\left(\frac{\delta_c}{p_{fo}}\right)\right]$	2
1/7	$m_p\left[\frac{b_p}{2}\left(\frac{\delta_b+p_{fi}\theta}{p_{fi}}-\theta\right)\right]$	$m_p\left[\frac{b_p}{2}\left(\frac{\delta_b}{p_{fi}}\right)\right]$	2
7/9	$m_p\left[\frac{g}{2}\left(\frac{\delta_b+p_{fi}\theta}{p_{fi}}-\theta\right)+p_{fi}\left(\frac{2\delta_b}{g}\right)\right]$	$m_p\left[\frac{g}{2}\left(\frac{\delta_b}{p_{fi}}\right)+\frac{2}{g}\left(p_{fi}\delta_b\right)\right]$	2
1/9	$m_p\left[\left(p_{fi}+\frac{p_b}{2}\right)\left(\frac{2\delta_b}{g}\right)\right]$	$m_p\left[\frac{2}{g}\left(\delta_b p_{fi}+\frac{\delta_b p_b}{2}\right)\right]$	2
1/11	$m_p\left[\left(s+\frac{p_b}{2}\right)\left(\frac{2\delta_a}{g}\right)\right]$	$m_p\left[\frac{2}{g}\left(\delta_a s+\frac{\delta_a p_b}{2}\right)\right]$	2
9/10	$m_p\left[\frac{g}{2}(\theta)+\frac{p_b}{2}\left(\frac{2\delta_b}{g}-\frac{\delta_a+\delta_b}{g}\right)\right]$	$m_p\left\{\frac{g}{2}(\theta)+\frac{2}{g}\left[\frac{p_b\left(\delta_b-\delta_a\right)}{4}\right]\right\}$	2
10/11	$m_p\left[\frac{g}{2}(\theta)+\frac{p_b}{2}\left(\frac{\delta_a+\delta_b}{g}-\frac{2\delta_a}{g}\right)\right]$	$m_p\left\{\frac{g}{2}(\theta)+\frac{2}{g}\left[\frac{p_b\left(\delta_b-\delta_a\right)}{4}\right]\right\}$	2
11/12	$m_p\left[\frac{g}{2}\left(\theta+\frac{\delta_a-s\theta}{s}\right)+s\left(\frac{2\delta_a}{g}\right)\right]$	$m_p\left[\frac{g}{2}\left(\frac{\delta_a}{s}\right)+\frac{2}{g}\left(s\delta_a\right)\right]$	2
10/8	$m_p\left[p_b\left(\frac{\delta_a+\delta_b}{g}\right)\right]$	$m_p\left\{\frac{2}{g}\left[\frac{p_b\left(\delta_a+\delta_b\right)}{2}\right]\right\}$	2
7/8	$m_p\left[\frac{b_p-g}{2}\left(\frac{\delta_b+p_{fi}\theta}{p_{fi}}\right)\right]$	$m_p\left[\frac{b_p}{2}\left(\frac{\delta_b}{p_{fi}}+\theta\right)-\frac{g}{2}\left(\frac{\delta_b}{p_{fi}}+\theta\right)\right]$	2
8/12	$m_p\left[\frac{b_p-g}{2}\left(\frac{\delta_a-s\theta}{s}\right)\right]$	$m_p\left[\frac{b_p}{2}\left(\frac{\delta_a}{s}-\theta\right)-\frac{g}{2}\left(\frac{\delta_a}{s}-\theta\right)\right]$	2
1/12	$m_p\left[\frac{b_p}{2}\left(\theta+\frac{\delta_a-s\theta}{s}\right)\right]$	$m_p\left[\frac{b_p}{2}\left(\frac{\delta_a}{s}\right)\right]$	2

Summing up the internal work given in Table 2-38 and substituting $\delta_a = h_4\theta$, $\delta_b = h_3\theta$, $\delta_c = h_2\,\theta$, and $\delta_d = h_1\,\theta$ results in the following equation for internal work:

$$W_I = 4m_p\theta \left\{ \begin{array}{l} \dfrac{b_p}{2}\left[h_2\left(\dfrac{1}{p_{fo}}\right) + h_3\left(\dfrac{1}{p_{fi}}\right) + h_4\left(\dfrac{1}{s}\right) - \dfrac{1}{2} \right] + \ldots \\ \dfrac{2}{g}\left[h_1\left(\dfrac{3p_b}{4} + d_e\right) + h_2\left(\dfrac{p_b}{4} + p_{fo}\right) + h_3\left(\dfrac{3p_b}{4} + p_{fi}\right) + h_4\left(\dfrac{p_b}{4} + s\right) \right] + \dfrac{5g}{4} \end{array} \right\} \tag{2-96}$$

The external work, W_E, is given by Eq. (2-97). Setting the internal work and external work equal results in Eq. (2-98).

$$W_E = M_{pl}\theta \tag{2-97}$$

$$M_{pl} = 4m_p \left\{ \begin{array}{l} \dfrac{b_p}{2}\left[h_2\left(\dfrac{1}{p_{fo}}\right) + h_3\left(\dfrac{1}{p_{fi}}\right) + h_4\left(\dfrac{1}{s}\right) - \dfrac{1}{2} \right] + \ldots \\ \dfrac{2}{g}\left[h_1\left(\dfrac{3p_b}{4} + d_e\right) + h_2\left(\dfrac{p_b}{4} + p_{fo}\right) + h_3\left(\dfrac{3p_b}{4} + p_{fi}\right) + h_4\left(\dfrac{p_b}{4} + s\right) \right] + \dfrac{5g}{4} \end{array} \right\} \tag{2-98}$$

This equation is further simplified into the form given in Eq. (2-99) by substituting the moment capacity per unit length, m_p, from Chapter 1, and defining the yield line parameter, Y, as given in Eq. (2-100).

$$M_{pl} = F_{yp}t_p^{\,2}Y \tag{2-99}$$

$$Y = \left\{ \begin{array}{l} \dfrac{b_p}{2}\left[h_2\left(\dfrac{1}{p_{fo}}\right) + h_3\left(\dfrac{1}{p_{fi}}\right) + h_4\left(\dfrac{1}{s}\right) - \dfrac{1}{2} \right] + \ldots \\ \dfrac{2}{g}\left[h_1\left(\dfrac{3p_b}{4} + d_e\right) + h_2\left(\dfrac{p_b}{4} + p_{fo}\right) + h_3\left(\dfrac{3p_b}{4} + p_{fi}\right) + h_4\left(\dfrac{p_b}{4} + s\right) \right] + \dfrac{5g}{4} \end{array} \right\} \tag{2-100}$$

Note: Use $p_{fi}=s$ if $p_{fi} > s$ Use $p_{fo}=s$ if $p_{fo} > s$

To obtain an equation for the dimension s, the equation for moment strength, M_{pl}, is minimized. The derivative of Eq. (2-99), taken with respect to the variable s, is set equal to zero and solved for the variable s. The result is Eq. (2-101).

$$s = \frac{1}{2}\sqrt{b_p g} \tag{2-101}$$

2.15 Twelve Bolt Multiple Row Extended 1/3 Four-Wide / Two-Wide Unstiffened End-Plate

The yield line pattern is shown in Figure 2-20. The rotation of each facet (facets are labeled in Figure 2-20) is given in Table 2-39 and the internal work associated with rotation along each yield line is given in Table 2-40. The yield lines are identified by the adjacent facet numbers (e.g., yield line 1/2 separates facets 1 and 2). Variables associated with the geometry of the connection are shown in Figure 2-20. Variables associated with the virtual rotations, displacement, and end-plate moment strength per unit length are described in Chapter 1. It is noted that hatched areas represent facets that are not rotating.

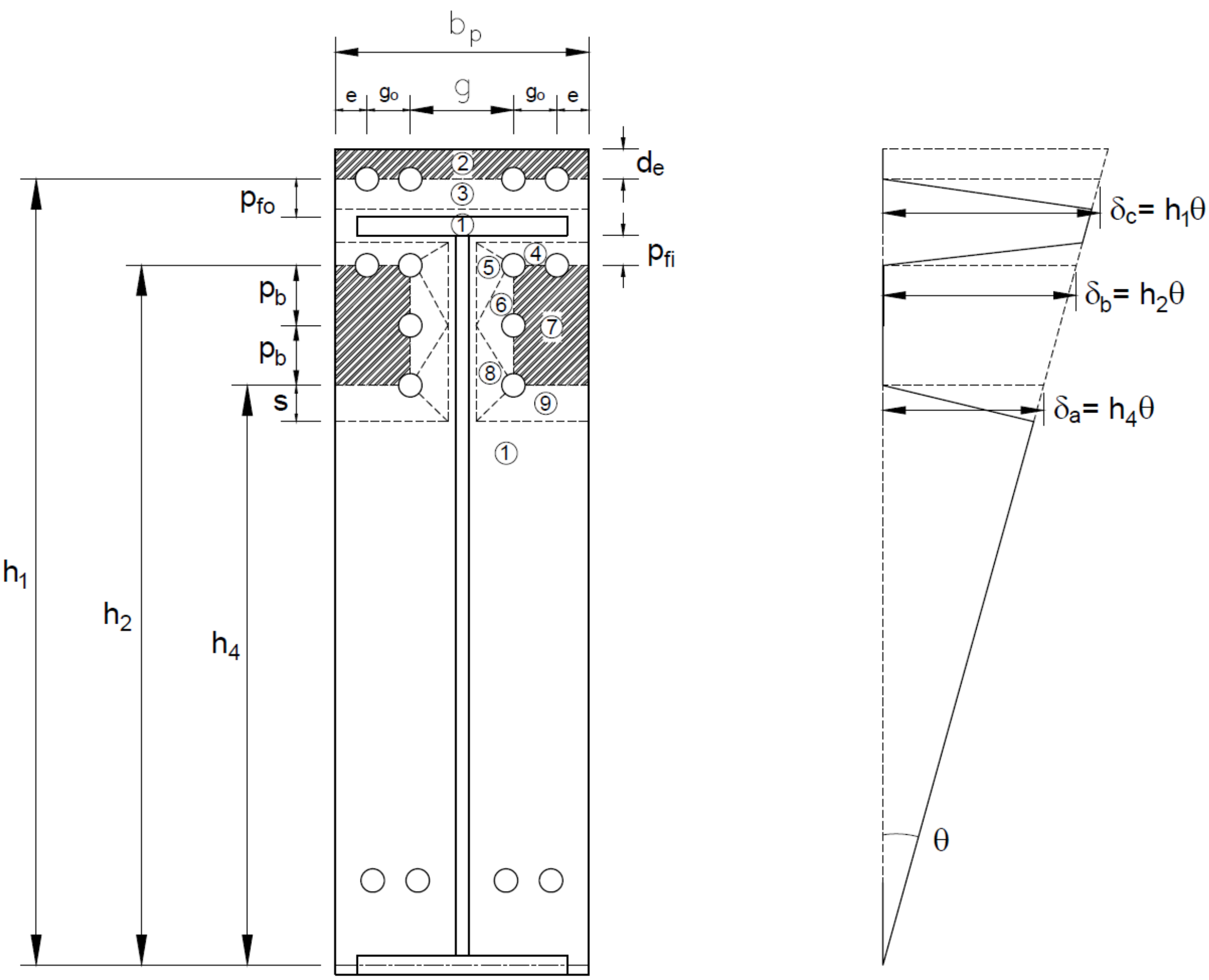

Figure 2-20 Yield Line Pattern for the
Twelve Bolt MRE 1/3 Four-Wide / Two-Wide Unstiffened End-Plate

Table 2-39 Rotation for Each Facet in the Twelve Bolt MRE 1/3 Four-Wide / Two-Wide Unstiffened End-Plate

Facet	θ_x	θ_y
1	θ	0
2	0	0
3	$-(\delta_c - p_{fo}\theta)/p_{fo}$	0
4	$(\delta_b + p_{fi}\theta)/p_{fi}$	0
5	θ	$2\delta_b/g$
6	0	$(\delta_b + \delta_a)/g$
7	0	0
8	θ	$2\delta_a/g$
9	$-(\delta_a - s\theta)/s$	0

Table 2-40 Internal Work Associated with Each Yield Line in the Twelve Bolt MRE 1/3 Four-Wide / Two-Wide Unstiffened End-Plate (Part 1 of 2)

Yield Line	Internal Work	Simplified Internal Work	Number of Lines
2/3	$m_p\left[b_p\left(\frac{\delta_c - p_{fo}\theta}{p_{fo}}\right)\right]$	$m_p\left[\frac{b_p}{2}\left(\frac{2\delta_c - 2p_{fo}\theta}{p_{fo}}\right)\right]$	1
1/3	$m_p\left[b_p\left(\theta+\frac{\delta_c - p_{fo}\theta}{p_{fo}}\right)\right]$	$m_p\left[\frac{b_p}{2}\left(\frac{2\delta_c}{p_{fo}}\right)\right]$	1
1/4	$m_p\left[\frac{b_p}{2}\left(\frac{\delta_b + p_{fi}\theta}{p_{fi}}-\theta\right)\right]$	$m_p\left[\frac{b_p}{2}\left(\frac{\delta_b}{p_{fi}}\right)\right]$	2
4/5	$m_p\left[\frac{g}{2}\left(\frac{\delta_b + p_{fi}\theta}{p_{fi}}-\theta\right)+p_{fi}\left(\frac{2\delta_b}{g}\right)\right]$	$m_p\left[\frac{g}{2}\left(\frac{\delta_b}{p_{fi}}\right)+\frac{2}{g}\left(p_{fi}\delta_b\right)\right]$	2
5/6	$m_p\left[\frac{g}{2}(\theta)+p_b\left(\frac{2\delta_b}{g}-\frac{\delta_b+\delta_a}{g}\right)\right]$	$m_p\left[\frac{g}{2}(\theta)+\frac{2}{g}\left(\frac{p_b\delta_b}{2}-\frac{p_b\delta_a}{2}\right)\right]$	2
6/8	$m_p\left[\frac{g}{2}(\theta)+p_b\left(\frac{\delta_b+\delta_a}{g}-\frac{2\delta_a}{g}\right)\right]$	$m_p\left[\frac{g}{2}(\theta)+\frac{2}{g}\left(\frac{p_b\delta_b}{2}-\frac{p_b\delta_a}{2}\right)\right]$	2
8/9	$m_p\left[\frac{g}{2}\left(\theta+\frac{\delta_a - s\theta}{s}\right)+s\left(\frac{2\delta_a}{g}\right)\right]$	$m_p\left[\frac{g}{2}\left(\frac{\delta_a}{s}\right)+\frac{2}{g}(s\delta_a)\right]$	2
1/5	$m_p\left[\left(p_{fi}+p_b\right)\left(\frac{2\delta_b}{g}\right)\right]$	$m_p\left[\frac{2}{g}\left(\delta_b p_{fi}+\delta_b p_b\right)\right]$	2
1/8	$m_p\left[\left(s+p_b\right)\left(\frac{2\delta_a}{g}\right)\right]$	$m_p\left[\frac{2}{g}\left(\delta_a s+\delta_a p_b\right)\right]$	2
4/7	$m_p\left[\left(\frac{b_p-g}{2}\right)\left(\frac{\delta_b+p_{fi}\theta}{p_{fi}}\right)\right]$	$m_p\left[\frac{b_p}{2}\left(\frac{\delta_b+p_{fi}\theta}{p_{fi}}\right)-\frac{g}{2}\left(\frac{\delta_b+p_{fi}\theta}{p_{fi}}\right)\right]$	2
6/7	$m_p\left[2p_b\left(\frac{\delta_b+\delta_a}{g}\right)\right]$	$m_p\left[\frac{2}{g}\left(p_b\delta_b+p_b\delta_a\right)\right]$	2

Table 2-40 Internal Work Associated with Each Yield Line in the Twelve Bolt MRE 1/3 Four-Wide / Two-Wide Unstiffened End-Plate (Part 2 of 2)

7/9	$m_p\left[\left(\frac{b_p-g}{2}\right)\left(\frac{\delta_a-s\theta}{s}\right)\right]$	$m_p\left[\frac{b_p}{2}\left(\frac{\delta_a-s\theta}{s}\right)-\frac{g}{2}\left(\frac{\delta_a-s\theta}{s}\right)\right]$	2
1/9	$m_p\left[\frac{b_p}{2}\left(\theta+\frac{\delta_a-s\theta}{s}\right)\right]$	$m_p\left[\frac{b_p}{2}\left(\frac{\delta_a}{s}\right)\right]$	2

Summing up the internal work given in Table 2-40 and substituting $\delta_a = h_4\,\theta$, $\delta_b = h_2\,\theta$, *and* $\delta_c = h_1\,\theta$ results in the following equation for internal work:

$$W_I = 4m_p\theta\left\{\frac{b_p}{2}\left[h_1\left(\frac{1}{p_{fo}}\right)+h_2\left(\frac{1}{p_{fi}}\right)+h_4\left(\frac{1}{s}\right)-\frac{1}{2}\right]+\frac{2}{g}\left[h_2\left(p_{fi}+\frac{3p_b}{2}\right)+h_4\left(\frac{p_b}{2}+s\right)\right]+\frac{g}{2}\right\} \tag{2-102}$$

The external work, W_E, is given by Eq. (2-103). Setting the internal work and external work equal results in Eq. (2-104).

$$W_E = M_{pl}\theta \tag{2-103}$$

$$M_{pl} = 4m_p\left\{\frac{b_p}{2}\left[h_1\left(\frac{1}{p_{fo}}\right)+h_2\left(\frac{1}{p_{fi}}\right)+h_4\left(\frac{1}{s}\right)-\frac{1}{2}\right]+\frac{2}{g}\left[h_2\left(p_{fi}+\frac{3p_b}{2}\right)+h_4\left(\frac{p_b}{2}+s\right)\right]+\frac{g}{2}\right\} \tag{2-104}$$

This equation is further simplified into the form given in Eq. (2-105) by substituting the moment capacity per unit length, m_p, from Chapter 1, and defining the yield line parameter, Y, as given in Eq. (2-106).

$$M_{pl} = F_{yp}t_p^{\,2}Y \tag{2-105}$$

$$Y = \frac{b_p}{2}\left[h_1\left(\frac{1}{p_{fo}}\right)+h_2\left(\frac{1}{p_{fi}}\right)+h_4\left(\frac{1}{s}\right)-\frac{1}{2}\right]+\frac{2}{g}\left[h_2\left(p_{fi}+\frac{3p_b}{2}\right)+h_4\left(\frac{p_b}{2}+s\right)\right]+\frac{g}{2} \tag{2-106}$$

Note: Use $p_{fi}=s$ if $p_{fi} > s$

To obtain an equation for the dimension s, the equation for moment strength, M_{pl}, is minimized. The derivative of Eq. (2-105), taken with respect to the variable s, is set equal to zero and solved for the variable s. The result is Eq. (2-107).

$$s = \frac{1}{2}\sqrt{b_p g} \tag{2-107}$$

2.16 Twelve Bolt Extended Stiffened End-Plate

The yield line pattern is shown in Figure 2-21. The rotation of each facet (facets are labeled in Figure 2-21) is given in Table 2-41 and the internal work associated with rotation along each yield line is given in Table 2-42. The yield lines are identified by the adjacent facet numbers (e.g., yield line 1/2 separates facets 1 and 2). Variables associated with the geometry of the connection are shown in Figure 2-21. Variables associated with the virtual rotations, displacement, and end-plate moment strength per unit length are described in Chapter 1. It is noted that hatched areas represent facets that are not rotating.

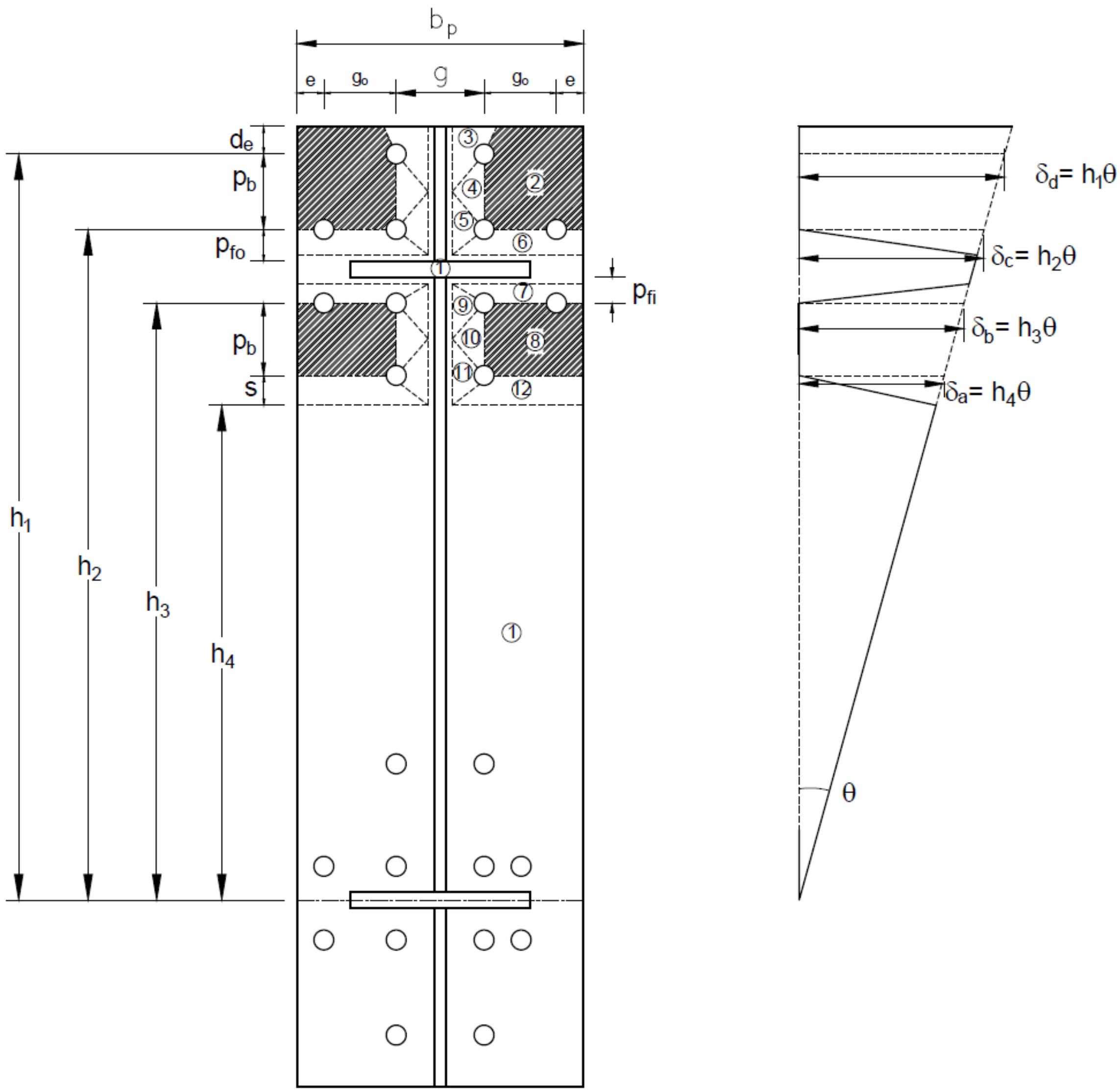

Figure 2-21 Yield Line Pattern for the Twelve Bolt Extended Stiffened End-Plate

Table 2-41 Rotation for Each Facet in the Twelve Bolt Extended Stiffened End-Plate

Facet	θ_x	θ_y
1	θ	0
2	0	0
3	θ	$2\delta_d / g$
4	0	$(\delta_c + \delta_d) / g$
5	θ	$2\delta_c / g$
6	$-(\delta_c - p_{fo}\theta) / p_{fo}$	0
7	$(\delta_b + p_{fi}\theta) / p_{fi}$	0
8	0	0
9	θ	$2\delta_b / g$
10	0	$(\delta_a + \delta_b) / g$
11	θ	$2\delta_a / g$
12	$-(\delta_a - s\theta) / s$	0

Table 2-42 Internal Work Associated with Each Yield Line in the Twelve Bolt Extended Stiffened End-Plate (Part 1 of 2)

Yield Line	Internal Work	Simplified Internal Work	Number of Lines
1/3	$m_p\left[\left(d_e + \frac{p_b}{2}\right)\left(\frac{2\delta_d}{g}\right)\right]$	$m_p\left[\frac{2}{g}\left(\delta_d d_e + \frac{\delta_d p_b}{2}\right)\right]$	2
1/5	$m_p\left[\left(P_{fo} + \frac{p_b}{2}\right)\left(\frac{2\delta_c}{g}\right)\right]$	$m_p\left[\frac{2}{g}\left(\delta_c p_{fo} + \frac{\delta_c p_b}{2}\right)\right]$	2
2/3	$m_p\left[d_e\left(\frac{2\delta_d}{g}\right)\right]$	$m_p\left[\frac{2}{g}(d_e\delta_d)\right]$	2
3/4	$m_p\left[\frac{g}{2}(\theta) + \frac{p_b}{2}\left(\frac{2\delta_d}{g} - \frac{\delta_c + \delta_d}{g}\right)\right]$	$m_p\left[\frac{g}{2}(\theta) + \frac{2}{g}\left(\frac{p_b\delta_d}{2} - \frac{p_b(\delta_c + \delta_d)}{4}\right)\right]$	2
4/5	$m_p\left[\frac{g}{2}(\theta) + \frac{p_b}{2}\left(\frac{\delta_c + \delta_d}{g} - \frac{2\delta_c}{g}\right)\right]$	$m_p\left[\frac{g}{2}(\theta) + \frac{2}{g}\left(\frac{p_b(\delta_c + \delta_d)}{4} - \frac{p_b\delta_c}{2}\right)\right]$	2
5/6	$m_p\left[\frac{g}{2}\left(\theta + \frac{\delta_c - p_{fo}\theta}{p_{fo}}\right) + p_{fo}\left(\frac{2\delta_c}{g}\right)\right]$	$m_p\left[\frac{g}{2}\left(\frac{\delta_c}{p_{fo}}\right) + \frac{2}{g}(\delta_c p_{fo})\right]$	2

Table 2-42 Internal Work Associated with Each Yield Line in the Twelve Bolt Extended Stiffened End-Plate (Part 2 of 2)

Yield Line	Internal Work	Simplified Internal Work	Number of Lines
4/2	$m_p\left[p_b\left(\frac{\delta_c+\delta_d}{g}\right)\right]$	$m_p\left[\frac{2}{g}\left(\frac{p_b\delta_c+p_b\delta_d}{2}\right)\right]$	2
2/6	$m_p\left[\frac{b_p-g}{2}\left(\frac{\delta_c-p_{fo}\theta}{p_{fo}}\right)\right]$	$m_p\left[\frac{b_p}{2}\left(\frac{\delta_c}{p_{fo}}-\theta\right)-\frac{g}{2}\left(\frac{\delta_c}{p_{fo}}-\theta\right)\right]$	2
1/6	$m_p\left[\frac{b_p}{2}\left(\theta+\frac{\delta_c-p_{fo}\theta}{p_{fo}}\right)\right]$	$m_p\left[\frac{b_p}{2}\left(\frac{\delta_c}{p_{fo}}\right)\right]$	2
1/7	$m_p\left[\frac{b_p}{2}\left(\frac{\delta_b+p_{fi}\theta}{p_{fi}}-\theta\right)\right]$	$m_p\left[\frac{b_p}{2}\left(\frac{\delta_b}{p_{fi}}\right)\right]$	2
7/9	$m_p\left[\frac{g}{2}\left(\frac{\delta_b+p_{fi}\theta}{p_{fi}}-\theta\right)+p_{fi}\left(\frac{2\delta_b}{g}\right)\right]$	$m_p\left[\frac{g}{2}\left(\frac{\delta_b}{p_{fi}}\right)+\frac{2}{g}\left(p_{fi}\delta_b\right)\right]$	2
1/9	$m_p\left[\left(p_{fi}+\frac{p_b}{2}\right)\left(\frac{2\delta_b}{g}\right)\right]$	$m_p\left[\frac{2}{g}\left(\delta_b p_{fi}+\frac{\delta_b p_b}{2}\right)\right]$	2
1/11	$m_p\left[\left(s+\frac{p_b}{2}\right)\left(\frac{2\delta_a}{g}\right)\right]$	$m_p\left[\frac{2}{g}\left(\delta_a s+\frac{\delta_a p_b}{2}\right)\right]$	2
9/10	$m_p\left[\frac{g}{2}(\theta)+\frac{p_b}{2}\left(\frac{2\delta_b}{g}-\frac{\delta_a+\delta_b}{g}\right)\right]$	$m_p\left\{\frac{g}{2}(\theta)+\frac{2}{g}\left[\frac{p_b\left(\delta_b-\delta_a\right)}{4}\right]\right\}$	2
10/11	$m_p\left[\frac{g}{2}(\theta)+\frac{p_b}{2}\left(\frac{\delta_a+\delta_b}{g}-\frac{2\delta_a}{g}\right)\right]$	$m_p\left\{\frac{g}{2}(\theta)+\frac{2}{g}\left[\frac{p_b\left(\delta_b-\delta_a\right)}{4}\right]\right\}$	2
11/12	$m_p\left[\frac{g}{2}\left(\theta+\frac{\delta_a-s\theta}{s}\right)+s\left(\frac{2\delta_a}{g}\right)\right]$	$m_p\left[\frac{g}{2}\left(\frac{\delta_a}{s}\right)+\frac{2}{g}\left(s\delta_a\right)\right]$	2
10/8	$m_p\left[p_b\left(\frac{\delta_a+\delta_b}{g}\right)\right]$	$m_p\left\{\frac{2}{g}\left[\frac{p_b\left(\delta_a+\delta_b\right)}{2}\right]\right\}$	2
7/8	$m_p\left[\frac{b_p-g}{2}\left(\frac{\delta_b+p_{fi}\theta}{p_{fi}}\right)\right]$	$m_p\left[\frac{b_p}{2}\left(\frac{\delta_b}{p_{fi}}+\theta\right)-\frac{g}{2}\left(\frac{\delta_b}{p_{fi}}+\theta\right)\right]$	2
8/12	$m_p\left[\frac{b_p-g}{2}\left(\frac{\delta_a-s\theta}{s}\right)\right]$	$m_p\left[\frac{b_p}{2}\left(\frac{\delta_a}{s}-\theta\right)-\frac{g}{2}\left(\frac{\delta_a}{s}-\theta\right)\right]$	2
1/12	$m_p\left[\frac{b_p}{2}\left(\theta+\frac{\delta_a-s\theta}{s}\right)\right]$	$m_p\left[\frac{b_p}{2}\left(\frac{\delta_a}{s}\right)\right]$	2

Summing up the internal work given in Table 2-42 and substituting $\delta_a = h_4\theta$, $\delta_b = h_3\theta$, $\delta_c = h_2\theta$, and $\delta_d = h_1\theta$ results in the following equation for internal work:

$$W_I = 4m_p\theta\begin{Bmatrix} \frac{b_p}{2}\left[h_2\left(\frac{1}{p_{fo}}\right)+h_3\left(\frac{1}{p_{fi}}\right)+h_4\left(\frac{1}{s}\right)-\frac{1}{2}\right]+\ldots \\ \frac{2}{g}\left[h_1\left(\frac{3p_b}{4}+d_e\right)+h_2\left(\frac{p_b}{4}+p_{fo}\right)+h_3\left(\frac{3p_b}{4}+p_{fi}\right)+h_4\left(\frac{p_b}{4}+s\right)\right]+\frac{5g}{4}\end{Bmatrix} \tag{2-108}$$

The external work, W_E, is given by Eq. (2-109). Setting the internal work and external work equal results in Eq. (2-110).

$$W_E = M_{pl}\theta \tag{2-109}$$

$$M_{pl} = 4m_p\begin{Bmatrix} \frac{b_p}{2}\left[h_2\left(\frac{1}{p_{fo}}\right)+h_3\left(\frac{1}{p_{fi}}\right)+h_4\left(\frac{1}{s}\right)-\frac{1}{2}\right]+\ldots \\ \frac{2}{g}\left[h_1\left(\frac{3p_b}{4}+d_e\right)+h_2\left(\frac{p_b}{4}+p_{fo}\right)+h_3\left(\frac{3p_b}{4}+p_{fi}\right)+h_4\left(\frac{p_b}{4}+s\right)\right]+\frac{5g}{4}\end{Bmatrix} \tag{2-110}$$

This equation is further simplified into the form given in Eq. (2-111) by substituting the moment capacity per unit length, m_p, from Chapter 1, and defining the yield line parameter, Y, as given in Eq. (2-112).

$$M_{pl} = F_{yp}t_p^2Y \tag{2-111}$$

$$Y = \begin{Bmatrix} \frac{b_p}{2}\left[h_2\left(\frac{1}{p_{fo}}\right)+h_3\left(\frac{1}{p_{fi}}\right)+h_4\left(\frac{1}{s}\right)-\frac{1}{2}\right]+\ldots \\ \frac{2}{g}\left[h_1\left(\frac{3p_b}{4}+d_e\right)+h_2\left(\frac{p_b}{4}+p_{fo}\right)+h_3\left(\frac{3p_b}{4}+p_{fi}\right)+h_4\left(\frac{p_b}{4}+s\right)\right]+\frac{5g}{4}\end{Bmatrix} \tag{2-112}$$

Note: Use $p_{fi}=s$ if $p_{fi} > s$ Use $p_{fo}=s$ if $p_{fo} > s$

To obtain an equation for the dimension s, the equation for moment strength, M_{pl}, is minimized. The derivative of Eq. (2-111), taken with respect to the variable s, is set equal to zero and solved for the variable s. The result is Eq. (2-113).

$$s = \frac{1}{2}\sqrt{b_p g} \tag{2-113}$$

3 COLUMN SIDE YIELD LINE SOLUTIONS

3.1 Two-Bolt Configurations

The configuration of two bolts on the column is associated with the two-bolt unstiffened flush end-plate connection. Figure 3-1 shows the different configurations with varied stiffening and proximity to the top of the column. The dimension, h_1, is the distance from the center of the beam compression flange to the tension bolt line.

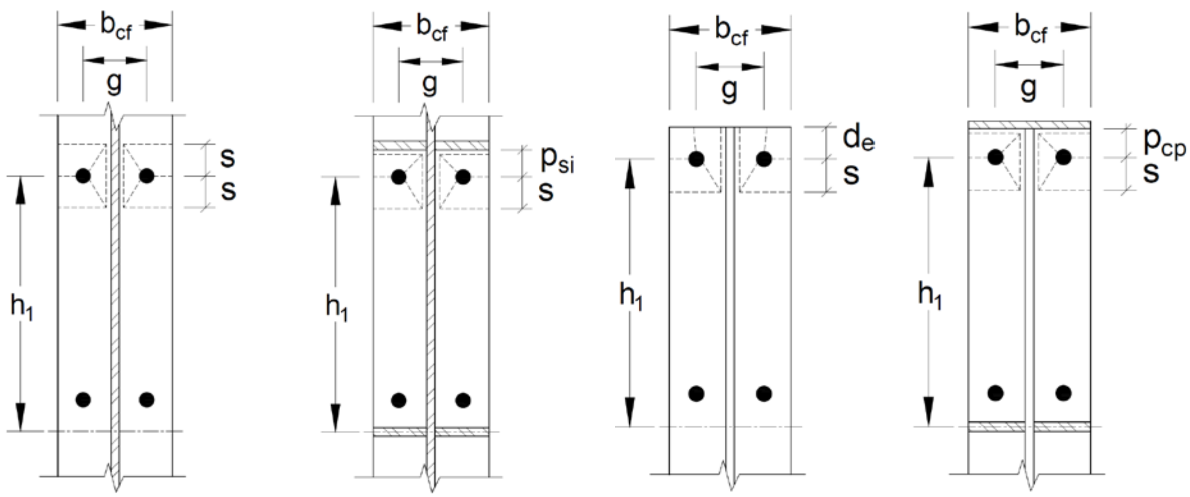

a) Continuous Column Unstiffened | b) Continuous Column Stiffened | c) Top of Column Unstiffened | d) Top of Column with Cap Plate

Figure 3-1 Yield Line Pattern for Two-Bolt Configurations

The following describes how the equation for each yield line parameter was obtained. Table 3-1 summarizes the resulting yield line parameters.

a) Continuous column that is unstiffened (Fig. 3-1(a)). The yield line parameter derivation is the same as two-bolt unstiffened flush end plate with the following substitutions: $p_{fi} = s$ and $b_p = b_{cf}$.

b) Continuous column that is stiffened (Fig. 3-1(b)). The derivation is the same as the two-bolt unstiffened flush end plate with the following substitutions: $p_{fi} = p_{si}$ and $b_p = b_{cf}$.

c) Top of column that is unstiffened (Fig. 3-1(c)). The derivation is provided later in this section.

d) Top of column with cap plate (Fig. 3-1(d)). The derivation is the same as the two-bolt unstiffened flush end-plate with the following substitutions: $p_{fi} = p_{cp}$ and $b_p = b_{cf}$.

Table 3-1 Summary of Column Side Yield Line Parameters for Two-Bolt Configurations

Configuration	Yield Line Parameter
Continuous Unstiffened Column [Fig. 3-1(a)]	$Y_c = \frac{b_{cf} h_1}{s} + \frac{4 h_1 s}{g}$
Continuous Stiffened Column [Fig. 3-1(b)]	$Y_c = \frac{b_{cf}}{2}\left[h_1\left(\frac{1}{p_{si}} + \frac{1}{s}\right)\right] + \frac{2}{g}\left[h_1\left(p_{si} + s\right)\right]$ Note: Use $p_{si}=s$ if $p_{si} > s$
Top of Column, Unstiffened [Fig. 3-1(c)]	$Y_c = \left\{\frac{b_{cf}}{2}\left[h_1\left(\frac{1}{s}\right) - \frac{1}{2}\right] + \frac{2}{g}\left[h_1\left(s + d_e\right)\right] + \frac{g}{4}\right\}$
Top of Column with Cap Plate [Fig. 3-1(d)]	$Y_c = \frac{b_{cf}}{2}\left[h_1\left(\frac{1}{p_{cp}} + \frac{1}{s}\right)\right] + \frac{2}{g}\left[h_1\left(p_{cp} + s\right)\right]$ Note: Use $p_{cp}=s$ if $p_{cp} > s$

__Derivation for the Unstiffened Top of a Column__

The yield line pattern is shown in Figure 3-2. The rotation of each facet (facets are labeled in Figure 3-2) is given in Table 3-2 and the internal work associated with rotation along each yield line is given in Table 3-3. The yield lines are identified by the adjacent facet numbers (e.g., yield line 1/2 separates facets 1 and 2). Variables associated with the geometry of the connection are shown in Figure 3-2. Variables associated with the virtual rotations, displacement, and end-plate moment strength per unit length are described in Chapter 1.

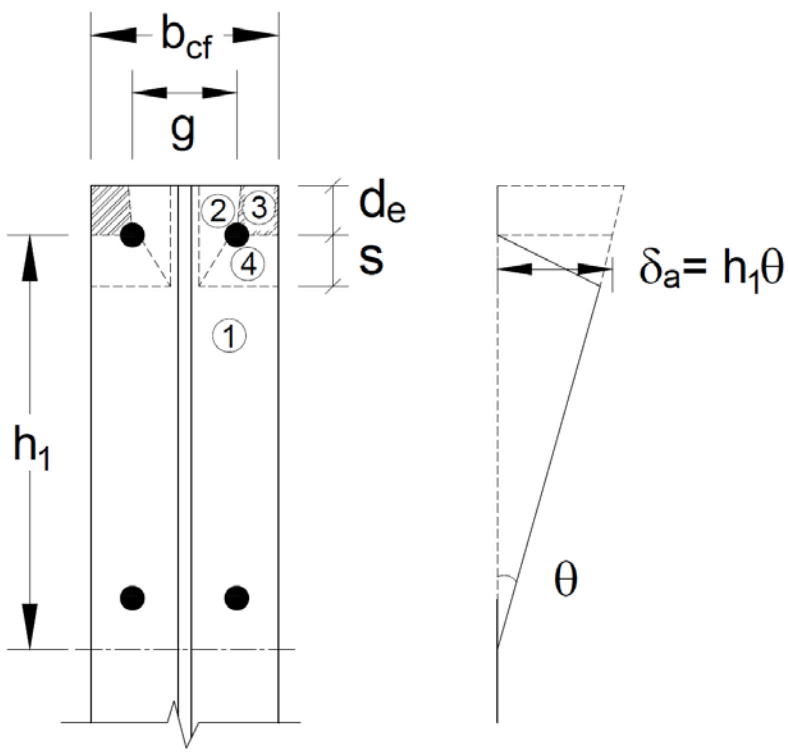

Figure 3-2 Yield Line Pattern for the Unstiffened Top of the Column

Table 3-2 Rotation for Each Facet in the Unstiffened Top of the Column

Facet	θ_x	θ_y
1	θ	0
2	θ	$2\delta_a / g$
3	0	0
4	$-(\delta_a - s\theta)/s$	0

Table 3-3 Internal Work Associated with Each Yield Line in the Unstiffened Top of the Column

Yield Line	Internal Work	Simplified Internal Work	Number of Lines
2/3	$m_p[d_e(\frac{2\delta_a}{g})]$	$m_p[\frac{2}{g}(\delta_a d_e)]$	2
2/4	$m_p\left[\frac{g}{2}\left(\theta+\frac{\delta_a - s\theta}{s}\right)+s\left(\frac{2\delta_a}{g}\right)\right]$	$m_p\left[\frac{g}{2}\left(\frac{\delta_a}{s}\right)+\frac{2}{g}(s\delta_a)\right]$	2
3/4	$m_p\left[\frac{b_{cf}-g}{2}\left(\frac{\delta_a - s\theta}{s}\right)\right]$	$m_p\left[\frac{b_{cf}}{2}\left(\frac{\delta_a}{s}-\theta\right)-\frac{g}{2}\left(\frac{\delta_a}{s}-\theta\right)\right]$	2
1/2	$m_p\left[(d_e+s)\left(\frac{2\delta_a}{g}\right)\right]$	$m_p\left\{\frac{2}{g}\left[\delta_a\left(d_e+s\right)\right]\right\}$	2
1/4	$m_p\left[\frac{b_{cf}}{2}\left(\theta+\frac{\delta_a - s\theta}{s}\right)\right]$	$m_p\left[\frac{b_{cf}}{2}\left(\frac{\delta_a}{s}\right)\right]$	2

Summing up the internal work given in Table 3-3 and substituting $\delta_a = h_1\theta$ results in the following equation for internal work:

$$W_I = 4m_p\theta\left\{\frac{b_{cf}}{2}\left[h_1\left(\frac{1}{s}\right)-\frac{1}{2}\right]+\frac{2}{g}\left[h_1\left(s+d_e\right)\right]+\frac{g}{4}\right\} \tag{3-1}$$

The external work, W_E, is given by Eq. (3-2). Setting the internal work and external work equal results in Eq. (3-3).

$$W_E = M_{pl}\theta \tag{3-2}$$

$$M_{pl} = 4m_p\left\{\frac{b_{cf}}{2}\left[h_1\left(\frac{1}{s}\right)-\frac{1}{2}\right]+\frac{2}{g}\left[h_1\left(s+d_e\right)\right]+\frac{g}{4}\right\} \tag{3-3}$$

This equation is further simplified into the form given in Eq. (3-4) by substituting the moment capacity per unit length, m_p, from Chapter 1, and defining the yield line parameter, Y, as given in Eq. (3-5).

$$M_{pl} = F_{yp}t_p{}^2Y_c \tag{3-4}$$

$$Y_c = \left\{\frac{b_{cf}}{2}\left[h_1\left(\frac{1}{s}\right)-\frac{1}{2}\right]+\frac{2}{g}\left[h_1\left(s+d_e\right)\right]+\frac{g}{4}\right\} \tag{3-5}$$

To obtain an equation for the dimension s, the equation for moment strength, M_{pl}, is minimized. The derivative of Eq. (3-4), taken with respect to the variable s, is set equal to zero and solved for the variable s. The result is Eq. (3-6).

$$s = \frac{1}{2}\sqrt{b_{cf}\,g} \tag{3-6}$$

3.2 Four-Bolt Configurations

The configuration of four bolts on the column is associated with the following end-plate connections: four-bolt unstiffened flush, four-bolt flush stiffened between the tension bolts, four-bolt flush stiffened below the tension bolts or four-bolt extended stiffened. Figure 3-3 shows the different configurations with varied stiffening and proximity to the top of the column. The dimensions, h_1, and h_2, are the distance from the center of the beam compression flange to the tension bolt lines.

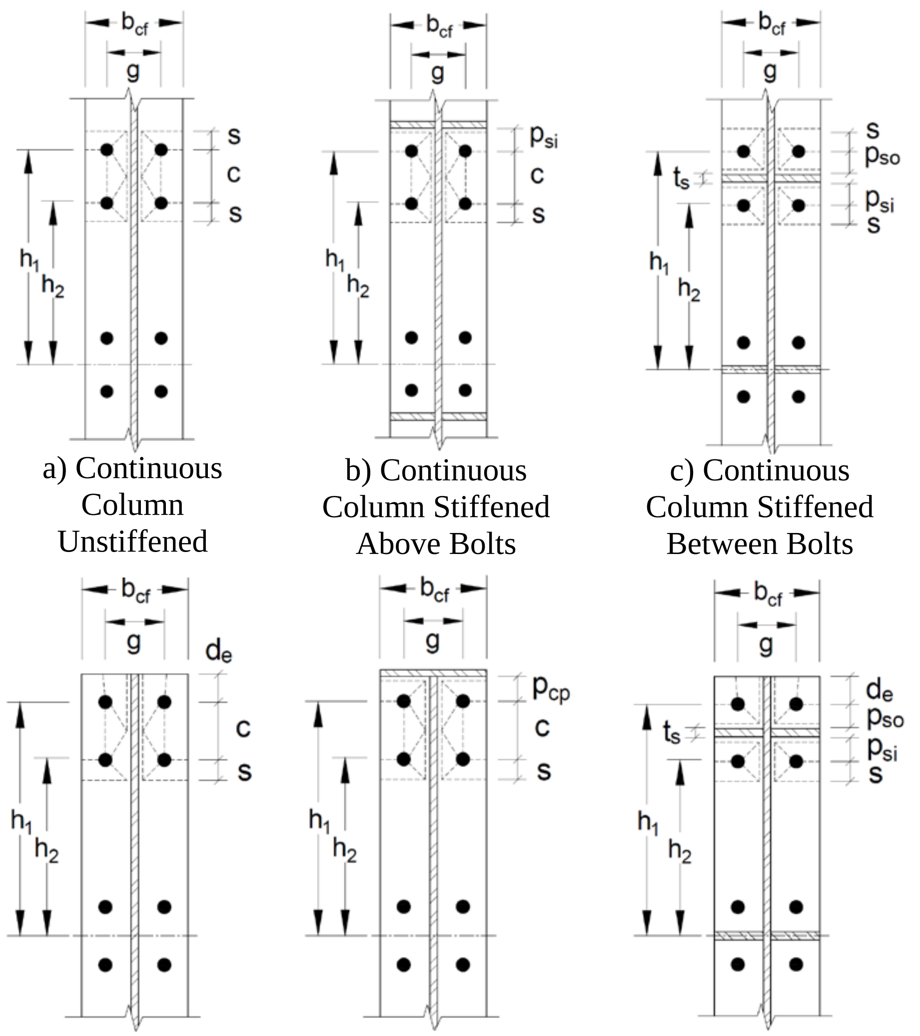

a) Continuous Column Unstiffened

b) Continuous Column Stiffened Above Bolts

c) Continuous Column Stiffened Between Bolts

d) Top of Column Unstiffened

e) Top of Column with Cap Plate

f) Top of Column Stiffened Between Bolts

Note: h_1 and h_2 are the distance from the center of the beam compression flange to the tension bolt lines.

Figure 3-3 Yield Line Pattern for Four-Bolt Configurations

The following describes how the equation for each yield line parameter was obtained. Table 3-4 summarizes the resulting yield line parameters.

a) Continuous column that is unstiffened (Fig. 3-3(a)). The derivation for the yield line parameter is the same as the four-bolt unstiffened flush end-plate with the following substitutions: $p_{fi} = s$, $b_p = b_{cf}$ and $p_b = c$.

b) Continuous column that is stiffened (Fig. 3-3(b)). The derivation is the same as the four-bolt unstiffened flush end-plate with the following substitutions: $p_{fi} = p_{si}$, $b_p = b_{cf}$ and $p_b = c$.

c) Continuous column that is stiffened between the bolt lines (Fig. 3-3(c)). The derivation is the same as the four-bolt flush end-plate stiffened between the bolt lines with the following substitutions: $p_{fi} = s$ and $b_p = b_{cf}$..

d) Top of column that is unstiffened (Fig. 3-3(d)). The derivation is provided later in this section.

e) Top of column with cap plate (Fig. 3-3(e)). The derivation is the same as the four-bolt unstiffened flush end-plate with the following substitutions: $p_{fi} = p_{cp}$, $b_p = b_{cf}$ and $p_b = c$.

f) Top of column stiffened between the bolt lines (Fig. 3-3(f)). The derivation is the same as the four-bolt extended stiffened end-plate with the following substitutions: $p_{fo} = p_{so}$, $p_{fi} = p_{si}$, and $b_p = b_{cf}$.

Table 3-4 Summary of Column Side Yield Line Parameters for Four-Bolt Configurations

Configuration	Yield Line Parameter
Continuous Unstiffened Column [Fig. 3-3(a)]	$Y_c = \frac{b_{cf}}{2}\left[h_1\left(\frac{1}{s}\right)+h_2\left(\frac{1}{s}\right)\right]+\frac{2}{g}\left[h_1\left(s+\frac{3}{4}c\right)+h_2\left(s+\frac{1}{4}c\right)\right]+\frac{g}{2}$
Continuous Column Stiffened Above the Bolts [Fig. 3-3(b)]	$Y_c = \frac{b_{cf}}{2}\left[h_1\left(\frac{1}{p_{si}}\right)+h_2\left(\frac{1}{s}\right)\right]+\frac{2}{g}\left[h_1\left(p_{si}+\frac{3}{4}c\right)+h_2\left(s+\frac{1}{4}c\right)\right]+\frac{g}{2}$ Note: Use $p_{si}=s$ if $p_{si} > s$
Continuous Column Stiffened Between the Bolts [Fig. 3-3(c)]	$Y_c = \frac{b_{cf}}{2}\left[h_1\left(\frac{1}{s}+\frac{1}{p_{so}}\right)+h_2\left(\frac{1}{p_{si}}+\frac{1}{s}\right)\right]+\frac{2}{g}\left[h_1\left(s+p_{so}\right)+h_2\left(p_{si}+s\right)\right]$ Note: Use $p_{si}=s$ if $p_{si} > s$ Use $p_{so}=s$ if $p_{so} > s$
Top of Column, Unstiffened [Fig. 3-3(d)]	$Y_c = \frac{b_{cf}}{2}\left[h_2\left(\frac{1}{s}\right)-\frac{1}{2}\right]+\frac{2}{g}\left[h_1\left(d_e+\frac{3}{4}c\right)+h_2\left(s+\frac{1}{4}c\right)\right]+\frac{3g}{4}$
Top of Column with Cap Plate [Fig. 3-3(e)]	$Y_c = \frac{b_{cf}}{2}\left[h_1\left(\frac{1}{p_{cp}}\right)+h_2\left(\frac{1}{s}\right)\right]+\frac{2}{g}\left[h_1\left(p_{cp}+\frac{3}{4}c\right)+h_2\left(s+\frac{1}{4}c\right)\right]+\frac{g}{2}$ Note: Use $p_{cp}=s$ if $p_{cp} > s$
Top of Column Stiffened Between the Bolts [Fig. 3-3(f)]	$Y_c = \frac{b_{cf}}{2}\left[h_1\left(\frac{1}{p_{so}}\right)+h_2\left(\frac{1}{p_{si}}+\frac{1}{s}\right)-\frac{1}{2}\right]+\frac{2}{g}\left[h_1\left(d_{ce}+p_{so}\right)+h_2\left(s+p_{si}\right)\right]+\frac{g}{4}$ Note: Use $p_{si}=s$ if $p_{si} > s$ Use $p_{so}=s$ if $p_{so} > s$

Derivation for the Unstiffened Top of a Column

The yield line pattern is shown in Figure 3-4. The rotation of each facet (facets are labeled in Figure 3-4, hatching represents non-rotating facet) is given in Table 3-5 and the internal work associated with rotation along each yield line is given in Table 3-6. The yield lines are identified by the adjacent facet numbers (e.g., yield line 1/2 separates facets 1 and 2). Variables associated with the geometry of the connection are shown in Figure 3-4. Variables associated with the virtual rotations, displacement, and end-plate moment strength per unit length are described in Chapter 1. Dimensions, h_1, and h_2, are the distance from the center of the beam compression flange to the tension bolt lines.

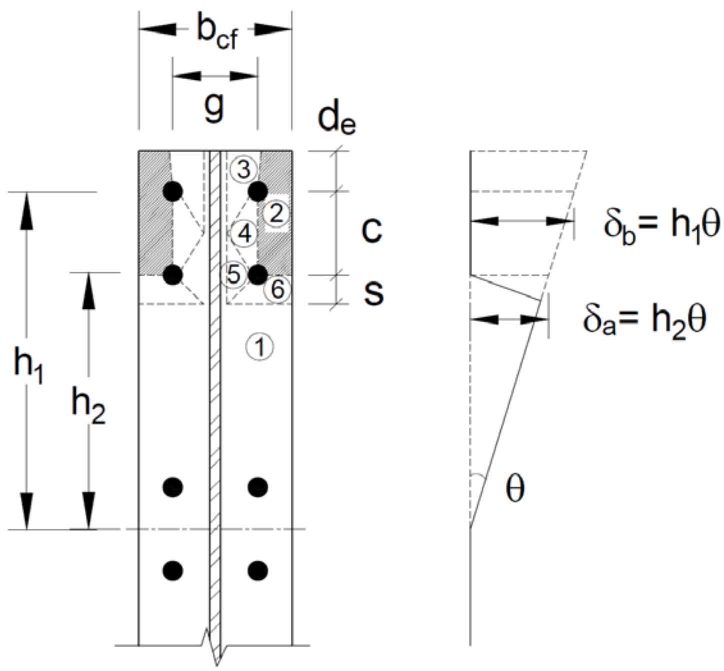

Figure 3-4 Yield Line Pattern for the Unstiffened Top of a Column

Table 3-5 Rotation for Each Facet in the Unstiffened Top of a Column

Facet	θ_x	θ_y
1	θ	0
2	0	0
3	θ	$2\delta_b / g$
4	0	$(\delta_a + \delta_b) / g$
5	θ	$2\delta_a / g$
6	$-(\delta_a - s\theta) / s$	0

Table 3-6 Internal Work Associated with Each Yield Line in the Unstiffened Top of a Column

Yield Line	Internal Work	Simplified Internal Work	Number of Lines
1/3	$m_p\left[\left(d_e+\frac{c}{2}\right)\left(\frac{2\delta_b}{g}\right)\right]$	$m_p\left[\frac{2}{g}\delta_b\left(d_e+\frac{c}{2}\right)\right]$	2
1/5	$m_p\left[\left(s+\frac{c}{2}\right)\left(\frac{2\delta_a}{g}\right)\right]$	$m_p\left[\frac{2}{g}\delta_a\left(s+\frac{c}{2}\right)\right]$	2
1/6	$m_p\left[\frac{b_{cf}}{2}\left(\theta+\frac{\delta_a-s\theta}{s}\right)\right]$	$m_p\left[\frac{b_{cf}}{2}\left(\frac{\delta_a}{s}\right)\right]$	2
3/4	$m_p\left[\frac{g}{2}(\theta)+\frac{c}{2}\left(\frac{2\delta_b}{g}-\frac{\delta_a+\delta_b}{g}\right)\right]$	$m_p\left[\frac{g}{2}(\theta)+\frac{2}{g}c\left(\frac{\delta_b-\delta_a}{4}\right)\right]$	2
4/5	$m_p\left[\frac{g}{2}(\theta)+\frac{c}{2}\left(\frac{\delta_a+\delta_b}{g}-\frac{2\delta_a}{g}\right)\right]$	$m_p\left[\frac{g}{2}(\theta)+\frac{2}{g}c\left(\frac{\delta_b-\delta_a}{4}\right)\right]$	2
2/6	$m_p\left[\frac{b_{cf}-g}{2}\left(\frac{\delta_a-s\theta}{s}\right)\right]$	$m_p\left[\frac{b_{cf}}{2}\left(\frac{\delta_a}{s}-\theta\right)-\frac{g}{2}\left(\frac{\delta_a}{s}-\theta\right)\right]$	2
2/3	$m_p\left[d_e\left(\frac{2\delta_b}{g}\right)\right]$	$m_p\left[\frac{2}{g}(d_e\delta_b)\right]$	2
2/4	$m_p\left[c\left(\frac{\delta_a+\delta_b}{g}\right)\right]$	$m_p\left[\frac{2}{g}c\left(\frac{\delta_a+\delta_b}{2}\right)\right]$	2
5/6	$m_p\left[\frac{g}{2}\left(\theta+\frac{\delta_a-s\theta}{s}\right)+s\left(\frac{2\delta_a}{g}\right)\right]$	$m_p\left[\frac{g}{2}\left(\frac{\delta_a}{s}\right)+\frac{2}{g}(s\delta_a)\right]$	2

Summing up the internal work given in Table 3-6 and substituting $\delta_a = h_2\,\theta$ and $\delta_b = h_1\,\theta$ results in the following equation for internal work:

$$W_I = 4m_p\theta\left\{\frac{b_{cf}}{2}\left[h_2\left(\frac{1}{s}\right)-\frac{1}{2}\right]+\frac{2}{g}\left[h_1\left(d_e+\frac{3}{4}c\right)+h_2(s+\frac{1}{4}c)\right]+\frac{3g}{4}\right\} \tag{3-7}$$

The external work, W_E, is given by Eq. (3-8). Setting the internal work and external work equal results in Eq. (3-9).

$$W_E = M_{pl}\theta \tag{3-8}$$

$$M_{pl} = 4m_p\left\{\frac{b_{cf}}{2}\left[h_2\left(\frac{1}{s}\right)-\frac{1}{2}\right]+\frac{2}{g}\left[h_1\left(d_e+\frac{3}{4}c\right)+h_2(s+\frac{1}{4}c)\right]+\frac{3g}{4}\right\} \tag{3-9}$$

This equation is further simplified into the form given in Eq. (3-10) by substituting the moment capacity per unit length, m_p, from Chapter 1, and defining the yield line parameter, Y, as given in Eq. (3-11).

$$M_{pl} = F_{yp} t_p^{\,2} Y_c \tag{3-10}$$

$$Y_c = \frac{b_{cf}}{2}\left[h_2\left(\frac{1}{s}\right) - \frac{1}{2}\right] + \frac{2}{g}\left[h_1\left(d_e + \frac{3}{4}c\right) + h_2\left(s + \frac{1}{4}c\right)\right] + \frac{3g}{4} \tag{3-11}$$

To obtain an equation for the dimension s, the equation for moment strength, M_{pl} is minimized. The derivative of Eq. (3-10), taken with respect to the variable s, is set equal to zero and solved for the variable s. The result is Eq. (3-12).

$$s = \frac{1}{2}\sqrt{b_{cf}\, g} \tag{3-12}$$

3.3 Six-Bolt 4W/2W Configurations

The four wide / two wide configuration of six bolts on the column is associated with the Six-Bolt Flush Four-Wide Flush End-Plate. Figure 3-5 shows the different configurations with varied stiffening and proximity to the top of the column. The dimensions, h_1, and h_2, are the distance from the center of the beam compression flange to the tension bolt lines.

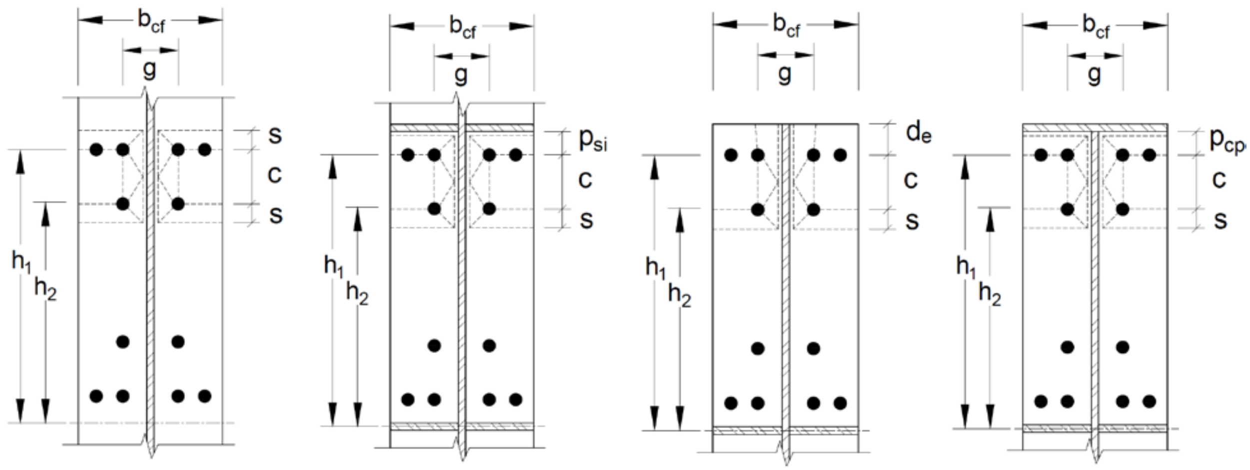

a) Continuous Column Unstiffened | b) Continuous Column Stiffened Above Bolts | c) Top of Column Unstiffened | d) Top of Column with Cap Plate

Figure 3-5 Yield Line Pattern for Six-Bolt 4W/2W Configurations

The following describes how the equation for each yield line parameter was obtained. Table 3-7 summarizes the resulting yield line parameters.

1. Continuous column that is unstiffened (Fig. 3-5(a)). The derivation for the yield line parameter is the same as the four-bolt unstiffened flush end-plate with the following substitutions: $p_{fi} = s$, $b_p = b_{cf}$ and $p_b = c$
2. Continuous column that is stiffened above the bolts (Fig. 3-5(b)). The derivation is same as the six-bolt flush four-wide unstiffened end-plate with the following substitutions: $p_{fi} = p_{si}$, $b_p = b_{cf}$ and $p_b = c$
3. Top of column that is unstiffened (Fig. 3-5(c)). The derivation is the same as the column-side yield line parameter for the four-bolt configuration at the top of the column.

4. Top of column with cap plate (Fig. 3-5(d)). The derivation is the same as the six-bolt flush four wide flush end-plate with the following substitutions: $p_{fi} = p_{cp}$, $b_p = b_{cf}$ and $p_b = c$.

Table 3-7 Summary of Column Side Yield Line Parameters for Six-Bolt 4W/2W Configurations

Configuration	Yield Line Parameter
Continuous Unstiffened Column [Fig. 3-5(a)]	$Y_c = \frac{b_{cf}}{2}\left[h_1\left(\frac{1}{s}\right)+h_2\left(\frac{1}{s}\right)\right]+\frac{2}{g}\left[h_1\left(s+\frac{3}{4}c\right)+h_2\left(s+\frac{1}{4}c\right)\right]+\frac{g}{2}$
Continuous Column Stiffened Above the Bolts [Fig. 3-5(b)]	$Y_c = \frac{b_{cf}}{2}\left[h_1\left(\frac{1}{p_{si}}\right)+h_2\left(\frac{1}{s}\right)\right]+\frac{2}{g}\left[h_1\left(p_{si}+\frac{3}{4}c\right)+h_2\left(s+\frac{1}{4}c\right)\right]+\frac{g}{2}$ Note: Use $p_{si}=s$ if $p_{si} > s$
Top of Column, Unstiffened [Fig. 3-5(c)]	$Y_c = \frac{b_{cf}}{2}\left[h_2\left(\frac{1}{s}\right)-\frac{1}{2}\right]+\frac{2}{g}\left[h_1\left(d_e+\frac{3}{4}c\right)+h_2\left(s+\frac{1}{4}c\right)\right]+\frac{3g}{4}$
Top of Column with Cap Plate [Fig. 3-5(d)]	$Y_c = \frac{b_{cf}}{2}\left[h_1\left(\frac{1}{p_{cp}}\right)+h_2\left(\frac{1}{s}\right)\right]+\frac{2}{g}\left[h_1\left(p_{cp}+\frac{3}{4}c\right)+h_2\left(s+\frac{1}{4}c\right)\right]+\frac{g}{2}$ Note: Use $p_{cp}=s$ if $p_{cp} > s$

3.4 Six-Bolt, 3 Rows Configurations

This configuration of six bolts on the column is associated with the MRE Extended 1/2 Unstiffened End-Plate. Figure 3-6 shows the different configurations with varied stiffening and proximity to the top of the column. The dimensions, h_1, h_2, and h_3, are the distance from the center of the beam compression flange to the tension bolt lines.

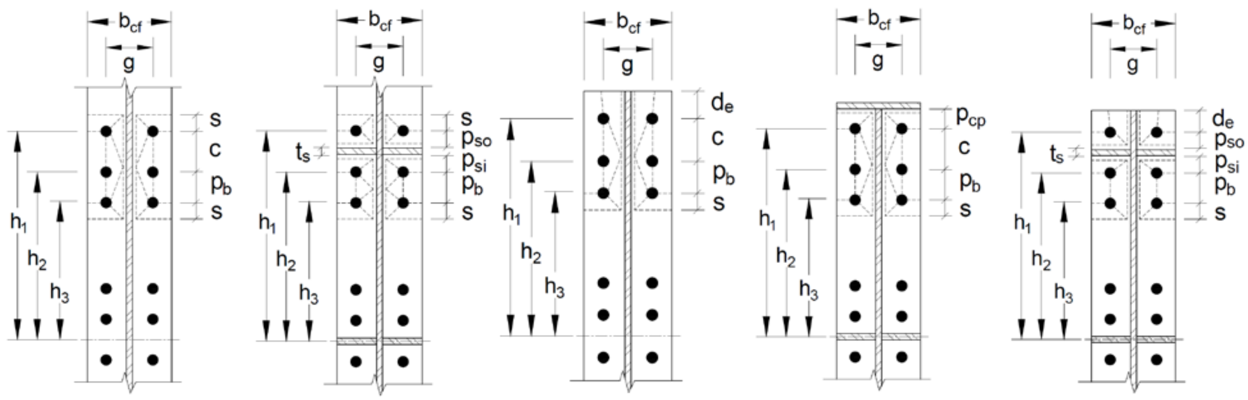

a) Continuous Column Unstiffened

b) Continuous Column Stiffened Between Bolts

c) Top of Column Unstiffened

d) Top of Column with Cap Plate

e) Top of Column Stiffened Between Bolts

Figure 3-6 Yield Line Pattern for Six-Bolt, 3 Rows Configurations

The following describes how the equation for each yield line parameter was obtained. Table 3-8 summarizes the resulting yield line parameters.

a) Continuous column that is unstiffened (Fig. 3-6(a)). The derivation for the yield line parameter is the same as the four-bolt unstiffened flush end-plate with the following substitutions: $p_b = c+p_b$, $h_2 = h_3$, $p_{fi} = s$ and $b_p = b_{cf}$.
b) Continuous column that is stiffened between the bolts (Fig. 3-6(b)). The derivation is provided later in this section.
c) Top of a column that is unstiffened (Fig. 3-6(c)). The derivation is the same as the column-side yield line parameter for the four-bolt configuration at the top of the column and c was replaced by $c+p_b$.

d) Top of column with cap plate (Fig. 3-6(d)). The derivation is the same as the four-bolt flush unstiffened end-plate with the following substitutions: $p_{fi} = p_{cp}$, $b_p = b_{cf}$, $h_2 = h_3$, and $p_b = c + p_b$.

e) Top of column stiffened between bolts (Fig. 3-6(d)). The derivation is the same as the MRE Extended 1/3 Stiffened End-Plate (alternative pattern) with the following substitutions: $p_{fo} = p_{so}$, $p_{fi} = p_{si}$, $b_p = b_{cf}$ and $p_b = p_b/2$.

Table 3-8 Summary of Column Side Yield Line Parameters for Six-Bolt, 3 Rows Configurations

Configuration	Yield Line Parameter
Continuous Unstiffened Column [Fig. 3-6(a)]	$Y_c = \frac{b_{cf}}{2}\left[h_1\left(\frac{1}{s}\right)+h_3\left(\frac{1}{s}\right)\right]+\frac{2}{g}\left[h_1\left(s+\frac{3}{4}p_b+\frac{3}{4}c\right)+h_3\left(s+\frac{1}{4}p_b+\frac{1}{4}c)\right)\right]+\frac{g}{2}$
Continuous Column Stiffened Between the Bolts [Fig. 3-6(b)]	$Y_c = \left\{\begin{array}{l}\frac{b_{cf}}{2}\left[h_1\left(\frac{1}{p_{so}}+\frac{1}{s}\right)+h_2\left(\frac{1}{p_{si}}\right)+h_3\left(\frac{1}{s}\right)\right]+\ldots\\ \frac{2}{g}\left[h_1\left(p_{so}+s\right)+h_2\left(p_{si}+\frac{3}{4}p_b\right)+h_3\left(s+\frac{1}{4}p_b\right)\right]+\frac{g}{2}\end{array}\right\}$ Note: Use $p_{si}=s$ if $p_{si} > s$ Use $p_{so}=s$ if $p_{so} > s$
Top of Column, Unstiffened [Fig. 3-6(c)]	$Y_c = \frac{b_{cf}}{2}\left[h_3\left(\frac{1}{s}\right)-\frac{1}{2}\right]+\frac{2}{g}\left[h_1\left(d_e+\frac{3}{4}p_b+\frac{3}{4}c\right)+h_3\left(s+\frac{1}{4}p_b+\frac{1}{4}c\right)\right]+\frac{3g}{4}$
Top of Column with Cap Plate [Fig. 3-6(d)]	$Y_c = \frac{b_{cf}}{2}\left[h_1\left(\frac{1}{p_{cp}}\right)+h_3\left(\frac{1}{s}\right)\right]+\frac{2}{g}\left[h_1\left(p_{cp}+\frac{3}{4}p_b+\frac{3}{4}c\right)+h_3\left(s+\frac{1}{4}p_b+\frac{1}{4}c\right)\right]+\frac{g}{2}$ Note: Use $p_{cp}=s$ if $p_{cp} > s$
Top of Column Stiffened Between Bolts [Fig. 3-6(e)]	$Y_c = \frac{b_{cf}}{2}\left[h_1\left(\frac{1}{p_{so}}\right)+h_2\left(\frac{1}{p_{si}}\right)+h_3\left(\frac{1}{s}\right)-\frac{1}{2}\right]+$ $\frac{2}{g}\left[h_1\left(p_{so}+d_e\right)+h_2\left(p_{si}+\frac{3}{4}p_b\right)+h_3\left(\frac{1}{4}p_b+s\right)\right]+\frac{3g}{4}$ Note: Use $p_{si}=s$ if $p_{si} > s$ Use $p_{so}=s$ if $p_{so} > s$

Derivation for the Continuous Column Stiffened Between the Bolts

The yield line pattern is shown in Figure 3-7. The rotation of each facet (facets are labeled in Figure 3-7, hatching represents non-rotating facet) is given in Table 3-9 and the internal work associated with rotation along each yield line is given in Table 3-10. The yield lines are identified by the adjacent facet numbers (e.g., yield line 1/2 separates facets 1 and 2). Variables associated with the geometry of the connection are shown in Figure 3-7. Variables associated with the virtual rotations, displacement, and end-plate moment strength per unit length are described in Chapter 1.

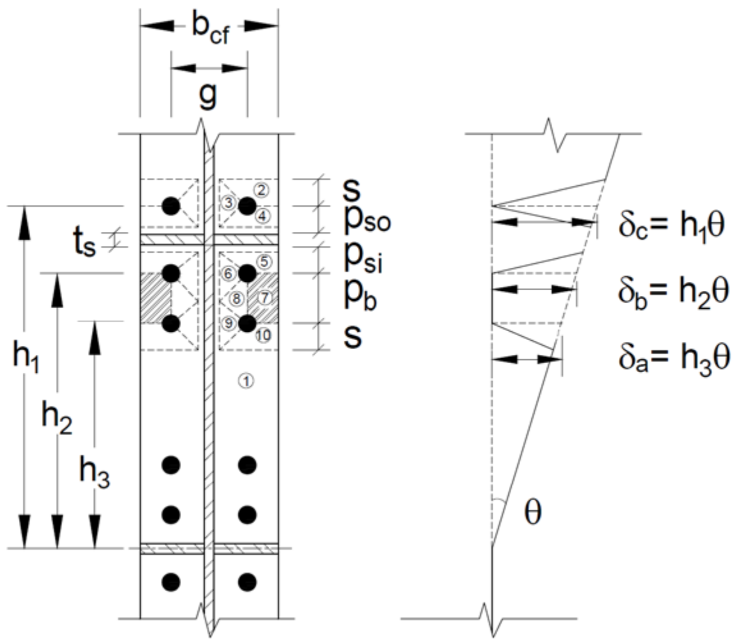

Figure 3-7 Yield Line Pattern for the Unstiffened Top of a Column

Table 3-9 Rotation for Each Facet in the Continuous Column Stiffened Between the Bolts

Facet	θ_x	θ_y
1	θ	0
2	$(\delta_c + s\theta)/s$	0
3	θ	$2\delta_c/g$
4	$-(\delta_c - p_{so}\theta)/p_{so}$	0
5	$(\delta_b + p_{si}\theta)/p_{si}$	0
6	θ	$2\delta_b/g$
7	0	0
8	0	$(\delta_a + \delta_b)/g$
9	θ	$2\delta_a/g$
10	$-(\delta_a - s\theta)/s$	0

Table 3-10 Internal Work Associated with Each Yield Line in the Continuous Column Stiffened Between the Bolts

Yield Line	Internal Work	Simplified Internal Work	Number of Lines
1/2	$m_p\left[\left(\frac{b_{cf}}{2}\right)\left(\frac{\delta_c+s\theta}{s}-\theta\right)\right]$	$m_p\left[\left(\frac{b_{cf}}{2}\right)\left(\frac{\delta_c}{s}\right)\right]$	2
1/3	$m_p\left[(s+p_{so})\left(\frac{2\delta_c}{g}\right)\right]$	$m_p\left[\frac{2}{g}(s\delta_c+\delta_c p_{so})\right]$	2
2/3	$m_p\left[\frac{g}{2}(\frac{\delta_c+s\theta}{s}-\theta)+s\left(\frac{2\delta_c}{g}\right)\right]$	$m_p\left[\frac{g}{2}(\frac{\delta_c}{s})+\frac{2}{g}(\delta_c s)\right]$	2
2/4	$m_p\left[\frac{b_{cf}-g}{2}\left(\frac{\delta_c+s\theta}{s}+\frac{\delta_c-p_{so}\theta}{p_{so}}\right)\right]$	$m_p\left[\frac{b_{cf}}{2}\delta_c\left(\frac{1}{s}+\frac{1}{p_{so}}\right)-\frac{g}{2}\delta_c\left(\frac{1}{s}+\frac{1}{p_{so}}\right)\right]$	2
3/4	$m_p\left[\frac{g}{2}\left(\theta+\frac{\delta_c-p_{so}\theta}{p_{so}}\right)+p_{so}\left(\frac{2\delta_c}{g}\right)\right]$	$m_p\left[\frac{g}{2}\left(\frac{\delta_c}{p_{fo}}\right)+\frac{2}{g}(\delta_c p_{fo})\right]$	2
1/4	$m_p\left[\frac{b_{cf}}{2}\left(\theta+\frac{\delta_c-p_{so}\theta}{p_{so}}\right)\right]$	$m_p\left[\frac{b_{cf}}{2}\left(\frac{\delta_c}{p_{so}}\right)\right]$	2
1/5	$m_p\left[\frac{b_{cf}}{2}\left(\frac{\delta_b+p_{si}\theta}{p_{si}}-\theta\right)\right]$	$m_p\left[\frac{b_{cf}}{2}\left(\frac{\delta_b}{p_{si}}\right)\right]$	2
1/6	$m_p\left[\left(\frac{p_{cf}}{2}+p_{si}\right)\left(\frac{2\delta_b}{g}\right)\right]$	$m_p\left[\frac{2}{g}\left(\delta_b\frac{p_b}{2}+\delta_b p_{si}\right)\right]$	2
5/6	$m_p\left[\frac{g}{2}\left(\frac{\delta_b+p_{si}\theta}{p_{si}}-\theta\right)+p_{si}\left(\frac{2\delta_b}{g}\right)\right]$	$m_p\left[\frac{g}{2}\left(\frac{\delta_b}{p_{fi}}\right)+\frac{2}{g}(\delta_b p_{fi})\right]$	2
5/7	$m_p\left[\frac{b_{cf}-g}{2}\left(\frac{\delta_b+p_{si}\theta}{p_{si}}\right)\right]$	$m_p\left[\frac{b_{cf}}{2}\left(\frac{\delta_b}{p_{si}}+\theta\right)-\frac{g}{2}\left(\frac{\delta_b}{p_{si}}+\theta\right)\right]$	2
6/8	$m_p\left[\frac{g}{2}(\theta)+\frac{p_b}{2}\left(\frac{2\delta_b}{g}-\frac{\delta_a+\delta_b}{g}\right)\right]$	$m_p\left\{\frac{g}{2}(\theta)+\frac{2}{g}\left[\frac{p_b}{2}\left(\frac{\delta_b-\delta_a}{2}\right)\right]\right\}$	2
7/8	$m_p\left[2\frac{p_b}{2}\left(\frac{\delta_a+\delta_b}{g}\right)\right]$	$m_p\left\{\frac{2}{g}\left[\frac{p_b}{2}(\delta_a+\delta_b)\right]\right\}$	2
8/9	$m_p\left[\frac{g}{2}(\theta)+\frac{p_b}{2}\left(\frac{\delta_a+\delta_b}{g}-\frac{2\delta_a}{g}\right)\right]$	$m_p\left\{\frac{g}{2}(\theta)+\frac{2}{g}\left[\frac{p_b}{2}\left(\frac{\delta_b-\delta_a}{2}\right)\right]\right\}$	2
7/10	$m_p\left[\frac{b_{cf}-g}{2}\left(\frac{\delta_a-s\theta}{s}\right)\right]$	$m_p\left[\frac{b_{cf}}{2}\left(\frac{\delta_a}{s}-\theta\right)-\frac{g}{2}\left(\frac{\delta_a}{s}-\theta\right)\right]$	2
1/9	$m_p\left[\left(\frac{p_b}{2}+s\right)\left(\frac{2\delta_a}{g}\right)\right]$	$m_p\left[\frac{2}{g}\left(\delta_a\frac{p_b}{2}+\delta_a s\right)\right]$	2
9/10	$m_p\left[\frac{g}{2}\left(\theta+\frac{\delta_a-s\theta}{s}\right)+s\left(\frac{2\delta_a}{g}\right)\right]$	$m_p\left[\frac{g}{2}\left(\frac{\delta_a}{s}\right)+\frac{2}{g}(\delta_a s)\right]$	2
1/10	$m_p\left[\frac{b_{cf}}{2}\left(\theta+\frac{\delta_a-s\theta}{s}\right)\right]$	$m_p\left[\frac{b_{cf}}{2}\left(\frac{\delta_a}{s}\right)\right]$	2

Summing up the internal work given in Table 3-10 and substituting $\delta_a = h_3\,\theta$, $\delta_b = h_2\,\theta$, *and* $\delta_c = h_1\,\theta$ results in the following equation for internal work:

$$W_I = 4m_p\theta\left\{\begin{array}{l}\dfrac{b_{cf}}{2}\left[h_1\left(\dfrac{1}{p_{so}}+\dfrac{1}{s}\right)+h_2\left(\dfrac{1}{p_{si}}\right)+h_3\left(\dfrac{1}{s}\right)\right]+\ldots\\ \dfrac{2}{g}\left[h_1\left(p_{so}+s\right)+h_2\left(p_{si}+\dfrac{3}{4}p_b\right)+h_3\left(s+\dfrac{1}{4}p_b\right)\right]+\dfrac{g}{2}\end{array}\right\} \tag{2-13}$$

The external work, W_E, is given by Eq. (2-14). Setting the internal work and external work equal results in Eq. (2-15).

$$W_E = M_{pl}\theta \tag{2-14}$$

$$M_{pl} = 4m_p\left\{\begin{array}{l}\dfrac{b_{cf}}{2}\left[h_1\left(\dfrac{1}{p_{so}}+\dfrac{1}{s}\right)+h_2\left(\dfrac{1}{p_{si}}\right)+h_3\left(\dfrac{1}{s}\right)\right]+\ldots\\ \dfrac{2}{g}\left[h_1\left(p_{so}+s\right)+h_2\left(p_{si}+\dfrac{3}{4}p_b\right)+h_3\left(s+\dfrac{1}{4}p_b\right)\right]+\dfrac{g}{2}\end{array}\right\} \tag{2-15}$$

This equation is further simplified into the form given in Eq. (2-16) by substituting the moment capacity per unit length, m_p, from Chapter 1, and defining the yield line parameter, Y_c, as given in Eq. (2-17).

$$M_{pl} = F_{yp}t_p^{\,2}Y_c \tag{2-16}$$

$$Y_c = \left\{\begin{array}{l}\dfrac{b_{cf}}{2}\left[h_1\left(\dfrac{1}{p_{so}}+\dfrac{1}{s}\right)+h_2\left(\dfrac{1}{p_{si}}\right)+h_3\left(\dfrac{1}{s}\right)\right]+\ldots\\ \dfrac{2}{g}\left[h_1\left(p_{so}+s\right)+h_2\left(p_{si}+\dfrac{3}{4}p_b\right)+h_3\left(s+\dfrac{1}{4}p_b\right)\right]+\dfrac{g}{2}\end{array}\right\} \tag{2-17}$$

Note: Use $p_{fi}=s$ if $p_{fi} > s$ Use $p_{fo}=s$ if $p_{fo} > s$

To obtain an equation for the dimension s, the equation for moment strength, M_{pl}, is minimized. The derivative of Eq. (2-16), taken with respect to the variable s, is set equal to zero and solved for the variable s. The result is Eq. (2-18).

$$s = \frac{1}{2}\sqrt{b_p g} \tag{2-18}$$

3.5 Eight-Bolt, 4 Rows Configurations

This configuration of eight bolts on the column is associated with the MRE 1/3 Unstiffened End-Plate, MRE 1/3 Stiffened End-Plate, and Eight-Bolt Extended Stiffened End-Plate. Figure 3-8 shows the different configurations with varied stiffening and proximity to the top of the column. The dimensions, h_1, h_2, h_3, and h_4, are the distance from the center of the beam compression flange to the tension bolt lines.

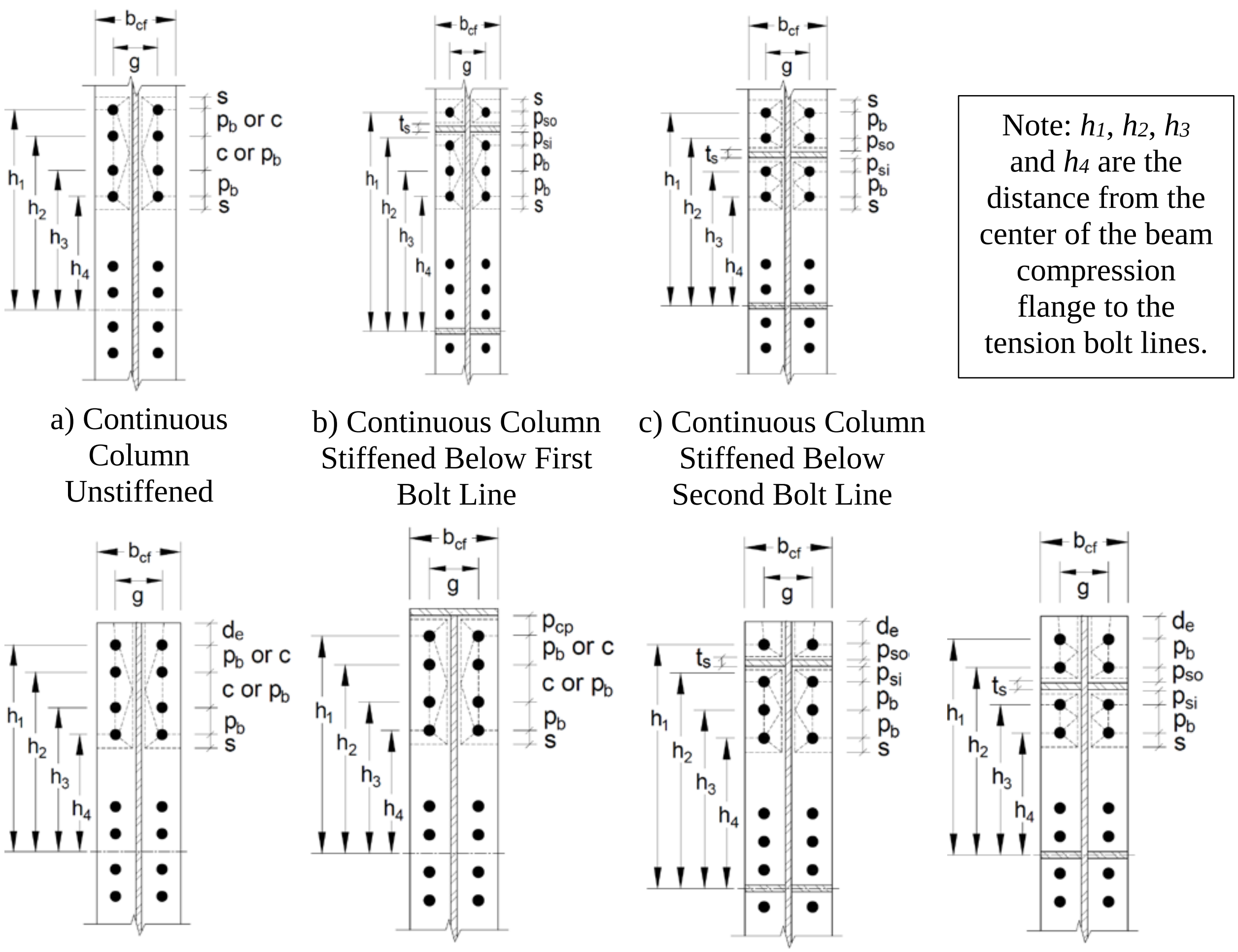

a) Continuous Column Unstiffened

b) Continuous Column Stiffened Below First Bolt Line

c) Continuous Column Stiffened Below Second Bolt Line

Note: h_1, h_2, h_3 and h_4 are the distance from the center of the beam compression flange to the tension bolt lines.

d) Top of Column Unstiffened

e) Top of Column Stiffened with Cap Plate

f) Top of Column Stiffened Below First Bolt Line

g) Top of Column Stiffened Below Second Bolt Line

Figure 3-8 Yield Line Pattern for Eight-Bolt, 4 Rows Configurations

The following describes how the equation for each yield line parameter was obtained. Table 3-11 summarizes the resulting yield line parameters.

a) Continuous column that is unstiffened (Fig. 3-8(a)). The derivation is provided later in this section.

b) Continuous column that is stiffened below the first bolt line (Fig. 3-8(b)). The derivation is same as the Continuous Column Stiffened Between the Bolts of 6-bolt Configuration (Figure 3.6b), p_b is replaced by $2p_b$ and h_3 is replaced by h_4.

c) Continuous column that is stiffened below the second bolt line (Fig. 3-8(c)). The derivation is provided later in this section.

d) Top of a column that is unstiffened (Fig. 3-8(d)). The derivation is the same as the column-side yield line parameter for the four-bolt configuration at the top of the column.

e) Top of column with cap plate (Fig. 3-8(e)). The derivation is the same as the four-bolt flush unstiffened end-plate with the following substitutions: $p_{fi} = p_{cp}$, $p_b = 2p_b+c$, $h_2 = h_4$ and $b_p = b_{cf}$.

f) Top of the column stiffened below the first bolt line (Fig. 3-8(f)). The derivation is the same as the MRE Extended 1/3 Stiffened End-Plate (Alternate Pattern) with the following substitutions: $p_{fi} = p_{si}$, $p_{fo} = p_{so}$ and $b_p = b_{cf}$.

g) Top of the column stiffened below the second bolt line (Fig. 3-8(g)). The derivation is the same as the Eight Bolt Extended Stiffened End-Plate (Alternate Pattern) with the following substitutions: $p_{fi} = p_{si}$, $p_{fo} = p_{so}$, and $b_p = b_{cf}$.

Table 3-11 Summary of Column Side Yield Line Parameters for Eight-Bolt, 4 Rows Configurations

Configuration	Yield Line Parameter
Continuous Unstiffened Column [Fig. 3-8(a)]	$Y_c = \frac{b_{cf}}{2}\left[h_1\left(\frac{1}{s}\right)+h_4\left(\frac{1}{s}\right)\right]+\frac{2}{g}\left[h_1\left(p_b+\frac{c}{2}+s\right)+h_2\left(\frac{p_b}{2}+\frac{c}{4}\right)+h_3\left(\frac{p_b}{2}+\frac{c}{4}\right)+h_4\left(s\right)\right]+\frac{g}{2}$
Continuous Column Stiffened Below the First Bolt Line [Fig. 3-8(b)]	$Y_c = \left\{\begin{array}{l}\frac{b_{cf}}{2}\left[h_1\left(\frac{1}{p_{so}}+\frac{1}{s}\right)+h_2\left(\frac{1}{p_{si}}\right)+h_4\left(\frac{1}{s}\right)\right]+\ldots \\ \frac{2}{g}\left[h_1\left(p_{so}+s\right)+h_2\left(p_{si}+\frac{3}{2}p_b\right)+h_4\left(s+\frac{1}{2}p_b\right)\right]+\frac{g}{2}\end{array}\right\}$ Note: Use $p_{si}=s$ if $p_{si} > s$ Use $p_{so}=s$ if $p_{so} > s$
Continuous Column Stiffened Below the Second Bolt Line [Fig. 3-8(c)]	$Y_c = \left\{\begin{array}{l}\frac{b_{cf}}{2}\left[h_1\left(\frac{1}{s}\right)+h_2\left(\frac{1}{p_{so}}\right)+h_3\left(\frac{1}{p_{si}}\right)+h_4\left(\frac{1}{s}\right)\right]+\ldots \\ \frac{2}{g}\left[h_1\left(\frac{3p_b}{4}+s\right)+h_2\left(\frac{p_b}{4}+p_{so}\right)+h_3\left(\frac{3p_b}{4}+p_{si}\right)+h_4\left(s+\frac{p_b}{4}\right)\right]+g\end{array}\right\}$ Note: Use $p_{si}=s$ if $p_{si} > s$ Use $p_{so}=s$ if $p_{so} > s$
Top of Column Unstiffened [Fig. 3-8(d)]	$Y_c = \frac{b_{cf}}{2}\left[h_4\left(\frac{1}{s}\right)-\frac{1}{2}\right]+\frac{2}{g}\left[h_1\left(d_e+\frac{3}{4}(2p_b+c)\right)+h_4\left(s+\frac{1}{4}(2p_b+c)\right)\right]+\frac{3g}{4}$
Top of Column with Cap Plate [Fig. 3-8(e)]	$Y_c = \frac{b_{cf}}{2}\left[h_1\left(\frac{1}{p_{cp}}\right)+h_4\left(\frac{1}{s}\right)\right]+\frac{2}{g}\left[h_1\left(p_{cp}+\frac{3}{4}(2p_b+c)\right)+h_4\left(s+\frac{1}{4}(2p_b+c)\right)\right]+\frac{g}{2}$ Note: Use $p_{cp}=s$ if $p_{cp} > s$
Top of Column Stiffened Below the First Bolt Line [Fig. 3-8(f)]	$Y_c = \left\{\begin{array}{l}\frac{b_{cf}}{2}\left[h_1\left(\frac{1}{p_{so}}\right)+h_2\left(\frac{1}{p_{si}}\right)+h_4\left(\frac{1}{s}\right)-\frac{1}{2}\right]+\ldots \\ \frac{2}{g}\left[h_1\left(p_{so}+d_e\right)+h_2\left(p_{si}+\frac{3}{2}p_b\right)+h_4\left(\frac{1}{2}p_b+s\right)\right]+\frac{3g}{4}\end{array}\right\}$ Note: Use $p_{si}=s$ if $p_{si} > s$ Use $p_{so}=s$ if $p_{so} > s$
Top of Column Stiffened Below the Second Bolt Line [Fig. 3-8(g)]	$Y_c = \left\{\begin{array}{l}\frac{b_{cf}}{2}\left[h_2\left(\frac{1}{p_{so}}\right)+h_3\left(\frac{1}{p_{si}}\right)+h_4\left(\frac{1}{s}\right)-\frac{1}{2}\right]+\ldots \\ \frac{2}{g}\left[h_1\left(\frac{3p_b}{4}+d_e\right)+h_2\left(\frac{p_b}{4}+p_{so}\right)+h_3\left(\frac{3p_b}{4}+p_{si}\right)+h_4\left(s+\frac{p_b}{4}\right)\right]+\frac{5g}{4}\end{array}\right\}$ Note: Use $p_{si}=s$ if $p_{si} > s$ Use $p_{so}=s$ if $p_{so} > s$

Derivation for the Continuous Unstiffened Column

The yield line pattern is shown in Figure 3-9. The rotation of each facet (facets are labeled in Figure 3-9) is given in Table 3-12 and the internal work associated with rotation along each yield line is given in Table 3-13. The yield lines are identified by the adjacent facet numbers (e.g., yield line 1/2 separates facets 1 and 2). Variables associated with the geometry of the connection are shown in Figure 3-9. Variables associated with the virtual rotations, displacement, and end-plate moment strength per unit length are described in Chapter 1.

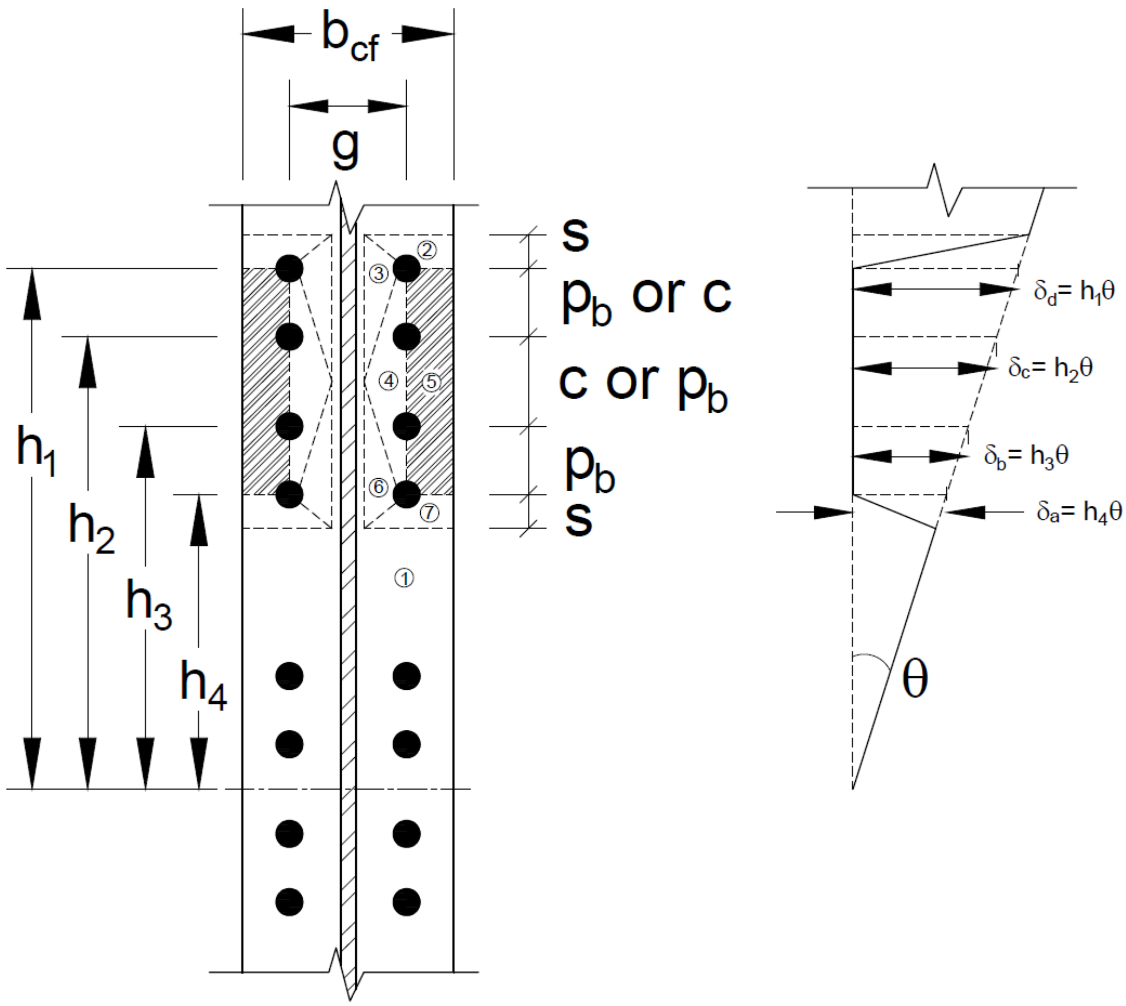

Figure 3-9 Yield Line Pattern for the Continuous Unstiffened Column

Table 3-12 Rotation for Each Facet in the Continuous Unstiffened Column

Facet	θ_x	θ_y
1	θ	0
2	$(\delta_d + s\theta)/s$	0
3	θ	$2\delta_d / g$
4	0	$(\delta_a + \delta_d)/g = (\delta_b + \delta_c)/g$
5	0	0
6	θ	$2\delta_a / g$
7	$-(\delta_a - s\theta)/s$	0

Table 3-13 Internal Work Associated with Each Yield Line in the Continuous Unstiffened Column

Yield Line	Internal Work	Simplified Internal Work	Number of Lines
1/2	$m_p\left(\frac{b_{cf}}{2}\right)\left(\frac{\delta_d + s\theta}{s} - \theta\right)$	$m_p\left(\frac{b_{cf}}{2}\right)\left(\frac{\delta_d}{s}\right)$	2
2/3	$m_p\left[\left(\frac{g}{2}\right)\left(\frac{\delta_d + s\theta}{s} - \theta\right) + s\left(\frac{2\delta_d}{g}\right)\right]$	$m_p\left[\left(\frac{g}{2}\right)\frac{\delta_d}{s} + \left(\frac{2}{g}\right)s\delta_d\right]$	2
3/4	$m_p\left[\left(\frac{g}{2}\right)\theta + (\frac{c}{2} + p_b)\left(\frac{2\delta_d}{g} - \frac{\delta_a + \delta_d}{g}\right)\right]$	$m_p\left\{\left(\frac{g}{2}\right)\theta + \left(\frac{2}{g}\right)\left[(\frac{c}{2} + p_b)\left(\frac{\delta_d}{2} - \frac{\delta_a}{2}\right)\right]\right\}$	2
4/5	$m_p\left[(2p_b + c)\left(\frac{\delta_b + \delta_c}{g}\right)\right]$	$m_p\left(\frac{2}{g}\right)\left[(2p_b + c)\left(\frac{\delta_b + \delta_c}{2}\right)\right]$	2
4/6	$m_p\left[\left(\frac{g}{2}\right)\theta + (\frac{c}{2} + p_b)\left(\frac{\delta_d + \delta_a}{g} - \frac{2\delta_a}{g}\right)\right]$	$m_p\left\{\left(\frac{g}{2}\right)\theta + \left(\frac{2}{g}\right)\left[(\frac{c}{2} + p_b)\left(\frac{\delta_d}{2} - \frac{\delta_a}{2}\right)\right]\right\}$	2
6/7	$m_p\left[\left(\frac{g}{2}\right)\left(\theta + \frac{\delta_a - s\theta}{s}\right) + s\left(\frac{2\delta_a}{g}\right)\right]$	$m_p\left[\frac{g}{2}\left(\frac{\delta_a}{s}\right) + \frac{2}{g}(s\delta_a)\right]$	2
7/1	$m_p\left[\frac{b_{cf}}{2}\left(\theta + \frac{\delta_a - s\theta}{s}\right)\right]$	$m_p\left[\frac{b_{cf}}{2}\left(\frac{\delta_a}{s}\right)\right]$	2
6/1	$m_p\left[\left(s + p_b + \frac{c}{2}\right)\left(\frac{2\delta_a}{g}\right)\right]$	$m_p\left(\frac{2}{g}\right)\left[\left(s + p_b + \frac{c}{2}\right)\delta_a\right]$	2
3/1	$m_p\left[\left(s + p_b + \frac{c}{2}\right)\left(\frac{2\delta_d}{g}\right)\right]$	$m_p\left(\frac{2}{g}\right)\left[\left(s + p_b + \frac{c}{2}\right)\delta_d\right]$	2
2/5	$m_p\left[\left(\frac{b_{cf} - g}{2}\right)\left(\frac{\delta_d + s\theta}{s}\right)\right]$	$m_p\left[\frac{b_{cf}}{2}\left(\frac{\delta_d}{s} + \theta\right) - \frac{g}{2}\left(\frac{\delta_d}{s} + \theta\right)\right]$	2
5/7	$m_p\left[\left(\frac{b_{cf} - g}{2}\right)\left(\frac{\delta_a - s\theta}{s}\right)\right]$	$m_p\left[\frac{b_{cf}}{2}\left(\frac{\delta_a}{s} - \theta\right) - \frac{g}{2}\left(\frac{\delta_a}{s} - \theta\right)\right]$	2

Summing up the internal work given in Table 3-13 and substituting $\delta_a = h_4\,\theta$, $\delta_b = h_3\,\theta$, $\delta_c = h_2\,\theta$, and $\delta_d = h_1\,\theta$ results in the following equation for internal work:

$$W_I = 4m_p\theta\left\{\frac{b_{cf}}{2}\left[h_1\left(\frac{1}{s}\right)+h_4\left(\frac{1}{s}\right)\right]+\frac{2}{g}\left[h_1\left(p_b+\frac{c}{2}+s\right)+h_2\left(\frac{p_b}{2}+\frac{c}{4}\right)+h_3\left(\frac{p_b}{2}+\frac{c}{4}\right)+h_4\left(s\right)\right]+\frac{g}{2}\right\} \quad (3\text{-}19)$$

The external work, W_E, is given by Eq. (3-20). Setting the internal work and external work equal results in Eq. (3-21).

$$W_E = M_{pl}\theta \quad (3\text{-}20)$$

$$M_{pl} = 4m_p\left\{\frac{b_{cf}}{2}\left[h_1\left(\frac{1}{s}\right)+h_4\left(\frac{1}{s}\right)\right]+\frac{2}{g}\left[h_1\left(p_b+\frac{c}{2}+s\right)+h_2\left(\frac{p_b}{2}+\frac{c}{4}\right)+h_3\left(\frac{p_b}{2}+\frac{c}{4}\right)+h_4\left(s\right)\right]+\frac{g}{2}\right\} \quad (3\text{-}21)$$

This equation is further simplified into the form given in Eq. (3-22) by substituting the moment capacity per unit length, m_p, from Chapter 1, and defining the yield line parameter, Y, as given in Eq. (3-23).

$$M_{pl} = F_{yp}t_p^{\,2}Y_c \quad (3\text{-}22)$$

$$Y_c = \frac{b_{cf}}{2}\left[h_1\left(\frac{1}{s}\right)+h_4\left(\frac{1}{s}\right)\right]+\frac{2}{g}\left[h_1\left(p_b+\frac{c}{2}+s\right)+h_2\left(\frac{p_b}{2}+\frac{c}{4}\right)+h_3\left(\frac{p_b}{2}+\frac{c}{4}\right)+h_4\left(s\right)\right]+\frac{g}{2} \quad (3\text{-}23)$$

To obtain an equation for the dimension s, the equation for moment strength, M_{pl}, is minimized. The derivative of Eq. (3-22), taken with respect to the variable s, is set equal to zero and solved for the variable s. The result is Eq. (3-24).

$$s = \frac{1}{2}\sqrt{b_{cf}\,g} \quad (3\text{-}24)$$

Derivation for the Continuous Column Stiffened Below the Second Bolt Line

The yield line pattern is shown in Figure 3-10. The rotation of each facet (facets are labeled in Figure 3-10) is given in Table 3-14 and the internal work associated with rotation along each yield line is given in Table 3-15. The yield lines are identified by the adjacent facet numbers (e.g., yield line 1/2 separates facets 1 and 2). Variables associated with the geometry of the connection are shown in Figure 3-10. Variables associated with the virtual rotations, displacement, and end-plate moment strength per unit length are described in Chapter 1.

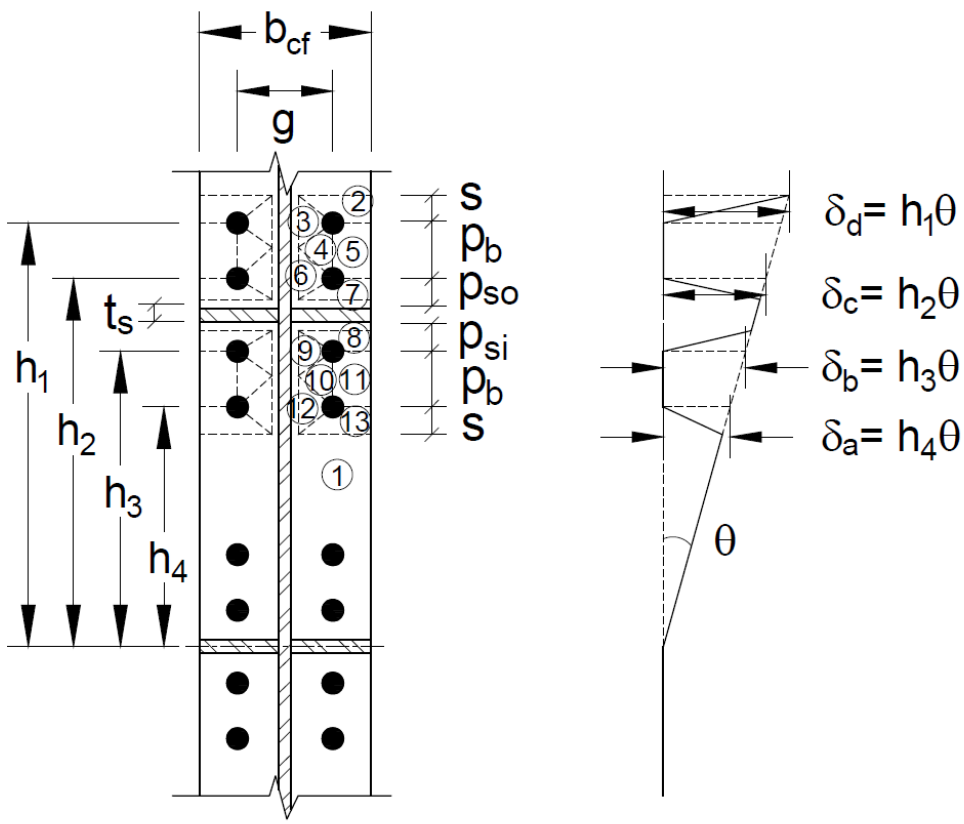

Figure 3-10 Yield Line Pattern for the Continuous Column Stiffened Below the Second Bolt Line

Table 3-14 Rotation for Each Facet in the Continuous Column Stiffened Below the Second Bolt Line

Facet	θ_x	θ_y
1	θ	0
2	$(\delta_d + s\theta)/s$	0
3	θ	$2\delta_d / g$
4	0	$(\delta_c + \delta_d)/g$
5	0	0
6	0	$2\delta_c / g$
7	$-(\delta_c - p_{so}\theta)/p_{so}$	0
8	$(\delta_b + p_{si}\theta)/p_{si}$	0
9	θ	$2\delta_b / g$
10	0	$(\delta_a + \delta_b)/g$
11	0	0
12	θ	$2\delta_a / g$
13	$-(\delta_a - s\theta)/s$	0

Table 3-15 Internal Work Associated with Each Yield Line in the Continuous Column Stiffened Below the Second Bolt Line (Part 1 of 2)

Yield Line	Internal Work	Simplified Internal Work	Number of Lines
1/2	$m_p[\frac{b_{cf}}{2}(\frac{\delta_d + s\theta}{s} - \theta)]$	$m_p[\frac{b_{cf}}{2}(\frac{\delta_d}{s})]$	2
2/3	$m_p[\frac{g}{2}(\frac{\delta_d + s\theta}{s} - \theta) + s\frac{2\delta_d}{g}]$	$m_p[\frac{g}{2}(\frac{\delta_d}{s}) + \frac{2}{g}(s\delta_d)]$	2
2/5	$m_p[\frac{b_{cf} - g}{2}(\frac{\delta_d + s\theta}{s})]$	$m_p[\frac{b_{cf}}{2}(\frac{\delta_d}{s} + \theta) - \frac{g}{2}(\frac{\delta_d}{s} + \theta)]$	2
1/3	$m_p[(s + \frac{p_b}{2})\frac{2\delta_d}{g}]$	$m_p[\frac{2}{g}\delta_d(s + \frac{p_b}{2})]$	2
3/4	$m_p[\frac{g}{2}\theta + \frac{p_b}{2}(\frac{2\delta_d}{g} - \frac{\delta_c + \delta_d}{g})]$	$m_p\left\{\frac{g}{2}(\theta) + \frac{2}{g}\left[\frac{p_b(\delta_d - \delta_c)}{4}\right]\right\}$	2
4/5	$m_p\left[p_b\left(\frac{\delta_c + \delta_d}{g}\right)\right]$	$m_p\left[\frac{2}{g}\left(\frac{p_b\delta_c + p_b\delta_d}{2}\right)\right]$	2

Table 3-15 Internal Work Associated with Each Yield Line in the Continuous Column Stiffened Below the Second Bolt Line (Part 2 of 2)

Yield Line	Internal Work	Simplified Internal Work	Number of Lines
4/6	$m_p\left[\frac{g}{2}(\theta)+\frac{p_b}{2}\left(\frac{\delta_c+\delta_d}{g}-\frac{2\delta_c}{g}\right)\right]$	$m_p\left[\frac{g}{2}(\theta)+\frac{2}{g}\left(\frac{p_b(\delta_c+\delta_d)}{4}-\frac{p_b\delta_c}{2}\right)\right]$	2
1/6	$m_p\left[\left(p_{so}+\frac{p_b}{2}\right)\left(\frac{2\delta_c}{g}\right)\right]$	$m_p\left[\frac{2}{g}\left(\delta_c p_{so}+\frac{\delta_c p_b}{2}\right)\right]$	2
6/7	$m_p\left[\frac{g}{2}\left(\theta+\frac{\delta_c-p_{so}\theta}{p_{so}}\right)+p_{fo}\left(\frac{2\delta_c}{g}\right)\right]$	$m_p\left[\frac{g}{2}\left(\frac{\delta_c}{p_{so}}\right)+\frac{2}{g}(\delta_c p_{so})\right]$	2
5/7	$m_p\left[\frac{b_{cf}-g}{2}\left(\frac{\delta_c-p_{so}\theta}{p_{so}}\right)\right]$	$m_p\left[\frac{b_{cf}}{2}\left(\frac{\delta_c}{p_{so}}-\theta\right)-\frac{g}{2}\left(\frac{\delta_c}{p_{so}}-\theta\right)\right]$	2
1/7	$m_p\left[\frac{b_{cf}}{2}\left(\theta+\frac{\delta_c-p_{so}\theta}{p_{so}}\right)\right]$	$m_p\left[\frac{b_{cf}}{2}\left(\frac{\delta_c}{p_{so}}\right)\right]$	2
1/8	$m_p\left[\frac{b_{cf}}{2}\left(\frac{\delta_b+p_{si}\theta}{p_{si}}-\theta\right)\right]$	$m_p\left[\frac{b_{cf}}{2}\left(\frac{\delta_b}{p_{si}}\right)\right]$	2
8/9	$m_p\left[\frac{g}{2}\left(\frac{\delta_b+p_{si}\theta}{p_{si}}-\theta\right)+p_{si}\left(\frac{2\delta_b}{g}\right)\right]$	$m_p\left[\frac{g}{2}\left(\frac{\delta_b}{p_{si}}\right)+\frac{2}{g}(p_{si}\delta_b)\right]$	2
8/11	$m_p\left[\frac{b_{cf}-g}{2}\left(\frac{\delta_b+p_{si}\theta}{p_{si}}\right)\right]$	$m_p\left[\frac{b_{cf}}{2}\left(\frac{\delta_b}{p_{si}}+\theta\right)-\frac{g}{2}\left(\frac{\delta_b}{p_{si}}+\theta\right)\right]$	2
1/9	$m_p\left[\left(p_{si}+\frac{p_b}{2}\right)\left(\frac{2\delta_b}{g}\right)\right]$	$m_p\left[\frac{2}{g}\left(\delta_b p_{si}+\frac{\delta_b p_b}{2}\right)\right]$	2
9/10	$m_p\left[\frac{g}{2}(\theta)+\frac{p_b}{2}\left(\frac{2\delta_b}{g}-\frac{\delta_a+\delta_b}{g}\right)\right]$	$m_p\left\{\frac{g}{2}(\theta)+\frac{2}{g}\left[\frac{p_b(\delta_b-\delta_a)}{4}\right]\right\}$	2
10/11	$m_p\left[p_b\left(\frac{\delta_a+\delta_b}{g}\right)\right]$	$m_p\left\{\frac{2}{g}\left[\frac{p_b(\delta_a+\delta_b)}{2}\right]\right\}$	2
10/12	$m_p\left[\frac{g}{2}(\theta)+\frac{p_b}{2}\left(\frac{\delta_a+\delta_b}{g}-\frac{2\delta_a}{g}\right)\right]$	$m_p\left\{\frac{g}{2}(\theta)+\frac{2}{g}\left[\frac{p_b(\delta_b-\delta_a)}{4}\right]\right\}$	2
11/13	$m_p\left[\frac{b_{cf}-g}{2}\left(\frac{\delta_a-s\theta}{s}\right)\right]$	$m_p\left[\frac{b_{cf}}{2}\left(\frac{\delta_a}{s}-\theta\right)-\frac{g}{2}\left(\frac{\delta_a}{s}-\theta\right)\right]$	2
12/13	$m_p\left[\frac{g}{2}\left(\theta+\frac{\delta_a-s\theta}{s}\right)+s\left(\frac{2\delta_a}{g}\right)\right]$	$m_p\left[\frac{g}{2}\left(\frac{\delta_a}{s}\right)+\frac{2}{g}(s\delta_a)\right]$	2
1/12	$m_p\left[\left(s+\frac{p_b}{2}\right)\left(\frac{2\delta_a}{g}\right)\right]$	$m_p\left[\frac{2}{g}\left(\delta_a s+\frac{\delta_a p_b}{2}\right)\right]$	2
1/13	$m_p\left[\frac{b_{cf}}{2}\left(\theta-\frac{-\delta_a+s\theta}{s}\right)\right]$	$m_p\left[\frac{b_{cf}}{2}\left(\frac{\delta_a}{s}\right)\right]$	2

Summing up the internal work given in Table 3-15 and substituting $\delta_a = h_4 \theta$, $\delta_b = h_3 \theta$, $\delta_c = h_2 \theta$, and $\delta_d = h_1 \theta$ results in the following equation for internal work:

$$W_I = 4m_p\theta\left\{\begin{aligned}&\frac{b_{cf}}{2}\left[h_1\left(\frac{1}{s}\right)+h_2\left(\frac{1}{p_{so}}\right)+h_3\left(\frac{1}{p_{si}}\right)+h_4\left(\frac{1}{s}\right)\right]+\ldots\\&\frac{2}{g}\left[h_1\left(\frac{3p_b}{4}+s\right)+h_2\left(\frac{p_b}{4}+P_{so}\right)+h_3\left(\frac{3p_b}{4}+p_{si}\right)+h_4\left(s+\frac{p_b}{4}\right)\right]+g\end{aligned}\right\} \tag{3-25}$$

The external work, W_E, is given by Eq. (3-26). Setting the internal work and external work equal results in Eq. (3-27).

$$W_E = M_{pl}\theta \tag{3-26}$$

$$M_{pl} = 4m_p\left\{\begin{aligned}&\frac{b_{cf}}{2}\left[h_1\left(\frac{1}{s}\right)+h_2\left(\frac{1}{p_{so}}\right)+h_3\left(\frac{1}{p_{si}}\right)+h_4\left(\frac{1}{s}\right)\right]+\ldots\\&\frac{2}{g}\left[h_1\left(\frac{3p_b}{4}+s\right)+h_2\left(\frac{p_b}{4}+P_{so}\right)+h_3\left(\frac{3p_b}{4}+P_{si}\right)+h_4\left(s+\frac{p_b}{4}\right)\right]+g\end{aligned}\right\} \tag{3-27}$$

This equation is further simplified into the form given in Eq. (3-28) by substituting the moment capacity per unit length, m_p, from Chapter 1, and defining the yield line parameter, Y, as given in Eq. (3-29).

$$M_{pl} = F_{yp}t_p^{\,2}Y_c \tag{3-28}$$

$$Y_c = \left\{\begin{aligned}&\frac{b_{cf}}{2}\left[h_1\left(\frac{1}{s}\right)+h_2\left(\frac{1}{p_{so}}\right)+h_3\left(\frac{1}{p_{si}}\right)+h_4\left(\frac{1}{s}\right)\right]+\ldots\\&\frac{2}{g}\left[h_1\left(\frac{3p_b}{4}+s\right)+h_2\left(\frac{p_b}{4}+p_{so}\right)+h_3\left(\frac{3p_b}{4}+p_{si}\right)+h_4\left(s+\frac{p_b}{4}\right)\right]+g\end{aligned}\right\} \tag{3-29}$$

To obtain an equation for the dimension *s*, the equation for moment strength, M_{pl}, is minimized. The derivative of Eq. (3-28), taken with respect to the variable *s*, is set equal to zero and solved for the variable s. The result is Eq. (3-30).

$$s = \frac{1}{2}\sqrt{b_{cf}\,g} \tag{3-30}$$

3.6 Eight-Bolt Four-Wide Configurations

This configuration of eight bolts on the column is associated with Eight-Bolt Extended Four-Wide Unstiffened End-Plate. Figure 3-11 shows the different configurations with varied stiffening and proximity to the top of the column. The dimensions, h_1, and h_2, are the distance from the center of the beam compression flange to the tension bolt lines.

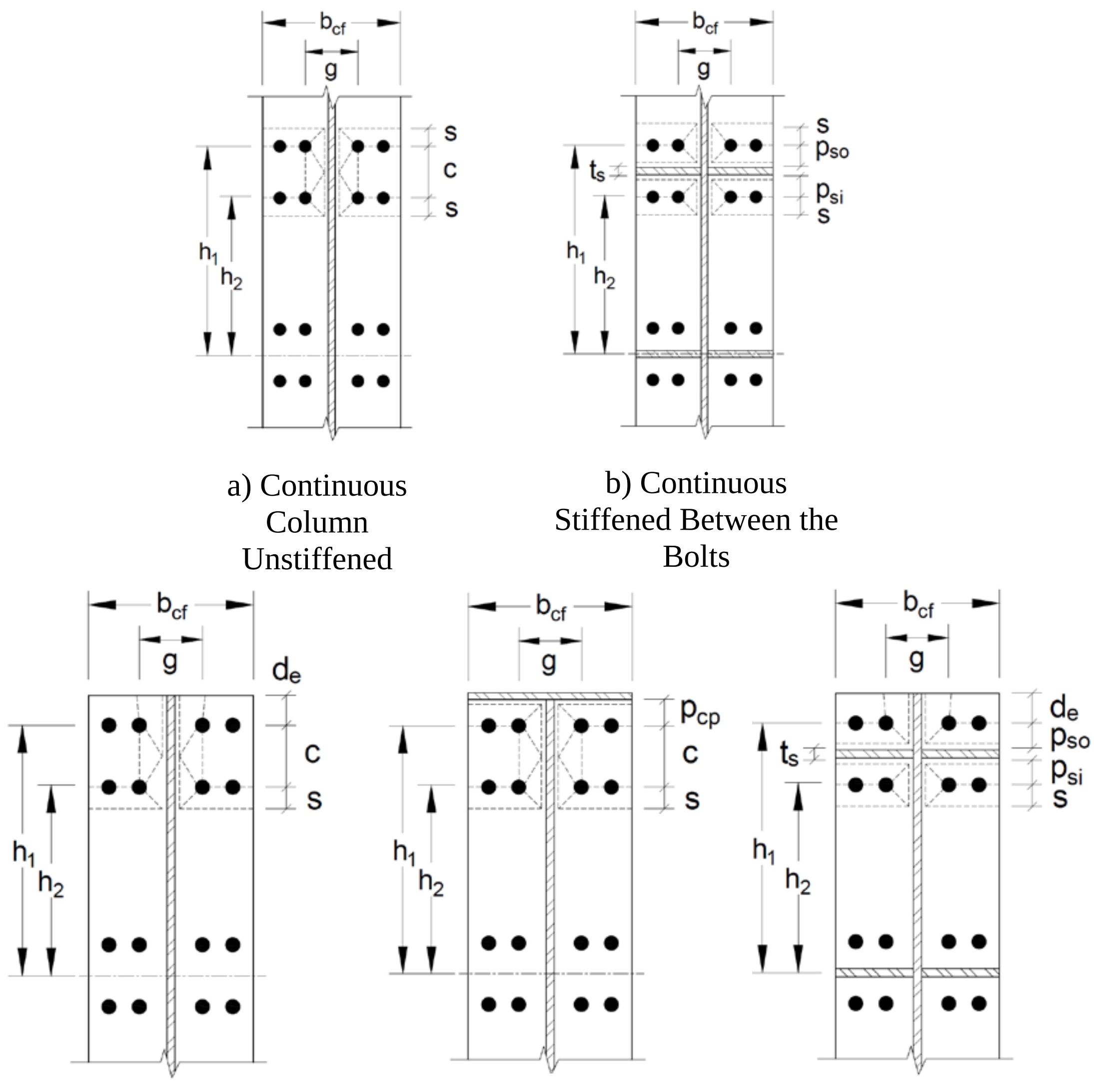

a) Continuous Column Unstiffened

b) Continuous Stiffened Between the Bolts

c) Top of Column Unstiffened

d) Top of Column Stiffened with Cap Plate

e) Top of Column Stiffened Between the Bolts

Figure 3-11 Yield Line Pattern for Eight-Bolt Four-Wide Configurations

The following describes how the equation for each yield line parameter was obtained. Table 3-16 summarizes the resulting yield line parameters.

a) Continuous column that is unstiffened (Fig. 3-11(a)). The derivation for the yield line parameter is the same as the four-bolt unstiffened flush end-plate with the following substitutions: $p_{fi} = s$, $p_b = c$ and $b_p = b_{cf}$.

b) Continuous column that is stiffened below the first bolt line (Fig. 3-11(b)). The derivation is same as the column-side yield line parameter for the four-bolt configuration stiffened between the bolts.

c) Top of a column that is unstiffened (Fig. 3-11(c)). The derivation is the same as the column-side yield line parameter for the four-bolt configuration at the top of the column.

d) Top of column with cap plate (Fig. 3-11(d)). The derivation is the same as the four-bolt unstiffened flush end-plate with the following substitutions: $p_{fi} = p_{cp}$, $p_b = c$ and $b_p = b_{cf}$.

e) Top of the column stiffened below the first bolt line (Fig. 3-11(e)). The derivation is the same as the four-bolt extended stiffened end-plate (Alternate Pattern) with the following substitutions: $p_{fi} = p_{si}$, $p_{fo} = p_{so}$, and $b_p = b_{cf}$.

Table 3-16 Summary of Column Side Yield Line Parameters for the Eight-Bolt Four-Wide Configurations

Configuration	Yield Line Parameter
Continuous Unstiffened Column [Fig. 3-11(a)]	$Y_c = \frac{b_{cf}}{2}\left[h_1\left(\frac{1}{s}\right)+h_2\left(\frac{1}{s}\right)\right]+\frac{2}{g}\left[h_1\left(s+\frac{3}{4}c\right)+h_2\left(s+\frac{1}{4}c\right)\right]+\frac{g}{2}$
Continuous Column Stiffened Between the Bolts [Fig. 3-11(b)]	$Y_c = \frac{b_{cf}}{2}\left[h_1\left(\frac{1}{s}+\frac{1}{p_{so}}\right)+h_2\left(\frac{1}{p_{si}}+\frac{1}{s}\right)\right]+\frac{2}{g}\left[h_1\left(s+p_{so}\right)+h_2\left(p_{si}+s\right)\right]$ Note: Use p_{si}=s if $p_{si} > s$ Use p_{so}=s if $p_{so} > s$
Top of Column Unstiffened [Fig. 3-11(c)]	$Y_c = \frac{b_{cf}}{2}\left[h_2\left(\frac{1}{s}\right)-\frac{1}{2}\right]+\frac{2}{g}\left[h_1\left(d_e+\frac{3}{4}c\right)+h_2\left(s+\frac{1}{4}c\right)\right]+\frac{3g}{4}$
Top of Column with Cap Plate [Fig. 3-11(d)]	$Y_c = \frac{b_{cf}}{2}\left[h_1\left(\frac{1}{p_{cp}}\right)+h_2\left(\frac{1}{s}\right)\right]+\frac{2}{g}\left[h_1\left(p_{cp}+\frac{3}{4}c\right)+h_2\left(s+\frac{1}{4}c\right)\right]+\frac{g}{2}$ Note: Use p_{cp}=s if $p_{cp} > s$
Top of Column Stiffened Between Bolts [Fig. 3-11(e)]	$Y_c = \frac{b_{cf}}{2}\left[h_1\left(\frac{1}{p_{so}}\right)+h_2\left(\frac{1}{p_{si}}+\frac{1}{s}\right)-\frac{1}{2}\right]+\frac{2}{g}\left[h_1\left(p_{so}+d_e\right)+h_2\left(p_{si}+s\right)\right]+\frac{g}{4}$ Note: Use p_{si}=s if $p_{si} > s$ Use p_{so}=s if $p_{so} > s$

3.7 Twelve Bolt 4Wx2/2Wx2 Configurations

This configuration of twelve bolts on the column is associated with Twelve-Bolt MRE 1/3 Unstiffened End-Plate. Figure 3-12 shows the different configurations with varied stiffening and proximity to the top of the column. The dimensions, h_1, h_2, h_3, and h_4, are the distance from the center of the beam compression flange to the tension bolt lines.

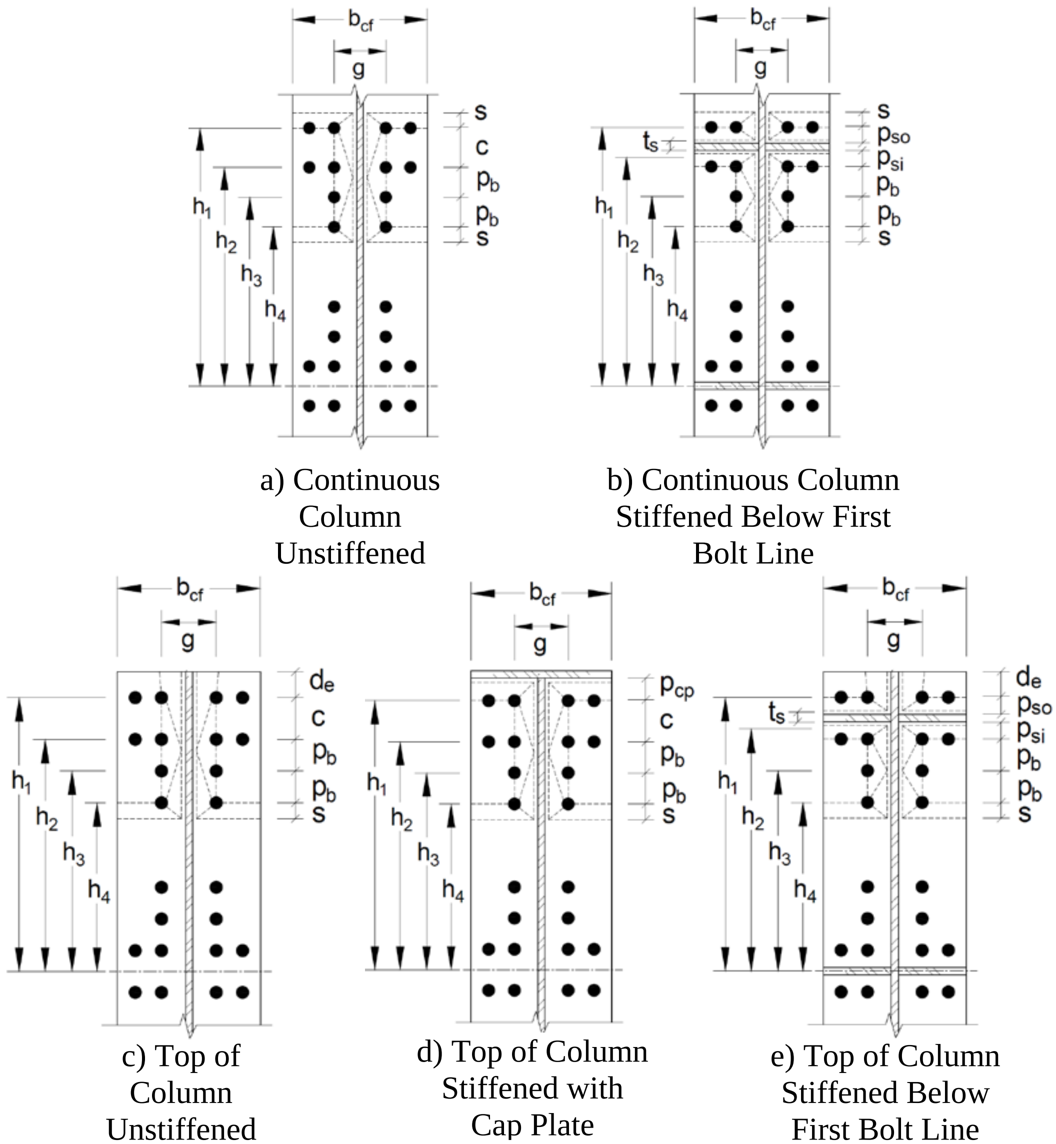

a) Continuous Column Unstiffened

b) Continuous Column Stiffened Below First Bolt Line

c) Top of Column Unstiffened

d) Top of Column Stiffened with Cap Plate

e) Top of Column Stiffened Below First Bolt Line

Figure 3-12 Yield Line Pattern for Twelve Bolt 4Wx2/2Wx2 Configurations

The following describes how the equation for each yield line parameter was obtained. Table 3-17 summarizes the resulting yield line parameters.

a) Continuous column that is unstiffened (Fig. 3-12(a)). The derivation for the yield line parameter is the same as the four-bolt unstiffened flush end-plate with the following substitutions: $p_b = 2p_b + c$, $h_2 = h_4$, $p_{fi} = s$ and $b_p = b_{cf}$.

   Continuous column that is stiffened below the first bolt line (Fig. 3-12(b)). The derivation is the same as the Continuous Column Stiffened Below First Bolt Line of 8-bolt Configuration (Figure 3.8b).

b) Top of a column that is unstiffened (Fig. 3-12(c)). The derivation is the same as the column-side yield line parameter for the four-bolt configuration at the top of the column with the following substitutions: $p_b = 2p_b + c$ and $h_2 = h_4$.

c) Top of column with cap plate (Fig. 3-12(d)). The derivation is the same as the four-bolt unstiffened flush with the following substitutions: $p_b = 2p_b + c$, $h_2 = h_4$, $p_{fi} = p_{cp}$ and $b_p = b_{cf}$.

d) Top of the column stiffened below the first bolt line (Fig. 3-12(e)). The derivation is the same as the MRE 1/3 Stiffened End-Plate (Alternate Pattern) configuration with the following substitutions: $p_{fi} = p_{si}$, $p_{fo} = p_{so}$, $h_3 = h_4$, and $b_p = b_{cf}$.

Table 3-17 Summary of Column Side Yield Line Parameters for Twelve Bolt 4Wx2/2Wx2 Configurations

Configuration	Yield Line Parameter
Continuous Unstiffened Column [Fig. 3-12(a)]	$Y_c = \frac{b_{cf}}{2}\left[h_1\left(\frac{1}{s}\right)+h_4\left(\frac{1}{s}\right)\right]+\frac{2}{g}\left[h_1\left(s+\frac{3}{2}p_b+\frac{3}{4}c\right)+h_4\left(s+\frac{1}{2}p_b+\frac{1}{4}c\right)\right]+\frac{g}{2}$
Continuous Column Stiffened Below the First Bolt Line [Fig. 3-12(b)]	$Y_c = \left\{\begin{matrix}\frac{b_{cf}}{2}\left[h_1\left(\frac{1}{p_{so}}+\frac{1}{s}\right)+h_2\left(\frac{1}{p_{si}}\right)+h_4\left(\frac{1}{s}\right)\right]+\ldots \\ \frac{2}{g}\left[h_1\left(p_{so}+s\right)+h_2\left(p_{si}+\frac{3}{2}p_b\right)+h_4\left(s+\frac{1}{2}p_b\right)\right]+\frac{g}{2}\end{matrix}\right\}$ Note: Use $p_{si}=s$ if $p_{si} > s$ Use $p_{so}=s$ if $p_{so} > s$
Top of Column Unstiffened [Fig. 3-12(c)]	$Y_c = \frac{b_{cf}}{2}\left[h_4\left(\frac{1}{s}\right)-\frac{1}{2}\right]+\frac{2}{g}\left[h_1\left(d_e+\frac{3}{2}p_b+\frac{3}{4}c\right)+h_4\left(s+\frac{1}{2}p_b+\frac{1}{4}c\right)\right]+\frac{3g}{4}$
Top of Column with Cap Plate [Fig. 3-12(d)]	$Y_c = \frac{b_{cf}}{2}\left[h_1\left(\frac{1}{p_{cp}}\right)+h_4\left(\frac{1}{s}\right)\right]+\frac{2}{g}\left[h_1\left(p_{cp}+\frac{3}{2}p_b+\frac{3}{4}c\right)+h_4\left(s+\frac{1}{2}p_b+\frac{1}{4}c\right)\right]+\frac{g}{2}$ Note: Use $p_{cp}=s$ if $p_{cp} > s$
Top of Column Stiffened Below the First Bolt Line [Fig. 3-12(e)]	$Y_c = \left\{\begin{matrix}\frac{b_{cf}}{2}\left[h_1\left(\frac{1}{p_{so}}\right)+h_2\left(\frac{1}{p_{si}}\right)+h_4\left(\frac{1}{s}\right)-\frac{1}{2}\right]+\ldots \\ \frac{2}{g}\left[h_1\left(p_{so}+d_e\right)+h_2\left(p_{si}+\frac{3}{2}p_b\right)+h_4\left(s+\frac{1}{2}p_b\right)\right]+\frac{3g}{4}\end{matrix}\right\}$ Note: Use $p_{si}=s$ if $p_{si} > s$ Use $p_{so}=s$ if $p_{so} > s$

3.8 Twelve Bolt 2W/4Wx2/2W Configurations

This configuration of twelve bolts on the column is associated with Twelve-Bolt Extended Stiffened End-Plate configuration. Figure 3-13 shows the different configurations with varied stiffening and proximity to the top of the column. The dimensions, h_1, h_2, h_3, and h_4, are the distance from the center of the beam compression flange to the tension bolt lines.

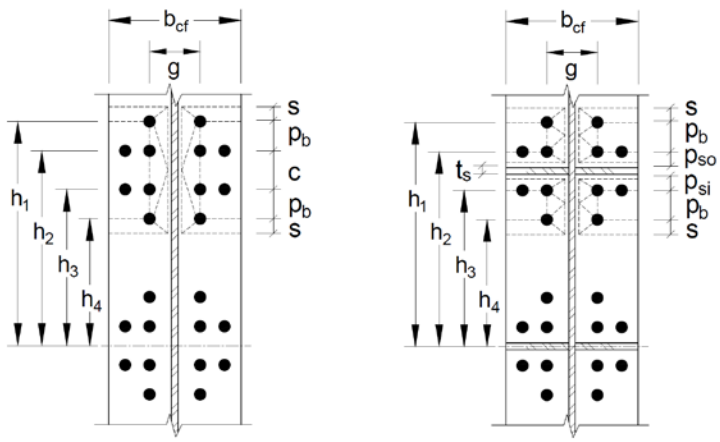

a) Continuous Column Unstiffened

b) Continuous Column Stiffened Below Second Bolt Line

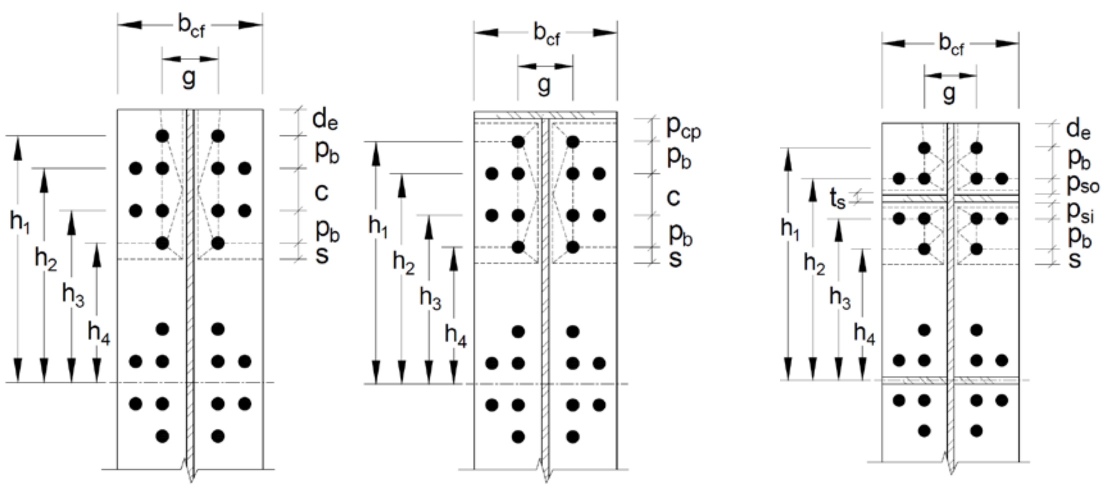

c) Top of Column Unstiffened

d) Top of Column Stiffened with Cap Plate

e) Top of Column Stiffened Below Second Bolt Line

Figure 3-13 Yield Line Pattern for Twelve Bolt 2W/4Wx2/2W Configurations

The following describes how the equation for each yield line parameter was obtained. Table 3-18 summarizes the resulting yield line parameters.

a) For a continuous column that is unstiffened (Fig. 3-13(a)), the derivation for the yield line parameter is the same as the four-bolt flush unstiffened end-plate with the following substitutions: $p_b = 2p_b + c$, $h_2 = h_4$, $p_{fi} = s$ and $b_p = b_{cf}$.

b) For a continuous column that is stiffened below the second bolt line (Fig. 3-13(b)), the derivation is the same as the column-side pattern for the Eight-Bolt 4 Rows configuration. (Figure 3-7c).

c) For the top of a column that is unstiffened (Fig. 3-13(c)), the derivation is the same as the column-side yield line parameter for the four-bolt configuration at the top of the column with the following substitutions: $h_2 = h_4$, $c = 2p_b+c$.

d) For the top of column with cap plate (Fig. 3-13(d)), the derivation is the same as the four-bolt flush unstiffened end-plate with the following substitutions: $h_2 = h_4$, $p_{fi} = p_{cp}$, $p_b = 2p_b+c$ and $b_p = b_{cf}$.

e) For the top of the column stiffened below the second bolt line (Fig. 3-13(e)), the derivation is the same as the Eight-Bolt Extended Stiffened End-Plate (alternate pattern) configuration with the following substitutions: $p_{fi} = p_{si}$, $p_{fo} = p_{so}$, and $b_p = b_{cf}$.

Table 3-18 Summary of Column Side Yield Line Parameters for Twelve Bolt 2W/4Wx2/2W Configurations

Configuration	Yield Line Parameter
Continuous Unstiffened Column [Fig. 3-13(a)]	$Y_c = \frac{b_{cf}}{2}\left[h_1\left(\frac{1}{s}\right)+h_4\left(\frac{1}{s}\right)\right]+\frac{2}{g}\left[h_1\left(s+\frac{3}{2}p_b+\frac{3}{4}c\right)+h_4\left(s+\frac{1}{2}p_b+\frac{1}{4}c\right)\right]+\frac{g}{2}$
Continuous Column Stiffened Below the Second Bolt Line [Fig. 3-13(b)]	$Y_c = \left\{\begin{matrix} \frac{b_{cf}}{2}\left[h_1\left(\frac{1}{s}\right)+h_2\left(\frac{1}{p_{so}}\right)+h_3\left(\frac{1}{p_{si}}\right)+h_4\left(\frac{1}{s}\right)\right]+\ldots \\ \frac{2}{g}\left[h_1\left(\frac{3p_b}{4}+s\right)+h_2\left(\frac{p_b}{4}+p_{so}\right)+h_3\left(\frac{3p_b}{4}+p_{si}\right)+h_4\left(\frac{p_b}{4}+s\right)\right]+g \end{matrix}\right\}$ Note: Use $p_{si}=s$ if $p_{si} > s$ Use $p_{so}=s$ if $p_{so} > s$
Top of Column Unstiffened [Fig. 3-13(c)]	$Y_c = \frac{b_{cf}}{2}\left[h_4\left(\frac{1}{s}\right)-\frac{1}{2}\right]+\frac{2}{g}\left[h_1\left(d_e+\frac{3}{2}p_b+\frac{3}{4}c\right)+h_4\left(s+\frac{1}{2}p_b+\frac{1}{4}c)\right)\right]+\frac{3g}{4}$
Top of Column with Cap Plate [Fig. 3-13(d)]	$Y_c = \left\{\frac{b_{cf}}{2}\left[h_1\left(\frac{1}{p_{cp}}\right)+h_4\left(\frac{1}{s}\right)\right]+\frac{2}{g}\left[h_1\left(p_{cp}+\frac{3}{2}p_b+\frac{3}{4}c\right)+h_4\left(s+\frac{1}{2}p_b+\frac{1}{4}c\right)\right]+\frac{g}{2}\right\}$ Note: Use $p_{cp}=s$ if $p_{cp} > s$
Top of Column Stiffened Below the Second Bolt Line [Fig. 3-13(e)]	$Y = \left\{\begin{matrix} \frac{b_{cf}}{2}\left[h_2\left(\frac{1}{p_{so}}\right)+h_3\left(\frac{1}{p_{si}}\right)+h_4\left(\frac{1}{s}\right)-\frac{1}{2}\right]+\ldots \\ \frac{2}{g}\left[h_1\left(\frac{3p_b}{4}+d_e\right)+h_2\left(\frac{p_b}{4}+p_{so}\right)+h_3\left(\frac{3p_b}{4}+p_{si}\right)+h_4\left(s+\frac{p_b}{4}\right)\right]+\frac{5g}{4} \end{matrix}\right\}$ Note: Use $p_{si}=s$ if $p_{si} > s$ Use $p_{so}=s$ if $p_{so} > s$

REFERENCES

Abel, M.S.M., and Murray, T.M., (1992), *Multiple Row, Extended Unstiffened End-Plate Connection Tests*, Virginia Tech Structural Engineering Report No. CE/VPI-ST-02/04, Blacksburg, VA.

Abel, M.S.M., and Murray, T.M. (1994), *Analytical and Experimental Investigation of the Extended Unstiffened Moment End-Plate Connection with Four Bolts at the Beam Tension Flange*, Virginia Tech Structural Engineering Report No. CE/VPI-ST-93/08, Blacksburg, VA.

Blumenbaum, S. and Murray, T. M. (2003), *Strength Evaluation of Four Extended Moment End-Plate Connections*, Virginia Tech Structural Engineering and Materials Report No. CEE/VPI-ST-04/02, Blacksburg, VA.

Blumenbaum, S. and Murray, T. M. (2004), *Response of Cyclically Loaded Extended End-Plate Moment Connections when used with Welded Built-up Sections*, Virginia Tech Structural Engineering and Materials Report No. CEE/VPI-ST-04/02, Blacksburg, VA.

Borgsmiller, J.T. (1995), *Simplified Method for Design of Moment End-Plate Connections*, M.S. Thesis, Virginia Tech, Blacksburg, VA.

Borgsmiller, J. T. Sumner, E. A. and Murray, T. M. (1995), *Extended Unstiffened Moment End-Plate Connection Tests*, Virginia Tech Structural Engineering Report No. CE/VPI-95/13, Blacksburg, VA.

Borgsmiller, J.T. (1995), *Simplified Method for Design of Moment End-Plate Connections*, M.S. Thesis, Virginia Tech, Blacksburg, VA.

Boorse, M. R. and Murray, T. M. (1999), *Evaluation of the Inelastic Rotation Capability of Flush End-Plate Moment Connections*, Virginia Tech Structural Engineering Report No. CE/VPI-ST 99/09, Blacksburg, VA.

Curtis, L.E., and Murray, T.M. (1989), “Column Flange Strength at Moment End-Plate Connections”, *Engineering Journal*, Vol 26, No. 2, pp. 41-50.

Eatherton, M.R., Toellner, B.W., Watkins, C.E., and Abbas, E. (2013), *The Effect of Powder Actuated Fasteners on the Seismic Performance of Protected Zones in Steel Moment Frames*, Virginia Tech Structural Engineering and Materials Report No. CE/VPI-ST-13/05.

Eatherton, M.R., Chen, Y., Laknejadi, K., and Murray, T.M. (2017), “Using Longitudinal Stiffeners to Mitigate Buckling of Noncompact and Slender Beam Webs in Ductile Moment Frame Connections”, *Annual Stability Conference Structural Stability Research Council*, San Antonio, TX.

Eatherton, M.R., Murray, T.M. (2021) Flush and Extended End-Plate Moment Connections, AISC Design Guide 4+16, Published by the American Institute of Steel Construction, Chicago, Il.

Ghassemieh, M., Kukreti, A. and Murray, T. M. (1983), *Inelastic Finite Element Analysis of Stiffened End-Plate Moment Connections*, FEARS Structural Engineering Laboratory Report No. FSEL/AISC 83-02, Norman OK.

Hendrick, D., Kukreti, A.R., and Murray, T. M. (1984), *Analytical and Experimental Investigation of Stiffened Flush End-Plate Connections with Four Bolts at the Tension Flange*, FEARS Structural Engineering Laboratory Report No. FSEL/MBMA 84-02, Norman, OK.

Italiano, V.M., and Murray, T.M., (2001), *Behavior of Diagonal Knee Moment-End Plate Connections*, Virginia Tech Structural Engineering Report No. CE/VPI-ST 01/01, Blacksburg, VA.

Jenner, R., Densford, T., Astaneh-Asl, A. and Murray, T. M. (1985), *Experimental Investigation of Rigid Frames Including Knee Connection Studies - Frame Assembly Tests*, FEARS Structural Engineering Laboratory Report No. FSEL/MESCO 85-0l, Norman, OK.

Jenner, R., Densford, T., Astaneh-Asl, A. and Murray, T. M. (1985a), *Experimental Investigation of Rigid Frames Including Knee Connection Studies - Frame Assembly Tests*, FEARS Structural Engineering Laboratory Report No. FSEL/MESCO 85-0l, Norman, OK.

Jenner, R., Densford, T., Astaneh-Asl, A. and Murray, T. M. (1985b), *Experimental Investigation of Rigid Frames Including Knee Connection Studies – Frame FR1 Tests*, FEARS Structural Engineering Laboratory Report No. FSEL/MESCO 85-02, Norman, OK.

Jenner, R., Densford, T., Astaneh-Asl, A. and Murray, T. M. (1985c), *Experimental Investigation of Rigid Frames Including Knee Connection Studies – Frame FR2 Tests*, FEARS Structural Engineering Laboratory Report No. FSEL/MESCO 85-03, Norman, OK.

Jain, N., Eatherton, M.R., and Murray, T.M. (2015), *Developing and Validating New Bolted End-Plate Moment Connection Configurations*, Virginia Tech Structural Engineering and Materials Report No. CE/VPI-ST-15/08, Blacksburg, VA.

Kline, D., Rojiani, K., and Murray, T. M. (1995), *Performance of Snug-Tight Bolts in Moment End-Plate Connections*, Virginia Tech Structural Engineering Report No. CE/VPI-ST-89/04, Blacksburg, VA.

Kukreti, A.R., Murray, T.M., and Abolmaali, A. (1987), "End-Plate Connection Moment-Rotation Relationship", *Journal of Constructional Steel Research*, Vol. 8, pp. 137-157.

Meng, R.L. (1996), *Design of Moment End-Plate Connections for Seismic Loading*, Ph.D. Dissertation, Virginia Tech, Blacksburg, VA.

Meng, R. L., and Murray, T. M. (1996), *Moment End-Plate Connections for Seismic Loading*, Virginia Tech Structural Engineering Report No. CE/VPI-ST-96/04, Blacksburg, VA.

Morrison, S. J., Astaneh-Asl, A. and Murray, T.M. (1985), *Analytical and Experimental Investigation of the Extended Stiffened Moment End-Plate Connection with Four Bolts at the Tension Flange*, FEARS Structural Engineering Laboratory Report No. FSEL/MBMA 85-05, Norman OK.

Morrison, S. J., Astaneh-Asl, A. and Murray, T.M. (1986), *Analytical and Experimental Investigation of the Multiple Row Extended Moment End-Plate Connection with Eight Bolts at the Beam Tension Flange*, FEARS Structural Engineering Laboratory Report No. FSEL/MBMA 86-01, Norman, OK.

Murray, T.M. (1989), *Tests to Determine the Adequacy of A490 Bolts in Moment End-Plate Connections*, Structural Engineers Inc. Report, Radford, VA.

Murray, T.M., and Sumner, E.A. (1999), *Brief Report of Steel Moment Connection Test – SAC Subtask 7.10, Testing and Analysis of Bolted End-Plate Connections*, Virginia Tech Report, Blacksburg, VA.

Srouji, R., Kukreti, A.R., and Murray, T. M. (1983), *Strength of Two Tension Bolt Flush End-Plate Connections*, FEARS Structural Engineering Laboratory Report No. FSEL/MBMA 83-03, Norman, OK.

Structural Engineers Inc. (1984), *Multiple Row, Extended End Plate Connection Tests*, Report, Norman, OK.

Sumner, E.A., and Murray, T.M. (1995), *Experimental Investigation of Rigid Knee Joints-Addendum*, Virginia Tech Structural Research Report No. CE/VPI-95/10, Blacksburg, VA.

Sumner, E.A., Mays, T.W., and Murray, T.M. (2000a), *Cyclic Testing of Bolted Moment End-Plate Connections*, SAC Report No. SAC/BD-00/21, Virginia Tech Structural Engineering Report No. CE/VPI-ST 00/03, Blacksburg, VA.

Sumner, E.A., and Murray, T.M. (2001a), *Experimental Investigation of the Multiple Row Extended 1/2 End-Plate Moment Connection*, Virginia Tech Structural Engineering Report No. CE/VPI-ST-01/14, Blacksburg, VA.

Sumner, E.A., and Murray, T.M. (2001b), *Experimental Investigation of Four Bolts Wide Extended End-Plate Moment Connections*, Virginia Tech Structural Engineering and Materials Report No. CE/VPI-ST 01/15, Blacksburg, VA.

Sumner, E.A., and Murray, T.M. (2002), "Behavior of Extended End-Plate Moment Connections Subjected to Cyclic Loading", *Journal of Structural Engineering*, Vol. 128, No. 4, pp. 501-508.

Szabo, T., Eatherton, M.R., He, X., and Murray, T.M. (2017), *Study of a Twelve Bolt Extended Stiffened End-Plate Moment Connection*, Virginia Tech Structural Engineering and Materials Report No. CE/VPI-ST-17/02.

Thompson, B.G., and Murray, T.M. (1975), *End-Plate Connection Tests and Analysis*, University of Oklahoma, School of Civil Engineering and Environmental Science Report, Norman OK.

Rodkey, R. W. and Murray, T. M. (1993b), *Eight-Bolt Extended Unstiffened End-Plate Connection Test*, Virginia Tech Structural Engineering Report No. CE/VPI-STG 93/10, Blacksburg, VA.

Ryan, J. C. Jr., and Murray, T. M. (1999), *Evaluation of the Inelastic Rotation Capability of Extended End-Plate Moment Connections*, Virginia Tech Structural Engineering and Materials Report No. CE/VPI-ST 99/13, Blacksburg, VA.

Young, J. and T. M. Murray, (1997), *Experimental Investigation of Positive Bending Moment Strength of Rigid Knee Connections*, Virginia Tech Structural Engineering Research Report